Visual Similarity Analysis of Web Pages based on Gestalt Theory

by

Zhen Xu

A thesis submitted in partial fulfillment of the requirements for the degree of

Doctor of Philosophy
in
Software Engineering & Intelligent Systems

Department of Electrical and Computer Engineering
University of Alberta

ABSTRACT

With the rapid development of internet technology, web page has evolved from a traditional rich-text information source to a multi-functional tool, which can serve images, audios and videos, act as the GUI (Graphical User Interface) components of distributed applications, and so on. Similarity evaluation of the modern web pages becomes more essential yet difficult. On one hand, while many search engine rely on keyword search, texts play less important roles in web pages. On the other hand, there exists a variety of browsers and platforms that support HMTL/CSS/JavaScript in different levels, causing a web page is displayed differently among browsers.

To address these issues, we propose four research topics. The first topic is to identify semantic blocks on web pages. We propose a model for merging web page content into semantic blocks based on human perception. To achieve this goal, we construct a layer tree to remove hierarchical inconsistencies between visual layout and DOM tree of web pages; we translate the Gestalt Laws of grouping to computer compatible rules can train a classifier to combine the laws to a unified rule to detect semantic blocks. The second topic is to estimate visual similarity of web pages. Existing approaches use DOM (Document Object Model) trees or images, but they either only focus on the structure of web pages or ignore inner connections among web page features. Therefore, we provide the block tree to combine both structural and visual information of web pages. Using this block tree structure, we propose a visual similarity measurement. The purpose of the third topic is to improve the visual similarity measurement and use it to detect visual differences in web pages when they are rendered in different browsers. The extended subtree model that maps sub trees instead of each single node is introduced for the precision improvement. The forth topic utilize the improved visual similarity measurement to create an automated testing framework for cross-browser visual incompatibility detection. An automated testing tool is also designed.

Major contribution of this thesis is two-folds. On the one hand, it enriches theoretical analysis in the detection of semantic content, visual similarity, and cross-browser differences for web pages. On the other hand, it also provides an insight for testing cross-browser incompatibilities in practice.

To my wife, my daughter, and my parents!

Acknowledgments

More than four years have passed since I came to Canada to pursuit my PhD degree. A lot of things have happened during this time period, and I cherish every moment of it, no matter they are happy or sad. I have millions to say to my family, teachers, and friends.

First of all, I would like to give my sincere thanks to my dear supervisor James Miller. He has always supported me, guided me, and gave me confidence during my study. He is such an excellent teacher that I can always find my direction under his supervision no matter what difficulties I met in the process of researching. He is such a responsible teacher that he always responses to my email quickly and he always put his students' benefits in the first place. Many times, even during weekends or holidays, he still can give me feedback very quickly. Without his push, I could not have made the progress I have achieved now. He is such an amiable teacher that he can always find a way to cheer me up when I did not make any progress at all. I would say he is the best teacher I have met and I owe him a lot.

Second, I want to give my thanks to my wife, Wenjing Wang, who has always supported me no matter what happens. She always stands on my side and encourages me. Especially when I encountered some difficulties in my research and felt frustrated, she never gave me up and she never imposed stresses on me. Instead, she enlightened me with gentle words and cooked me delicious food. I feel very lucky to have such a wonderful wife.

At last, I also feel grateful of my parents: my father Xinghua Xu and my mother Yuling Yan. Although they are back in China, they still care about me so much. Without their love and raise, I cannot grow up so healthy and strong. Additionally, I would like to thank my friends as well. Thanks for their help in my life. Without them, my life could not have been so fulfilling and colorful. Allow me name them here: Yanan Xie, Zhengrong Cheng, Jikai Liu, Xihui Liang, and many others. Thanks so much, buddies!

Table of Contents

List of Tables

List of Figures

CHAPTER 1 Introduction

Internet has brought many benefits and opportunities to our modern life, one of which is the development and usage of web pages. Web pages have changed our way of life in a variety of ways. Nowadays web pages are thriving and have invaded into every way of life, including banking, trading, shopping, education, and etc. Web pages become so important and prevalent that we can barely live without them. For example, online banking allows us to shop by browsing commercial web pages and later make a payment; major universities and colleges offer educational resources through their own web pages for students wherever they are as long as they have access to internet; e-commerce has changed the way of traditional marketing and brings about more convenience both to merchants and customers.

While we enjoy the convenience web pages have brought to our daily life, we should see that there are issues associated with them as well. For instance, many web pages are embedded with abundant irrelevant information, such as pop-up ads and extraneous images, which interrupts our reading efficiency and prevents us from acquiring the real information we are seeking. The similarity of web pages is also an issue. Some web pages are designed so similar that ordinary people can hardly see the differences between them. Malicious designers will mimic the design of major web sites deliberately so that they can trick users for illegal gains.

Since the technique behind web pages is complex, the usage of web pages is a double-edged sword. We can benefit from it if they are used properly or we can also suffer from them otherwise. In this thesis, we will look at web pages from the aspects of semantic content, similarity, and cross-browser issues.

1 Motivation and Goals

After reading relevant papers in the literature, we find that four issues are imminent and important in the area of web pages, these can be as summarized in the follows.

Firstly, web pages are inundated with vast of irrelevant information such as ads and extraneous images. The irrelevant information not only makes web pages more complicated, but also affects the efficiency and effectiveness of our knowledge acquisition.

Secondly, web pages have become increasingly important as we growing rely on them. As such, a number of illegal web pages have immerged by mimicking the real ones. Since ordinary users cannot tell the differences between the real web pages and the fake ones in many cases, it is necessary for web page designers and researchers to find a way to reduce the influence of web page misusage.

Thirdly, with the advent of various web browsers and platforms, web pages designed for a specified carrier cannot work well in another, which leads to cross-browser issues for web pages. How to detect these issues correctly and effectively becomes important and necessary for us to trust on web pages.

In order to tackle the above-mentioned issues, we seek to achieve the following goals in this thesis.

Regarding the first issue, we will find approaches to identify semantic content in web pages. By doing so, we attempt to provide a method for retrieving information from web pages effectively and efficiently.

Regarding the second, issue, our goal is to propose a method for estimating similarity of web pages. As a matter of fact, there are a number of methods available at present for estimating web page similarity. However, current methods are not feasible with regard to modern rich-format web pages.

Regarding the last issue, the purpose is to investigate cross-browser issues and develop an approach to detect differences existing in various web browsers and platforms. It is noted that we mainly focus on visual differences of web pages in this regard. Based on the proposed approach, we will further develop an automated testing framework for detecting cross-browser incompatibilities.

2 Main Contributions and Thesis Outline

The major contributions of this thesis are summarized as follows:

- Investigated and interpreted the Gestalt laws of grouping into computer compatible rules for web page content segmentation.
- Provided a semantic block tree model to represent web pages visual information.
- Proposed a numeric measurement for web page visual similarity evaluation.
- Improved the interpretation of Gestalt laws of grouping by a series of empirical experiments.
- Improved the visual similarity measurement by using the extended subtree model to replace the tree edit distance.

- Utilized the visual similarity measurement to evaluate cross-browser similarity of web pages.
- Designed an automated testing framework to detect cross-browser visual incompatibilities.

This thesis adopts the paper-based format and organized as follows. In Chapter 2, we present our first journal paper as it is published. This paper provides an approach to identify semantic blocks in web pages using the Gestalt laws of grouping. Chapter 3 presents our second journal paper as it is published. This paper offers a way to estimate similarity of rich web pages using visual information. In Chapter 4, we present our third journal paper as it is in review. This paper deals with detection of cross-browser differences for web page visual similarity. Chapter 5 shows our fourth journal paper as it is submitted. It describes an automated testing framework for detecting cross-browser differences. The last chapter summarizes and concludes the thesis as a whole.

CHAPTER 2 Identifying Semantic Blocks in Web Pages Using Gestalt Laws of Grouping[1]

Abstract

Semantic block identification is an approach to retrieve information from web pages and applications. As website design evolves, however, traditional methodologies cannot perform well any more. This chapter proposes a new model to merge web page content into semantic blocks by simulating human perception. A “layer tree” is constructed to remove hierarchical inconsistencies between the DOM tree representation and the visual layout of the web page. Subsequently, the Gestalt laws of grouping are interpreted as the rules for semantic block detection. During interpretation, the normalized Hausdorff distance, the CIE-Lab color difference, the normalized compression distance, and the series of visual information are proposed to operationalize these Gestalt laws. Finally, a classifier is trained to combine each operationalized law into a unified rule for identifying semantic blocks from the web page. Experiments are conducted to compare the efficiency of the model to a state-of-art algorithm, the VIPS. The comparison results of the first experiment show that the Gestalt layer merging (GLM) model generates more “true positives” and less “false negatives” than VIPS (VIsion-based Page Segmentation). The next experiment upon a large-scale test set produces an average precision of 90.53% and recall rate of 90.85%, which is approximately 25% better than that of VIPS.

1 Xu, Zhen, and James Miller. "Identifying semantic blocks in Web pages using Gestalt laws of grouping." World Wide Web 19.5 (2016): 957-978.

Keywords: DOM Tree; Gestalt Law of Grouping; Normalized Hausdorff Distance; CIE-Lab; Normalized Compression Distance.

1 Introduction

Modern web pages are much more complicated in both content and layout than ever before. Many pages include vast amounts of "irrelevant" information, such as pop-up ads, game animations, and extraneous images. Due to this, content identification is becoming more and more difficult. Nevertheless, it is the basis for further work, i.e., content extraction, data mining, anti-phishing, etc.; hence, it is important that a solution to this problem is found. The number of applications derived from semantic block identification in web pages, has climbed in recent years. To be specific, major applications include:

- Content extraction: with extensive information available on current rich-format web pages, removing "irrelevant" information and extracting target information quickly and exactly is a vital task.
- Data mining: it aims to investigate data patterns from the large amount of data carried by target web pages. Web page semantic block identification divides web pages into distinct blocks by their semantics, and this process will boost data mining mechanisms and thus improve their accuracy.
- Anti-phishing: current web pages carry both good and bad information, for example, a variety of fake web pages has emerged, trying to obtain illegal benefits from the public. Under this situation, anti-phishing becomes an important topic and assumes the heavy responsibility of distinguishing fake web pages. Through analyzing

contextual semantics, blocks with fake content can be detected and distinguished from genuine content.

- UI design: Despite technology improvements in web design, web pages becomes increasingly complex at the same time. An excellent web page should be one that serves the needs and demands of its target customers, rather than feed them with abundant irrelevant information. Thus, semantic block identification provides a potential guideline to enhance UI design of web pages and web sites.
- Web search: to search target information fast and accurately, the semantic meaning of the web page blocks is as important as its content and layout. That is, semantic block identification provides another insight into web search, on top of web page layout and pure text content.

Traditional methodologies on block identification work well on textual web pages, however, they cannot efficiently process rich-format modern web pages. It is obvious that people can recognize related web page content fast and correctly even before reading it, regardless of the complexity of the web pages. According to Gestalt psychology, this is because that humans group objects based on a series of laws – the Gestalt laws of grouping (Palmer 1990; Sternberg 2003; Koffka 1995).

Therefore, this chapter proposes the "Gestalt Layer Merging" (GLM) model to solve the problem of the traditional methodologies. The GLM model simulates human perception by utilizing the Gestalt laws of grouping and three tasks are mainly involved in this model:

- It extracts the web page content from the DOM tree and constructs a "layer tree". This layer tree has an identical hierarchy with the visual layout of the web page.

- It interprets the Gestalt laws of grouping. The Gestalt laws are translated into comparable measurements to evaluate and merge the layer tree nodes into semantic blocks.
- It combines different Gestalt laws into a unified rule for identification. The combination obtained by a classifier specifies how the web page content is merged, and how the final semantic blocks are displayed.

The organization of this chapter is as follows: Sect. 2 discusses an overview of related work on web page block identification; Sect. 3 describes the GLM model's outline; Sect. 4 gives details on the implementation of the model; Sect. 5 runs experiments to merge and identify web page blocks and evaluates the result by precision and recall; and finally, Sect. 6 draws conclusions from the experimental result.

2 Related Work

Web pages of ten years ago were not as rich in layout as that of today – they contained mostly plain text and text hyperlinks, while images, video, and audio streams were not very common. In addition, because many of the web pages focused on publishing (textual) articles, their layouts were usually very simple. Thus, the web pages can be identified by text extraction simply and directly. Besides, using tabular tags such as "`<TABLE>`", "`<TR>`" and "`<TD>`" to hold content was once very popular in web page design. Therefore, many researches extracted content blocks by such tabular clues. For example, Lin and Ho (2002) analyzed such web pages to extracted informative content blocks. Because modern web pages usually do not apply tabular skeleton, this method is not suitable any more.

Some other researchers have chosen to directly analyze the source HTML files. Gupta et al. (2003) applied two sets of filters to retrieve text. Their first filter set was a text filter that removed images, links, scripts and styles, and the second filter set contained four components, namely, an advertisement remover, a link list remover, an empty table remover, and a removed link retainer. By applying the two sets of filters, all images and stream media were removed from the web page. Although performed well on textual web pages, it can retrieve very limited information from rich format web pages. Reis et al. (2004) proposed the RTDM, a restricted top-down mapping algorithm based on the "tree edit distance". This methodology solved the structure-based page classification problem; and can extract news articles from web pages automatically. However, it focused only on the textual content while paid no attention on the layout, therefore had limitations on processing modern web pages. Kohlschütter and Nejdl (2008) proposed a densitometric approach, the "block fusion" algorithm, by which they merged (fused) text into blocks according to the density of the paragraphs. The number of "tokens" an "lines" are used to determine the density of the paragraphs. The disadvantage of the "block fusion" algorithm lies on its assumption that the maximum width of a line is 80 – this only applies to traditional monospaced terminals, but not to the varies of modern displaying devices. Kang et al. (2010) investigated the HTML tag repeat patterns. Based on the repetition patterns, their REPS algorithm splits the web page content (tags) into blocks. By applying proper value to the threshold of the "normalized importance weight", their algorithm worked well on block identification. However, many modern web pages, especially home pages of modern websites, are designed very simple in layout, containing very few of such repetition patterns. The REPS cannot identify blocks on such web pages as well as it did in traditional textual pages.

Evolution of browsers enables web pages to become richer in both content and layout. Due to the power of CSS and JavaScript, the source HTML files are no longer sufficient to represent what we see from the web page. Therefore, researchers have considered visual clues. Cai, et al. (2003a; 2003b; Yu, et al. 2003; Song, et al., 2004) proposed the VIPS algorithm in their research. The VIPS algorithm utilizes all the visual clues that CSS supported, considers each DOM element as a rectangular block (for separator identification), and segments web pages by iteratively detecting separators among these visual blocks. This work has been highly influential, and still represents the state-of-art in this area. However, although the visual clues of the web page layout were taken into consideration by the VIPS algorithm, the researchers still segmented pages in a "manual" way – they studied the rendering style of web pages and concluded limited segmenting rules, leading to an incompleteness of analyzing the visual clues. Meanwhile, the VIPS algorithm was proposed and evaluated on the traditional web pages with tabular skeleton, but performed less efficient on modern web pages. Chen et al. (2003) proposed a methodology similar to VIPS. They first evaluate the position of each DOM element to decide if it is a header, a footer, or a sidebar; and then detect the separators among such blocks. Based on these visual clues, they segment web pages into semantic blocks.

Visual based web page block identification is also useful for displaying web pages on small screen devices. Hattori et al. (2007) propose the "content distance" of HTML tags and derived a layout-based segmentation algorithm for visual block identification. The "content distance" is calculated based on the node depth of the DOM tree, which is a novel metric in this area. However, the implementation of this distance only parses the source HTML files, leading to missing important features such as dynamically loaded content or CSS properties. The layout-based segmentation algorithm pre-splits a page according to the "cell" size, which is divided by tabular skeleton or "`<DIV>`" wrappers, and the splitting procedure relies heavily on the parameter of "maximum cell size". However, the determination of such an important parameter is not solved in the chapter, making the algorithm un-implementable by third parties. Baluja (2006) propose a machine learning framework to identify blocks and recast web pages to fit cell phone screens. In the methodology, they calculated the entropy and the "information gain" based on the area of each DOM element, extract its spatial coordinates as features, and build a decision tree to split the web page into blocks. Specifically, the algorithm splits each web page into 9 grids, each mapped to a button in the number pad. By pressing a number, the user interacted with the corresponding grid (for example, zoom in/out). Although it seems to perform well, this algorithm can only identify a fixed number of blocks with a predefined spatial pattern, this makes it completely unsuitable for general purpose utilization! In addition, in many cases, it splits complete semantic blocks into different grids incorrectly because it evaluates the "information gain" of each vertical and horizontal line while ignores the actual boundaries of DOM elements. Therefore, this algorithm has a very limited application in the research area of web page semantic block identification. Besides, as the hardware evolves, small screen devices that need to display web pages draw much less popularity, leading to the demand of recasting web pages shrink. Instead, more mature solutions for recasting web pages (such as Bootstrap[2]) have been widely employed.

2 http://getbootstrap.com/

Some other researchers investigated the semantic block identification problem in other ways. Chakrabarti et al. (2008) formulated the problem in a combinatorial optimization framework. They constructed a weighted graph from the DOM tree of a web page, used the energy-minimizing cuts to perform machine learning of the weights, and finally split web page content into blocks by the learnt weights. Cao et al. (2010) transformed each page into an image of RGB colors, and then applied an edge detecting algorithm (Canny, et al. 1986) to "shrink" the image into several "dividing zones", which were the actual web page blocks. Their experiment demonstrated this image processing algorithm worked well on textual web pages.

3 Gestalt Layer Merging Model

The Gestalt layer merging (GLM) model aims to identify web page blocks by simulating human perception with the Gestalt laws of grouping. Three components are included in the model, namely, the layer tree constructor, the Gestalt laws translator, and the web page block identifier.

3.1 Layer Tree Constructor

The DOM tree is a fast and precise representation of a web page; however, it cannot be directly used as the input in this model. People read only visible content from the web pages, so the invisible DOM elements are useless, i.e., they are simply noise to this model. Meanwhile, the visual hierarchy of a web page sometimes differs from the corresponding DOM hierarchy, causing perception errors to this model. Such noise and errors must be eliminated before analyzing.

Definition: Given a web page WP, the *layer tree* LT of WP is a finite set where each element n (that is, *layer tree node*) of LT is a *layer* representing a visible element e from DOM tree DT of WP ($LT = \{n \mid n \leftarrow e, e \in DT\}$) and all elements follow the visual hierarchy of WP.

The layer tree constructor takes the DOM tree of a web page as a prototype to build up its layer tree. The construction includes removing the invisible DOM elements and fixing the hierarchy. An invisible DOM element is either an element with area of 0 (including the borders and shadows), an element without any actual content (text, image, background, etc.), or an element that is completely covered by its visible child elements. The visual hierarchy refers to the geometrical distribution and overlapping relationships of the DOM elements. The layer tree and layer tree nodes have the following properties:

Property 1: A layer tree node always represents a visible DOM element.

The DOM tree of a web page contains not only the content information, but also structural and other information. While the former information can be seen by people, the latter is often ignored, so it is not required in this model. For example, some "`DIV`" elements contain no direct content and only act as "wrappers" – holding other elements. Such elements will not be extracted into layer tree nodes.

Property 2: A layer tree node always represents a complete DOM element.

This follows the Gestalt laws of prägnanz. A DOM element may contain many kinds of sub content, for example, it may have both foreground text and a background image. Although, visually speaking, such a DOM element can be further split, we do not extract each of the sub content into a separate layer node. Instead, only one layer node is extracted representing the complete DOM element.

Property 3: A layer tree node is always a complete rectangle.

This follows the Gestalt laws of closure. In a web page, it is common that some layers overlap others, so that the parts of the lower layers that covered by the upper layers cannot be seen. For example, an input box may overlap its parental layer's background image. In fact, people still perceive such rectangles as complete. Therefore, it is reasonable to consider layer tree nodes as complete rectangles.

Property 4: The root node of a layer tree always represents the "`BODY`" element.

Visible content of a web page locates under the "`BODY`" subtree. However, the "`BODY`" element sometimes is empty, which means it is invisible. In such a case, the browser will still draw the web page on a white background. This browser behavior enables the "`BODY`" to become a visible DOM element. Consequently, it is correct to be selected as the root of the layer tree.

Property 5: A layer tree node is always located inside its parent layer (if it has a parent layer).

The layer tree is designed to represent a web page. It must follow the visual hierarchy of the page. In the DOM tree, child elements are located inside their parent elements by default; however, some CSS rules can manipulate locations, such as "`position`", "`float`", "`z-index`", etc. These rules sometimes cause the DOM hierarchy to be misaligned against the visual hierarchy. Therefore, in layer tree construction, such an inconsistency must be eliminated.

3.2 Gestalt Laws Translator

This translator interprets the Gestalt laws of grouping into machine compatible rules. The Gestalt laws explain the mechanisms of how humans perceive and understand things. When processing web pages (layer trees), two Gestalt laws are used to build up the layer tree, and other four Gestalt laws are expanded into six rules to identify web page blocks.

3.2.1 The Gestalt Law of Prägnanz

The Gestalt law of prägnanz is also referred to as Gestalt law of simplicity. Humans tend to perceive objects into the simplest organizations. This is the overarching Gestalt law of grouping. Based on this law, we take the assumption that every layer node in the layer tree represents a complete DOM element and such a layer node should not be split any further in the GLM model.

3.2.2 The Gestalt Law of Closure

Humans tend to perceive incomplete shapes as complete. While building up a layer tree, we interpret this law to be that each node of the layer tree represents a complete rectangle, no matter how it is actually displayed.

3.2.3 The Gestalt Law of Proximity

Humans tend to perceive objects that are close to others as a single group, while those objects that are far from each other are placed into separate groups. This law groups elements based on their distances.

Browser behavior tells us that web page layers are placed adjacently to each other by default. So if we use the edge distance of layers as proximity, the value will be 0 for many cases. In another case, if there are two big layers and another two small layers each having the same edge distance, the gaps between the pairs of layers will not be visually the same. To solve this issue, we utilize a variant of the Hausdorff distance (Chaudhuri and Rosenfeld 1999; Sim, et al. 1999; Zhao et al. 2005) between layers as a working definition of proximity. This is because it takes the sizes of the two objects into consideration.

3.2.4 The Gestalt Law of Similarity

Humans tend to perceive similar objects as a single group. The similarity of two objects is determined by their appearances.

As a layer node is always a rectangle, the appearance includes its size, background, and foreground. Consequently, this law is expanded into three laws, accordingly. The first expanded law compares the size, which consists of both its width and height; the second expanded law compares background content, which consists of the background color and image; and the third expanded law compares the foreground content, which are the textual styles.

3.2.5 The Gestalt Law of Continuity

Humans tend to perceive objects that are aligned together as a single group. This law evaluates the positions of layers.

The browser aligns content by top and left by default. Therefore, if some layers are right or bottom aligned, they may be deliberately placed together by the designer of the web page. Hence, such continuity provides a strong clue that these layers are semantically related.

3.2.6 The Gestalt Law of Common Fate

Humans tend to perceive objects that share the same motion trend as a single group.

Most of the layers in a web page do not move at all. Some layers may contain animations or videos, but the layers themselves do not move. Thus, it is not possible to directly evaluate the motion trend. However, this law can evaluate the "static" trend of the layers.

3.2.7 The Gestalt Law of Symmetry

Humans tend to perceive symmetric objects together as a single group, even if they are far from each other. As most web pages are not designed to have symmetric layers, we do not utilize this law.

3.3 Web Page Blocks Identifier

A classifier combines the rules from the Gestalt law translator to identify web page blocks. Taking the layer tree of a web page as the input, the identifier evaluates each layer and makes a decision whether the layers can be put into the same group. While only siblings can be grouped, layers having different parents will be automatically put into different groups. Such merged groups represent the final blocks. They will be collected and the web page will be updated.

The GLM model's working procedure is illustrated in **Figure 2.1**.

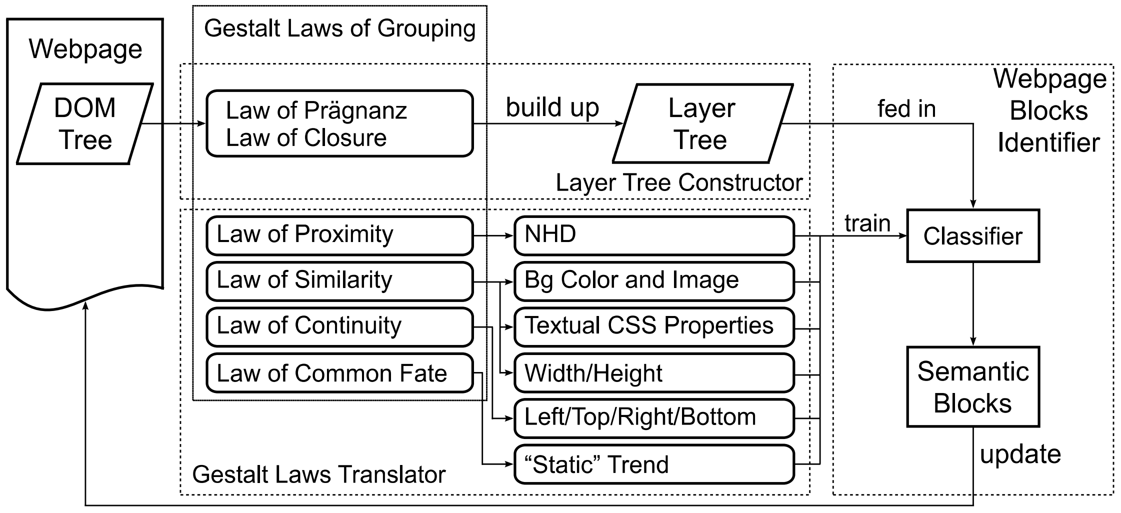

Figure 2.1 Working Procedure of GLM Model

4 Implementation

4.1 Buildup of the Layer Tree

Although the layer tree is similar to a subset of the DOM tree, building it is not just removing redundant nodes and information. Layer tree nodes must keep both content text and layout information, while the layer tree must keep the correct hierarchy of these nodes. Since CSS is able to float DOM elements to any place of the page, the DOM hierarchy is, for many cases, not identical to the rendered (visual) hierarchy. Thus, it is necessary to reconstruct the layer tree.

4.1.1 Create Layer Tree Nodes

The most important node of a tree is the root. For the layer tree, the root node is created from the "BODY" element. If a web page's "BODY" is invisible, it is set to a white background. Next, for each layer tree node, we create it as follows:

1) Acquire the corresponding DOM element.

2) Check if the DOM element is visible. Mark it as invisible and skip it if it meets any of these conditions: the HTML tag is invisible; either the element's height or width equals to 0; some of its CSS properties specify that it is not to be rendered; or it is completely transparent and empty.
3) If the DOM element is visible, calculate its geometric attributes representing the size. As mentioned previously, we consider every layer as a rectangle according to Gestalt law of closure. Therefore, the layer tree node's geometric attributes include the coordinates of its left top vertex as well as its height and width.
4) Identify the layout information of the layer tree node from the CSS styles. Every clue related to the layout can be interpreted from the CSS styles of the DOM element, so this step is actually retrieving useful CSS properties such as text styles, background styles, etc.
5) Different from DOM elements having more than one text node, the layer tree nodes contain only one text component, and this component is part of the node rather than its child nodes. So this step is to merge and trim all the DOM element's text nodes into one single property of the layer node.
6) Give the layer tree node a name. The name of a layer tree node is not necessary for applying Gestalt laws of grouping. It is only used for identifying the node. We simply use the XPath of the DOM element as the name.

4.1.2 Build Layer Tree with Nodes

The hierarchy of a layer tree is constructed from the DOM tree of the web page. As sometimes CSS styles replace the original layout and dis-render some DOM elements, the layer stacking hierarchy is not always identical with the DOM hierarchy. In addition, invisible elements existing in the DOM tree shall be removed when building up the layer tree. Thus, a modification is necessary.

To construct the layer tree, we manipulate nodes as follows:

1) Take the "BODY" layer node as the root node.
2) From the root node on, for every layer tree node, append all child (layer tree) nodes according to their corresponding DOM hierarchy.
3) If any node is completely located inside any of its sibling nodes, then move the node downward so that it becomes a child node of that sibling. Sibling nodes that geometrically overlap each other are acceptable in the layer tree model. They are still considered as sibling nodes.
4) If a DOM element is invisible or empty, then there is no corresponding layer tree node. However, its child DOM elements may have corresponding layer tree nodes. In this condition, these child layer tree nodes shall become children of the layer tree node which is related to this DOM element's first visible parent element.

Creating layer tree nodes from DOM elements is done simultaneously with building up the layer tree. This procedure starts from adding the root node to the layer tree, and then executes recursively until all visible DOM elements are extracted and added to the layer tree.

4.2 Translation of the Gestalt Laws

As mentioned above, the Gestalt law of similarity is expanded into three laws, namely, background similarity, text similarity, and size similarity. Among all the six laws:

- The Gestalt law of proximity is translated as to compare the distance between two layers. The distance in the GLM model is defined as the normalized Hausdorff distance between layers. Sect. 4.2.1 discusses details about the calculation.
- Background similarity is evaluated by both background color and image. Color comparison is conducted in CIE-Lab color space instead of RGB color space, and image comparison is done by calculating the normalized compression distance. They are discussed in Sect. 4.2.2 and Sect. 4.2.3.
- Text similarity is evaluated by comparing a set of text and paragraph related CSS properties. Similarly, with background color, the text colors are compared under CIE-Lab space; the other CSS styles are directly compared by their corresponding values.
- Size similarity is represented by both the width and height of the layers.
- The Gestalt law of continuity is interpreted to compare the left, top, right and bottom coordinates of layers. If any of the four edges between two layers share the same value, then they are continuous.
- The "Static trend" from the Gestalt law of common fate is represented by the "position" CSS property. By default, the positions are the same for semantically related layers. If any of a group of layers has a different "position", then it is designed to be separated from the others. Therefore, it belongs to a different block with others.

4.2.1 Normalized Hausdorff Distance

As mentioned previously, a normalized Hausdorff distance between two layers is used as the proximity. For the two layers L_1 and L_2, the Hausdorff distance (HD) between them is calculated as follows:

1) For any point l_1 in L_1 and l_2 in L_2, the distance between them is the length of the line segment:

$$\|l_1 - l_2\| = \sqrt{(x_{l_1} - x_{l_2})^2 + (y_{l_1} - y_{l_2})^2}\ ;$$

2) For any point l_1 in L_1, the distance between it and L_2 is the infimum of distances between l_1 and all points in L_2:

$$d(l_1, L_2) = \inf_{l_2 \in L_2} \|l_1 - l_2\|\ ;$$

3) Hausdorff distance from L_1 to L_2 ($hd_{1,2}$) is the supremum of distances between L_2 and all points in L_1:

$$hd_{1,2} = \sup_{l_1 \in L_1} d(l_1, L_2)\ ;$$

4) Hausdorff distance between L_1 and L_2 is the maximum value between the Hausdorff distance from L_1 to L_2 and the Hausdorff distance from L_2 to L_1, as shown in (2-1):

$$HD(L_1, L_2) = \max\{hd_{1,2}, hd_{2,1}\}\ . \qquad (2\text{-}1)$$

However, it is not sufficient to directly use HD as the proximity. This is because of a perceptual inconsistency: if there is a pair of large layers close to each other and another pair of small layers far from each other, the proximities of the two pairs are perceptually different (far vs. close), while the HD may have the same values. For example, as shown in **Figure 2.2**, L_1 and L_2 are both 50×50 while adjacent to each other; L_3 and L_4 are 10×10 while having an edge distance of 40. In this case the perceptual proximities of the two groups they are not the same, however, the NDs of the two pairs are both 50.

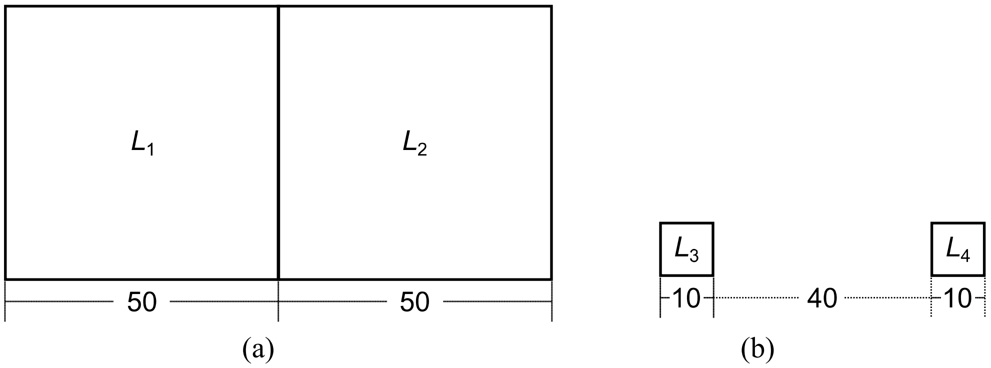

Figure 2.2 Paradox between Perceptual Proximity and Hausdorff Distance

Such inconsistency is caused by the sizes of the two layers. To eliminate it, we introduce a modification of the original Hausdorff distance as the proximity – the normalized Hausdorff distance (NHD). It is calculated by adding a normalizing factor – relevant length (Re) – to (2-1), as shown in (2-2):

$$NHD(L_1, L_2) = \max\left\{\frac{hd_{1,2}}{Re_{L_1}}, \frac{hd_{2,1}}{Re_{L_2}}\right\}, \tag{2-2}$$

where, L_1, L_2 are the two layers; sup and inf retrieve the supremum and infimum of a set of values; $\|l_1 - l_2\|$ is the norm (distance) between l_1 and l_2; and Re_{L_1}, Re_{L_2} are the relevant lengths, respectively.

Re can be either the height, width, or both (the diagonal) of the layer, depending on the related location of the two layers. Note that Re_{L_1} and Re_{L_2} in (2-2) may be different.

For example (**Figure 2.3**d), Re_{L_1} is the diagonal length of L_1 while Re_{L_2} is the height of L_2. As shown in **Figure 2.3**, having analyzed all possible distributions of two layers, we conclude the NHD calculation as follows:

1) L_1 is completely inside or outside of L_2. We do not deal with this condition and simply set NHD to 0 (although $hd_{2,1} \neq 0$ in **Figure 2.3**a). This only happens when calculating proximity between a parent and a child layer:

$$NHD(L_1, L_2) = 0\ .$$

2) L_1 is completely in the north/south area (between left and right edges) of L_2 (**Figure 2.3**b). In this condition, Re_{L_1} is the height of L_1, and $hd_{1,2}$ equals to the vertical distance between top edges (North) or bottom edges (South) of the two layers:

$$Re_{L_1} = height_{L_1}\ ;$$

$$hd_{1,2} = dist_{\mathrm{v}} = \begin{cases} \left|top_{L_1} - top_{L_2}\right|, \ c_y^1 < c_y^2 \\ \left|bottom_{L_1} - bottom_{L_2}\right|, \ c_y^1 > c_y^2 \end{cases},$$

Where, c_y^1 and c_y^2 are the y coordinates of the two layers' centroids, $c_y^1 \neq c_y^2$.

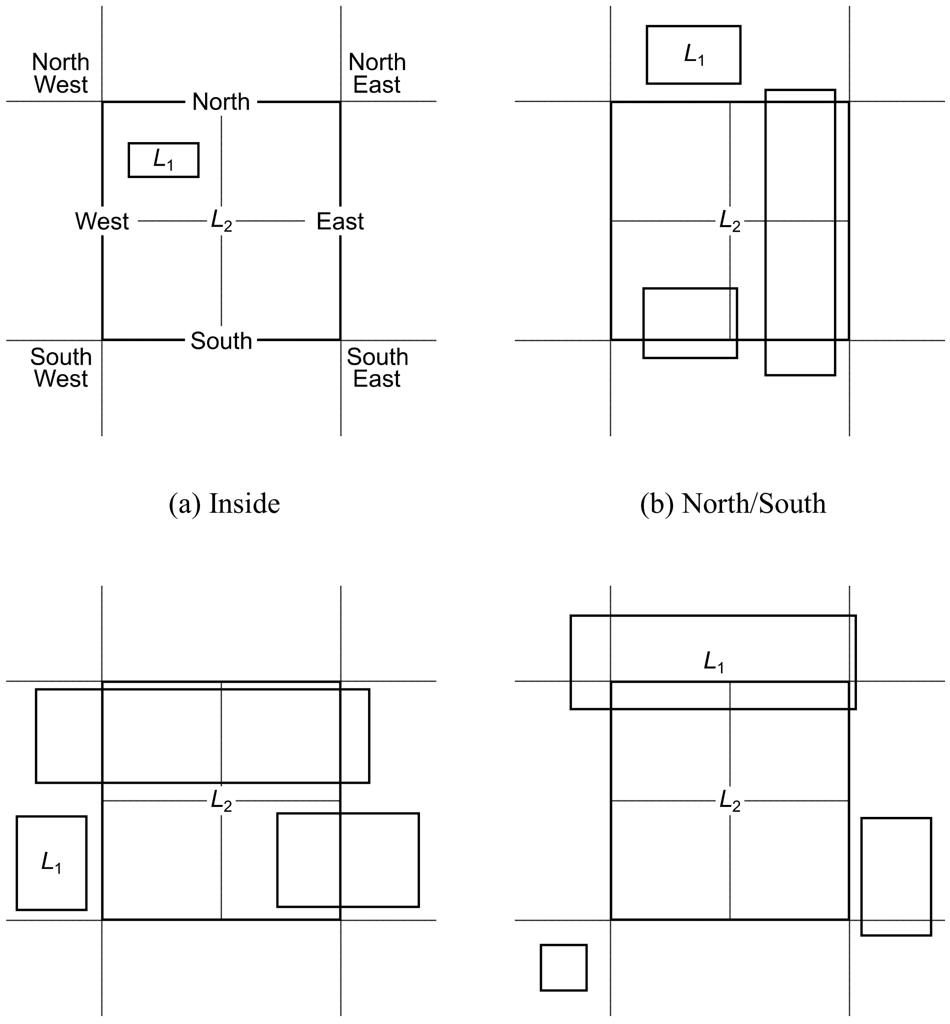

(a) Inside (b) North/South

(c) West/East (d) Corner Region(s)

Figure 2.3 Area definition and relevant length

3) L_1 is completely in the west/east area (between top and bottom edges) of L_2 (**Figure 2.3**c). Similarly, Re_{L_1} is the width of L_1, and $hd_{1,2}$ is the horizontal edge distance between their left edges (west) or right edges (east):

$$Re_{L_1} = width_{L_1} ;$$

$$hd_{1,2} = dist_{\mathrm{h}} = \begin{cases} |left_{L_1} - left_{L_2}|, \ c_x^1 < c_x^2 \\ |right_{L_1} - right_{L_2}|, \ c_x^1 > c_x^2 \end{cases},$$

Where, c_x^1 and c_x^2 are the x coordinates of the two layers' centroids, $c_x^1 \neq c_x^2$.

4) L_1 covers one or two corner areas of L_2 (**Figure 2.3**d). As none of the two rectangular layers completely locates inside of the other, L_1 can only cover one corner area or at most two adjacent corner areas of L_2. In this condition, both the height and the width of L_1 are the relevant lengths, so Re_{L_1} is the diagonal length of L_1; and $hd_{1,2}$ is the distance between the furthest vertices:

$$Re_{L_1} = diagonal_{L_1} = \sqrt{{width_{L_1}}^2 + \ {height_{L_1}}^2}\ ;$$

$$hd_{1,2} = \sqrt{{dist_{\mathrm{v}}}^2 + \ {dist_{\mathrm{h}}}^2}\ .$$

Having the NHD calculated, we can merge the layers according to Gestalt law of proximity. If a series of sibling layers share the same proximity, then they belong to one single group; however, if any pair of two layers has a different proximity than other pairs, they shall be put into a different group.

4.2.2 Comparing Two Colors

While most web pages use RGB color space, CIE-Lab color space is used in this chapter because it is designed to approximate human vision, and it provides standards to evaluate color differences.

When retrieving a CSS color, most browsers will return a RGB value or "transparent". The first step to compare colors is to fix the transparent color. In fact, if a layer has a transparent background color with no background image, the under layer's content will show. Thus "transparent" is not this layer's actual displaying background color

– it is its parent layer's background color. If all layers under the layer (that is, all the parent layers of it) are transparent and none of these parent layers contains any background image, then all the parent layers and the child layer will have a white background color. Having determined this, we can assign all layers with a non-transparent background color properly.

The non-transparent RGB colors are then converted into CIE-Lab through (2-3) and (2-4) (Connolly and Fleiss 1997; Johnson and Fairchild 2003):

$$\begin{pmatrix} X \\ Y \\ Z \end{pmatrix} = \begin{pmatrix} 0.4303 & 0.3416 & 0.1784 \\ 0.2219 & 0.7068 & 0.0713 \\ 0.0202 & 0.1296 & 0.9393 \end{pmatrix} \begin{pmatrix} R \\ G \\ B \end{pmatrix}, \qquad (2\text{-}3)$$

where, R, G, B are the red, green and blue channel of the RGB color; and X, Y Z are the X, Y, Z channel of the color in XYZ color space.

$$\begin{aligned} L^* &= 116\, f(Y \,/\, Y_0) - 16 \\ a^* &= 500\, [f(X \,/\, X_0) \;-\; f(Y \,/\, Y_0)]\,, \\ b^* &= 500\, [f(Y \,/\, Y_0) \;-\; f(Z \,/\, Z_0)] \end{aligned} \qquad (2\text{-}4)$$

where, L^*, a^*, b^* are the L*, a* and b* channel of the color; X_0, Y_0, Z_0 are the tristimulus values of CIE-Lab standard illuminant D_{50}; and $f(q)$ is calculated as:

$$f(q) = \begin{cases} \sqrt[3]{q} & q > 0.008856 \\ 7.787\, q + 0.1379 & q \le 0.008856 \end{cases}.$$

The CIE-Lab color difference is used to determine whether two colors can be considered as the same or not. Specifically, the color difference ΔE_{00}^{12} under the CIEDE2000 standard (Luo, et al. 2001; Sharma et al. 2005) is calculated, as shown in (2-5):

$$\Delta E_{00}^{12} = \sqrt{\left(\frac{\Delta L'}{k_L S_L}\right)^2 + \left(\frac{\Delta C'}{k_C S_C}\right)^2 + \left(\frac{\Delta H'}{k_H S_H}\right)^2 + R_T \left(\frac{\Delta C'}{k_C S_C}\right)\left(\frac{\Delta H'}{k_H S_H}\right)}\,. \qquad (2\text{-}5)$$

During comparison, if ΔE_{00}^{12} is greater than 3.30 (Liu, et al. 2012), then the two colors are considered as different.

4.2.3 Comparing Two Images

Background images are provided by CSS as URLs. However, it is not correct to simply compare the URLs because images with different URLs may still be the same. A correct way to compare images is to compare their content. We first retrieved images from URLs; and then convert them from RGB color space into CIE-Lab color space. To compare similarity of the two images (CIE-Lab color pixels), we calculate the normalized compression distance (NCD) as shown in (2-6) (Li, et al. 2004; Cilibrasi 2007):

$$NCD(x, y) = \frac{C(xy) - min\{C(x), C(y)\}}{max\{C(x), C(y)\}}, \tag{2-6}$$

where, x, y are the pixel representation of the two images; xy is the concatenation of x and y; and $C(q)$ calculates the length of the compressed data q.

We select LZMA as the compression algorithm. Having obtained $NCD(x, y)$, if it is smaller than 0.25 (Roshanbin and Miller 2011), then the two images x and y can be considered to contain the same content.

4.3 Identification of Web Page Blocks

Each of the six translated laws can provide a result that determines whether two layers should be merged together of not. The (final) result must combine the six sets of results together. However, it is not easy to analyze them after the application of the laws. An alternative solution is to combine the six laws together before the identification.

4.3.1 Combination of the Gestalt Laws

There exist no obvious rules on combining the Gestalt laws. Therefore, we choose the naive Bayes classifier (McCallum and Nigam 1998) to explore the hidden connection between them. In this classifier, the category variable C of the classifier is set as "0" and "1", representing "not merge" and "merge", respectively, while the feature vector consists of six variables, each representing the corresponding Gestalt law, as shown in **Table 2.1**.

Table 2.1 Variables used by the naive Bayes classifier

Variables			Values 0	Values 1
$\boldsymbol{F}$	F_1	Gestalt law of proximity	do not merge the layers	merge the layers
	F_2	Gestalt law of similarity (background)		
	F_3	Gestalt law of similarity (text style)		
	F_4	Gestalt law of similarity (layer size)		
	F_5	Gestalt law of continuity		
	F_6	Gestalt law of common fate		
C		all the above Gestalt laws		

To train the classifier, we do not build the training set with concrete web pages. This is because the training set shall contain all possible conditions of $\boldsymbol{F}$, such actual web pages are very rare. For example, it is hard to find a web page in the condition that all the layers follow and only follow the Gestalt law of proximity ($\boldsymbol{F} = (F_1, F_2, F_3, F_4, F_5, F_6) = (1,0,0,0,0,0)$). Due to this, we deliberately designed the sample pages to construct the training set, which has covered all values of $\boldsymbol{F}$. The training set consists of 64 cases ($2^6 = 64$). The training set is manually classified, and then fed to the classifier.

4.3.2 Collection of the Identification Results

The trained classifier reads the layer tree of a web page, evaluates the (sibling) layers by the six laws to create the corresponding feature vector $\boldsymbol{F}$, and finally categorizes the layers as "merge them" or "not merge them". The final identification results consist of a series of groups, where each group represents a semantic block. Layers in each block can be identified from the web page by its node name.

The blocks are stored into database. As we separate layers with different parents automatically into different groups, each semantic block will only contain sibling layers. Sometimes, a semantic block holds all sibling layers of a parent layer. In this condition, it is reasonable to replace all the child layers with the parent layer in the block.

As mentioned before, the advantage of Mozilla Firefox extension is that it is able to modify the web page in real-time. Therefore, in this implementation, having obtained the merging results, we update them to the original web page immediately. The updates are displayed by marking the corresponding DOM elements with a special background. For each semantic block, a different color (except black and white) is assigned, and each layer in this block is marked with this color as background. Meanwhile, border shadows are also added to make it clearer.

5 Experiments

We develop a Mozilla Firefox extension to implement the GLM model. This is because:

- Mozilla Firefox provides APIs for manipulating DOM elements without any extra effort such as parsing HTML code, JavaScript functions or CSS properties, making it possible to build up the layer tree easily and fast;
- The DOM tree provided in Mozilla Firefox is the one used for rendering the original web page, thus it is the most accurate data source of a web page we can find; and

- Any modification of the DOM tree is applied immediately, and shown (in real-time) to the users.

Experiment results of the GLM are compared with Cai's VIPS algorithm (Reis, et al. 2004), which is state-of-art and normally considered the most accurate web page segmentation algorithm. Algorithms by Hattori et al. (2007) and Baluja (2006) were also considered, but these algorithms are not implementable for this problem space. Details of the problems with these algorithms can be found in Sect. 2 .

5.1 Comparison Test

This test examines the identification results of the two algorithms on two test cases: the home pages of University of Alberta and IEEE standards association. For each of the two web pages, the two algorithms identify a series of blocks. However, some of the blocks are incorrect – they are the "false positive" results (FP); the correct blocks that any algorithms misses are the "false negative" results (FN); the correctly identified blocks are the "true positive" results (TP). The original pages and the result pages of are shown in **Figure 2.4**. Note that the screenshots of VIPS results are modified to illustrate results more clearly, because Cai's software cannot display all identified blocks in a single page.

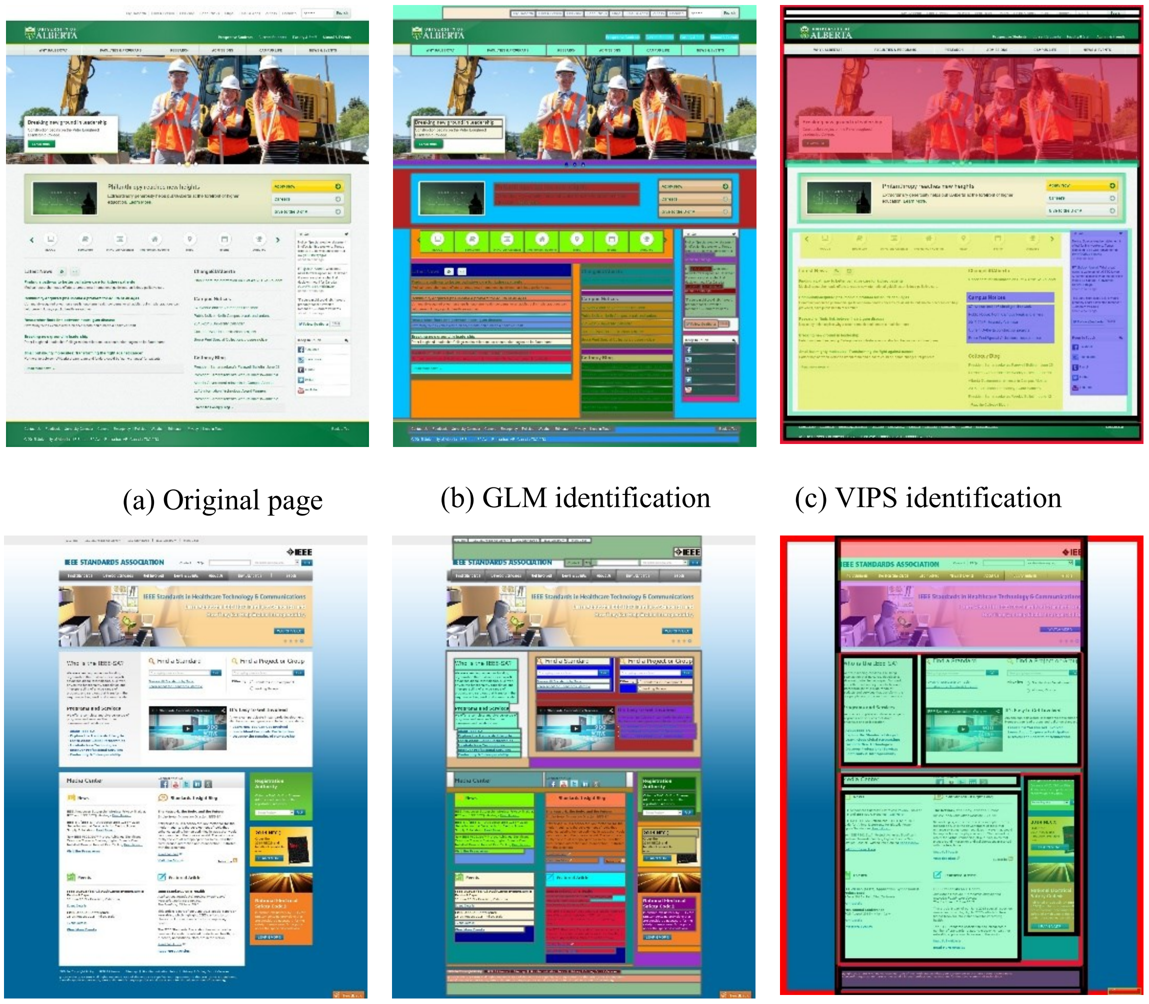

(a) Original page (b) GLM identification (c) VIPS identification

(d) Original page 2 (e) GLM identification (f) VIPS identification

Figure 2.4 Comparison of Identification Results

From the figure, observations can be found that the both GLM and VIPS have successfully identified correlated semantic blocks. For example, the middle navigation bar holding 7 icons (each element in the block is marked with yellow background) in **Figure 2.4**b, the big image block (marked with light red) in **Figure 2.4**c, the "news" block at the left bottom (marked with light green background) in **Figure 2.4**e, and the footer block (marked with purple) in **Figure 2.4**f, etc.

According to the observation, the GLM algorithm has performed better than VIPS on the two test cases. VIPS has identified very limited number of blocks, and misses a lot: for the UA home page, it only finds 28 blocks in total; while GLM finds 47 blocks; and for the IEEE home page, the total numbers of blocks found by the two algorithms are 15 and 41, respectively. This is because VIPS only identifies big blocks while it misses small ones. For example, as shown in **Figure 2.4**c, VIPS has identified the middle block (marked with light green border), but inside of this block, it fails to mark none of the three sub blocks – the left side image, the middle text block, and the right side buttons group. As a comparison in **Figure 2.4**b, GLM has identified both big block (marked with light blue background) and two of the three sub blocks, missing only the left side image. Furthermore, even when VIPS finds big blocks, many big blocks are still missed. For example, the "news" block (left part of the lower yellow block) in **Figure 2.4**c, the video block in in **Figure 2.4**f, etc. This drawback contributes to a high value of VIPS "false negatives", namely, 26 in IEEE home page, and 14 in UA home page. The statistics are summarized in **Table 2.2**.

Table 2.2 Numbers of TPs, FPs and FNs

Test	**GLM**			**VIPS**		
case	**TP**	**FP**	**FN**	**TP**	**FP**	**FN**
IEEE	38	3	3	10	5	26
UA	41	6	2	18	10	14

5.2 Efficiency Test

The second group of experiments evaluates the efficiency of the GLM and compare it with the VIPS through a large test set. Cai's VIPS software only provides manual operation for block identification and cannot displays all blocks together in the web page, therefore is not feasible for mass evaluation. To solve this problem, we chose this implementation[3].

The test set covers the homepages of the world's 500 top websites as defined from statistics produced by Alexa[4]. Before running the tests, we filter out "inappropriate" samples of websites such as duplicate sites (for example, "google.com", "google.ca", etc.), temporarily unavailable sites and sites that contain inappropriate content. The final test set consists of 381 websites.

5.2.1 Evaluation Metrics

The algorithm is evaluated by measuring its precision, recall and F-1 scores. Having acquired the numbers of TPs, FPs, and FNs for each web page, the three metrics can be calculated by (2-7):

$$\begin{aligned} P_i &= \frac{B_A \cap B_i}{B_A} = \frac{TP_i}{TP_i + FP_i} \\ R_i &= \frac{B_A \cap B_i}{B_i} = \frac{TP_i}{TP_i + FN_i}, \\ F_i &= \frac{2\, P_i R_i}{P_i + R_i} \end{aligned} \tag{2-7}$$

where, P_i, R_i, F_i are precision, recall and F-1 score of the ith web page, respectively; B_A is the number of blocks identified by the algorithm; B_i is the number of blocks that the ith web page contains; and TP_i, FP_i, FN_i are the number of "true positives", "false positives" and "false negatives", respectively.

As no computer system or software can count the correct TP_i, FP_i, FN_i automatically, we rely upon human judgement. In this chapter, we recruit five volunteers

[3] https://github.com/tpopela/vips_java
[4] http://www.alexa.com/topsites. The top sites were retrieved on April 4, 2014.

to evaluate all the 381 samples. The volunteers all utilize the Internet every day, so it is believed that they have sufficient experience to identify web page blocks correctly. They are required to judge the correctness of each result calculated by the algorithm. That is, to find the TP_i, FP_i and FN_i from both the screenshots of GLM and VIPS for each web page.

5.2.2 Inter Rater Reliability

The five volunteers evaluate each web page sample and count the TP_i, FP_i and FN_i independently. Before using their evaluations for the calculation of precision, recall and F-1 scores, a verification of inter-rater reliability (Gwet 2010) showing the agreement level among the five raters is needed. If they disagree with each other, then it will be meaningless to rely on their rates. During the verification, we calculate Cohen's Kappa (Jacob 1960) to verify it, as shown in (2-8):

$$\kappa = \frac{Pr(a) + Pr(e)}{1 - Pr(a)}, \tag{2-8}$$

where, $Pr(a)$ and $Pr(e)$ are the observed and expected percentage of agreement, respectively.

Mean κ values of all samples between each two raters' TP, FP and FN are listed in **Table 2.3**. The reason that κ values of GLM's TP are lower lies in the fact that TP blocks are the major parts of each web page. Of all the test cases, the average TP is 36.89 while average FP and FN are 3.35 and 3.03, respectively. Raters' disagreement level on the larger group is higher than that on the smaller groups:

1) The identification results contain blocks with different granularities. One rater considered small blocks as TP bocks while another rater considered them as FP

blocks. Such an example from **Figure 2.4**b is the green button inside the text rectangle floating upon the big image (See the yellow ellipse in **Figure 2.5**) – three of the raters believed the buttons should not be separated from the text, while the other two raters identified them as one block. Although almost every sample contained blocks where one was inside of another, less than 10% of them caused granularity issues in the five volunteers' ratings. However, this was the major source of deviations.

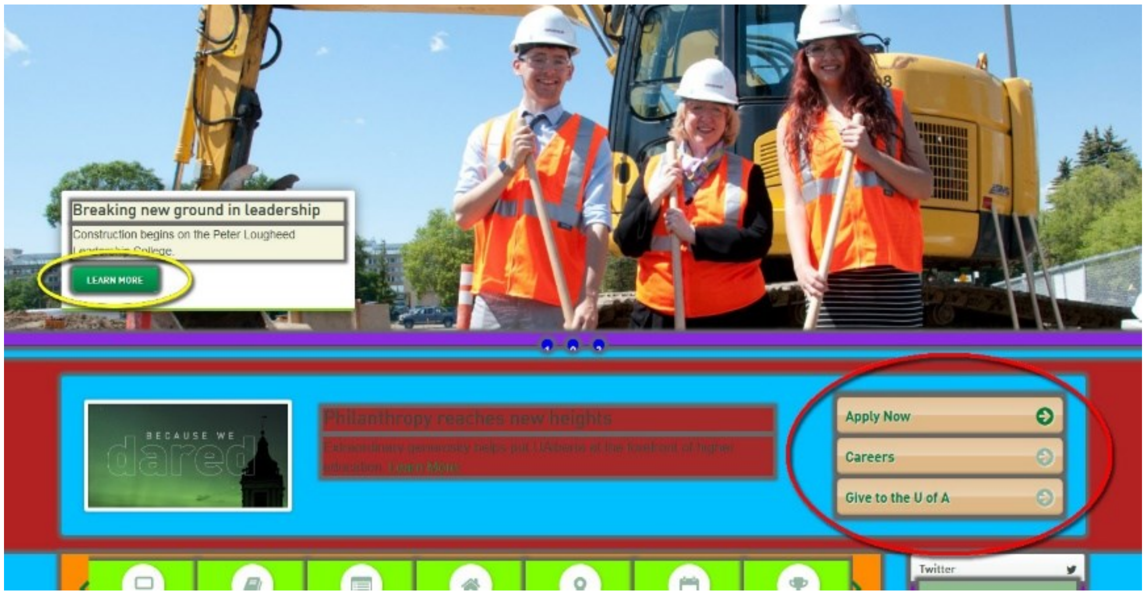
Breaking new ground in leadership
Construction begins on the Peter Lougheed Leadership College.
LEARN MORE
BECAUSE WE dared
Philanthropy reaches new heights
Apply Now
Careers
Give to the U of A
Twitter

Figure 2.5 Disagreement in GLM Blocks Identification Results

2) There are "hidden" blocks. This is actually because the background colors and shadow borders of these blocks are overlapped by their upper blocks, hence the view of these blocks was obscured. An example from **Figure 2.4**b is the block holding the three buttons at the right side of the middle area (red ellipse in **Figure 2.5**) – the buttons were identified as a block and marked (actually their parent layer was marked) with background color and shadow borders, however it was very

difficult to view due to its obscuration. Such human errors are less than 5% among the five volunteers' ratings, but contribute to the second largest category of deviations.

Results in **Table 2.3** provide strong evidence that even human "experts" are less than perfect when undertaking this task, and hence it is clearly a demanding task for an automated system.

Table 2.3 κ of two raters' evaluations

Raters		**GLM**				**VIPS**			
A	**B**	TP	FP	FN	**Overall**	TP	FP	FN	**Overall**
1	2	0.5746	0.9136	0.9475	0.6270	0.7137	0.7934	0.8977	0.7689
1	3	0.5106	0.9167	0.9320	0.5715	0.7384	0.7630	0.9045	0.7710
1	4	0.5319	0.9136	0.9320	0.5895	0.7662	0.7731	0.8807	0.7850
1	5	0.5000	0.9044	0.9351	0.5618	0.7416	0.7832	0.8943	0.7785
2	3	0.5267	0.9229	0.9475	0.5868	0.6708	0.7596	0.8840	0.7335
2	4	0.5534	0.9198	0.9413	0.6089	0.6770	0.7494	0.8841	0.7329
2	5	0.5028	0.9044	0.9444	0.5648	0.6523	0.7527	0.8670	0.7194
3	4	0.5374	0.9259	0.9567	0.5968	0.6771	0.7358	0.8705	0.7260
3	5	0.5161	0.9013	0.9413	0.5757	0.6801	0.7596	0.8841	0.7381
4	5	0.5373	0.9136	0.9444	0.5949	0.6925	0.7630	0.9011	0.7479

Table 2.4 shows the interpretations of the κ value (Landis and Koch 1997). From the table, the GLM's overall κ values between every two raters' rates are all in a moderate level ($\kappa > 0.5$) while VIPS' overall κ values all in a substantial level ($\kappa > 0.7$). Such agreement is equivalent to many works reporting inter-rate reliability statistics on complex visual and medical classification problems (Pereira, et al. 2009; Hauzeur, et al. 1999; Unwin 1998; Tewarie, et al. 2012; Albrecht, et al. 2012) and hence it is considered sufficient for the task. Therefore, we can infer that the five raters all agreed with each other.

Table 2.4 κ interpretation

κ	Strength of agreement
0.00 ~ 0.20	Slight
0.21 ~ 0.40	Fair
0.41 ~ 0.60	Moderate
0.61 ~ 0.80	Substantial
0.81 ~ 1.00	Almost perfect

5.2.3 Evaluation Results

By testing the precisions, recalls and F-1 scores of the two algorithms on the 381 web page samples, we conclude that GLM is more accurate than VIPS. Each of the five volunteers' rates as well as an average of these rates are evaluated. The evaluation results are shown in **Table 2.5**.

Table 2.5 Average precision, recall and F-1 score of both algorithms

Volunteers	GLM			VIPS		
	Precision	Recall	F-1 Score	Precision	Recall	F-1 Score
1	90.55%	90.87%	90.40%	65.79%	67.98%	63.80%
2	90.55%	90.88%	90.40%	65.87%	68.01%	63.87%
3	90.48%	90.79%	90.30%	65.80%	67.93%	63.79%
4	90.49%	90.84%	90.34%	65.69%	68.01%	63.76%
5	90.50%	90.86%	90.36%	65.77%	67.93%	63.79%
Average	90.53%	90.85%	90.37%	65.79%	67.98%	63.81%

As can be seen from **Table 2.5**, each volunteer produces results which are very similar to each other (errors within 1% and standard deviations within 0.001), providing a high degree of confidence that the results are independent of the volunteers and their performance. It clearly shows that GLM outperforms VIPS in every situation – the average GLM precision of the test samples is 90.53%, which is 24.74% better than VIPS. Meanwhile, GLM provides a high recall rate of 90.85% and a high F-1 score of 90.37% – 22.87% and 26.56% higher than VIPS, respectively.

Figure 2.6 shows the box plots of all the results, where "P" denotes precision, "R" denotes recall, and "F" denotes F-1 score. Visually we can conclude that the GLM distributions, for each of the three evaluation metrics, are clearly superior to its VIPS equivalent. In addition, if we look at the plots more closely:

1) Although both algorithms can identify samples with highest average precision (**Figure 2.6**e) as 100%, GLM's lowest precision is 56.45% (volunteer 2) and lowest average precision is 58.72% (both for "www.reddit.com") while VIPS' lowest average precision is 0% (18 samples). VIPS' lowest non-zero precision is 1.14% (volunteer 5) and lowest non-zero average precision is 1.21% ("www.y8.com").
2) The median of GLM's average precision, recall and F-1 score are 92.13%, 91.49% and 91.09% (**Figure 2.6**f), respectively, meaning that more than half of the results are over 91%. On contrary, VIPS provides the average precision, recall and F-1 score with medians of 74.68%, 74.19% and 72.08%, respectively.
3) The first quartile of GLM's average precision is 86.36% while the third quartile is 95.63%, meaning GLM can guarantee that more than half of its results have average precision within the range between 87% and 95%. The first and third quartiles of VIPS' precision are 42.86% and 100%, which is a much wider range. This shows that although VIPS can provide some better samples, it also provides many poorer samples than GLM.

From the data, we can find that the GLM algorithm works better than VIPS in general. The reason lies on the fact that the GLM model interprets most of the Gestalt laws of grouping to simulate a human's mechanism of perception, while VIPS relies mainly on visual of web pages to identify blocks. As modern web pages evolve, layouts are no longer as simple as ten years ago and the visual separators are much less obvious.

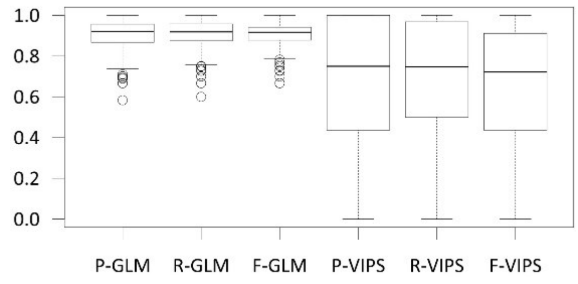

(a) Volunteer 1

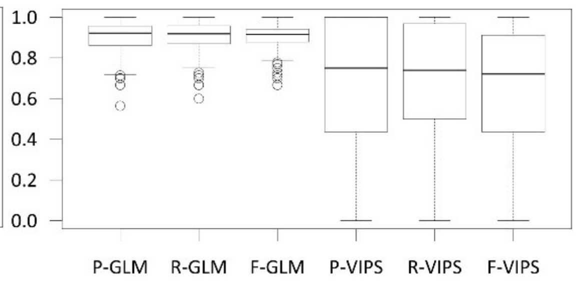

(b) Volunteer 2

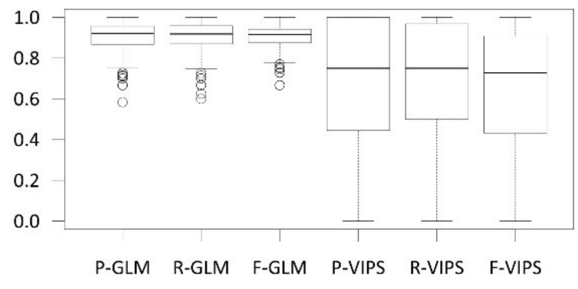

(c) Volunteer 3

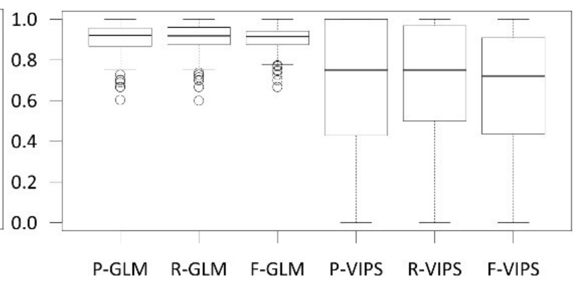

(d) Volunteer 4

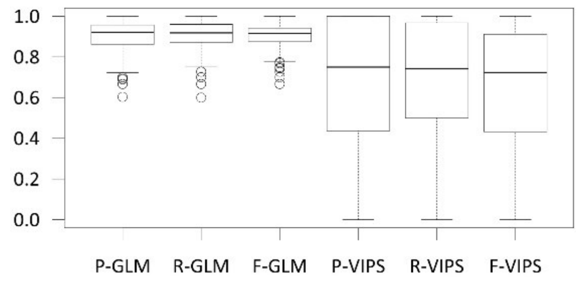

(e) Volunteer 5

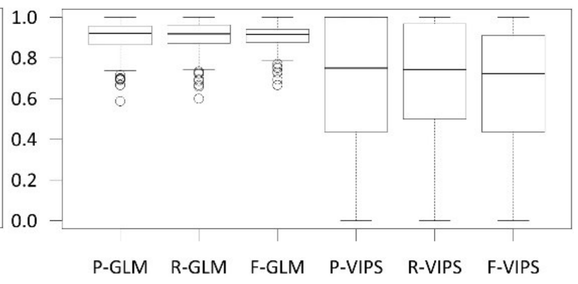

(f) Average

Figure 2.6 Evaluations of GLM and VIPS on the Test Set

6 Conclusions

This chapter proposes a web page semantic block identification algorithm utilizing the Gestalt laws of grouping, and applies two experiments to evaluate its efficiency. The GLM model consists of three components: the layer tree builder, the Gestalt law translator, and the web page blocks identifier. The layer tree builder produces input data to the Gestalt laws translator. It extracts visible DOM elements into layer nodes and builds the layer tree from DOM tree of the web page by fixing the hierarchical inconsistency. The Gestalt laws translator, the core component of the GLM model, interprets four of the major Gestalt laws of grouping. The web page blocks identifier combines each interpreted law into a unified law, applies it to the layer tree to obtain the semantic blocks, and finally feedbacks the blocks to both the original web page and the local database.

Two groups of experiments are conducted to evaluate the efficiency of the model by comparing with the VIPS algorithm. The first group runs two test cases to compare the two algorithms' identification results. The outcomes show that the GLM model generates more "true positives" and less "false negatives" than VIPS, which means that the VIPS does not perform well on modern rich format web pages. The second group tests home pages of the world's top 500 websites. Five volunteers are recruited to evaluate the identification results manually. Three metrics have been calculated by collecting their evaluations, namely, precision, recall and F-1 score. The testing results clearly demonstrates that the GLM model is superior to VIPS:

- GLM has higher precision, recall and F-1 score than VIPS;
- Medians of the GLM precisions and recalls are both higher than those of VIPS; and
- GLM provides steadier and higher distributions of precisions and recalls than VIPS.

Acknowledgement

The authors give thanks to China Scholarship Council (CSC) for their financial support.

References

Albrecht, P., M¨uller, A.-K., Ringelstein, M., Finis, D., Geerling, G., Cohn, E., Aktas, O., Hartung, H.-P., Hefter, H., Methner, A., 2013. Retinal neurodegeneration in wilsons disease revealed by spectral domain optical coherence tomography. In: Neurology. Vol. 80. Lippincott Williams & Wilkins 530 WALNUT ST, PHILADELPHIA, PA 19106-3621 USA.

Baluja, S., 2006. Browsing on small screens: recasting web-page segmentation into an efficient machine learning framework. In: Proceedings of the 15th international conference on World Wide Web. ACM, pp. 33–42.

Cai, D., Yu, S., Wen, J.-R., Ma, W.-Y., 2003a. Extracting content structure for web pages based on visual representation. In: Asia-Pacific Web Conference. Springer, pp. 406–417.

Cai, D., Yu, S., Wen, J.-R., Ma, W.-Y., 2003b. Vips: a vision-based page segmentation algorithm.

Canny, J., 1986. A computational approach to edge detection. IEEE Transactions on pattern analysis and machine intelligence (6), 679–698.

Cao, J., Mao, B., Luo, J., 2010. A segmentation method for web page analysis using shrinking and dividing. International Journal of Parallel, Emergent and Distributed Systems 25 (2), 93–104.

Chakrabarti, D., Kumar, R., Punera, K., 2008. A graph-theoretic approach to webpage segmentation. In: Proceedings of the 17th international conference on World Wide Web. ACM, pp. 377–386.

Chaudhuri, B. B., Rosenfeld, A., 1999. A modified hausdorff distance between fuzzy sets. Information Sciences 118 (1), 159–171.

Cilibrasi, R. L., et al., 2007. Statistical inference through data compression.

Cohen, J., 1960. A coefficient of agreement for nominal scales. Educational and psychological measurement 20 (1), 37–46.

Connolly, C., Fleiss, T., 1997. A study of efficiency and accuracy in the transformation from rgb to cielab color space. IEEE Transactions on Image Processing 6 (7), 1046–1048.

Gupta, S., Kaiser, G., Neistadt, D., Grimm, P., 2003. Dom-based content extraction of html documents. In: Proceedings of the 12th international conference on World Wide Web. ACM, pp. 207–214.

Gwet, K. L., 2014. Handbook of inter-rater reliability: The definitive guide to measuring the extent of agreement among raters. Advanced Analytics, LLC.

Hattori, G., Hoashi, K., Matsumoto, K., Sugaya, F., 2007. Robust web page segmentation for mobile terminal using content-distances and page layout information. In: Proceedings of the 16th international conference on World Wide Web. ACM, pp. 361–370.

Hauzeur, J., Mathy, L., De Maertelaer, V., 1999. Comparison between clinical evaluation and ultrasonography in detecting hydrarthrosis of the knee. The Journal of rheumatology 26 (12), 2681–2683.

Johnson, G. M., Fairchild, M. D., 2003. A top down description of s-cielab and ciede2000. Color Research & Application 28 (6), 425–435.

Kang, J., Yang, J., Choi, J., 2010. Repetition-based web page segmentation by detecting tag patterns for small-screen devices. IEEE Transactions on Consumer Electronics 56 (2).

Koffka, K., 2013. Principles of Gestalt psychology. Vol. 44. Routledge.

Kohlsch¨utter, C., Nejdl, W., 2008. A densitometric approach to web page segmentation. In: Proceedings of the 17th ACM conference on Information and knowledge management. ACM, pp. 1173–1182.

Landis, J. R., Koch, G. G., 1977. The measurement of observer agreement for categorical data. biometrics, 159–174.

Li, M., Chen, X., Li, X., Ma, B., Vit´anyi, P. M., 2004. The similarity metric. IEEE transactions on Information Theory 50 (12), 3250–3264.

Lin, S.-H., Ho, J.-M., 2002. Discovering informative content blocks from web documents. In: Proceedings of the eighth ACM SIGKDD international conference on Knowledge discovery and data mining. ACM, pp. 588–593.

Liu, H. X., Wu, B., Liu, Y., Huang, M., Xu, Y. F., 2013. A discussion on printing color diffierence tolerance by ciede2000 color diffierence formula. In: Applied Mechanics and Materials. Vol. 262. Trans Tech Publ, pp. 96–99.

Luo, M. R., Cui, G., Rigg, B., 2001. The development of the cie 2000 colour-diffierence formula: Ciede2000. Color Research & Application 26 (5), 340–350.

McCallum, A., Nigam, K., et al., 1998. A comparison of event models for naive bayes text classification. In: AAAI-98 workshop on learning for text categorization. Vol. 752. Madison, WI, pp. 41–48.

Palmer, S. E., 1990. Modern theories of gestalt perception. Mind & Language 5 (4), 289–323.

Pereira, A. C., Eggertsson, H., Martinez-Mier, E. A., Mialhe, F. L., Eckert, G. J., Zero, D. T., 2009. Validity of caries detection on occlusal surfaces and treatment decisions based on results from multiple caries-detection methods. European journal of oral sciences 117 (1), 51–57.

Reis, D. d. C., Golgher, P. B., Silva, A. S., Laender, A., 2004. Automatic web news extraction using tree edit distance. In: Proceedings of the 13th international conference on World Wide Web. ACM, pp. 502–511.

Roshanbin, N., Miller, J., 2011. Finding homoglyphs-a step towards detecting unicode-based visual spoofing attacks. Web Information System Engineering–WISE 2011, 1–14.

Sharma, G., Wu, W., Dalal, E. N., 2005. The ciede2000 color-diffierence formula: Implementation notes, supplementary test data, and mathematical observations. Color Research & Application 30 (1), 21–30.

Sim, D.-G., Kwon, O.-K., Park, R.-H., 1999. Object matching algorithms using robust hausdorff distance measures. IEEE Transactions on image processing 8 (3), 425–429.

Song, R., Liu, H.,Wen, J.-R., Ma,W.-Y., 2004. Learning block importance models for web pages. In: Proceedings of the 13th international conference on World Wide Web. ACM, pp. 203–211.

Sternberg, R. J., Sternberg, K., 2016. Cognitive psychology. Nelson Education.

Tewarie, P., Balk, L., Costello, F., Green, A., Martin, R., Schippling, S., Petzold, A., 2012. The oscar-ib consensus criteria for retinal oct quality assessment. PloS one 7 (4), e34823.

Unwin, N., Alberti, K., Bhopal, R., Harland, J., Watson, W., White, M., 1998. Comparison of the current who and new ada criteria for the diagnosis of diabetes mellitus in three ethnic groups in the uk. Diabetic medicine 15 (7), 554–557.

Yu, S., Cai, D., Wen, J.-R., Ma, W.-Y., 2003. Improving pseudo-relevance feedback in web information retrieval using web page segmentation. In: Proceedings of the 12th international conference on World Wide Web. ACM, pp. 11–18.

Zhao, C., Shi, W., Deng, Y., 2005. A new hausdorff distance for image matching. Pattern Recognition Letters 26 (5), 581–586.

CHAPTER 3 Estimating Similarity of Rich Internet Pages Using Visual Information[5]

Abstract

Traditional text-based web page similarity measures fail to handle rich-information-embedded modern web pages. Current approaches regard web pages as either DOM trees or images. However, the former only focuses on the web page structure, while the latter ignores the inner connections among different web page features. Therefore, they are not suitable for modern web pages. Hence, the idea of a block tree is introduced, which contains both structural and visual information of web pages. A visual similarity measurement is proposed as the edit distance between two block trees. Finally, an experiment is undertaken, by cross-comparing 500 web pages, illustrating that the model appears to be highly accurate, empirically demonstrating that the measurement is highly promising.

Keywords: Block Tree; Gestalt Laws of Grouping; Normalised Compression Distance; Tree Edit Distance; Web Page Classification.

1 Introduction

Recent years have witnessed a rapid development of the Internet, which brings about huge changes in people's daily life through the interaction with web sites. As a matter

5 Xu, Zhen, and James Miller. "Estimating Similarity of Rich Internet Pages Using Visual Information". Accepted by International Journal of Web Engineering and Technology on May 2017.

of fact, web pages have become an important tool and indispensable part of our life. For example, people read web pages to obtain the news or information they are interested in, get service through online systems from service providers (such as banking and socialising), or conduct e-business. Therefore, similarity analysis of web pages is essential and has a widespread automation application. First, it can serve as a preliminary task such as in an anti-phishing process, i.e., through detecting similar web pages, the search scope of potential phishing sites can be decreased to some extent. Second, it can perform version control and evolution of web pages. Web pages evolve very fast, and the similarity analysis provides a method to detect changes and adopt relevant control policies if necessary. Third, it can be used for software testing. For robust software, the page should be able to response correctly and display relevant information upon a user's input. We can detect whether the software functions correctly by comparing the actual page and the target page.

Due to its importance, web page similarity analysis has drawn the attention of many researchers. However, there are still some issues, which mainly result from the fact that modern web pages, with much more abundant information such as images and streaming media, present additional challenges to web page classification (Wei, et al. 2014). Hence, traditional approaches that rely heavily on textual content cannot handle modern web pages. From the observation of human behaviours, we found that no matter how complicated web pages are, people always have the ability of recognising and correlating content at a first glance. The theory behind it is that humans can read the visual information directly, rather than through the understanding of the textual content. Users do not examine web page details, but rather the layout and design of the page to create a single impression. This is analogous to the idea of "super signals" (Dörner 1996), a theory to account for human decision making under time constraints and massive numbers of stimuli. Dörner argues that humans collapse a number of features into a single composite impression. This thinking pattern presents us with an interesting question: if the computer can think, can they detect similarity more precisely? The answer is obvious, but the next question is how can we achieve this goal? The Gestalt laws of grouping summarise the characteristics of people's thinking patterns. We believe that the laws can be a potential way to introduce human-based analysis into the study of visual similarity. Therefore, in this chapter, we will investigate web page similarity from the visual perspective by using Gestalt laws of grouping. Our major contributions in this chapter are:

- We develop a data structure to represent web pages based on the Gestalt laws of grouping.
- We propose a model to evaluate the similarity of rich web pages according to a tree edit distance.

The rest of this chapter is organised as follows: in Section 2, we review the related work, and provide background on currently used classification methods; section 3 introduces the concept of the block tree, and puts forward an approach to interpret and apply the Gestalt laws of grouping; in Section 4, we come up with a visual similarity measurement and a classification model which exploits this measurement; section 5 prepares the test sets, outlines the experimental methodology, performs the experiment on aforementioned test sets, and analyse the outcomes; to finish, we summarise and conclude this chapter's contributions in Section 6.

2 Related Work

In general, two major orientations are widely applied including treating web pages as images or trees, to explore web page visual similarity.

In the first category, a web page is abstracted as an image before computing their similarities. Recently, many scholars have focused their study on image similarity (Chechik, et al. 2010; Rohlfing 2012). A feature-based image similarity measurement approach uses image phase congruency measurements to compute the similarities between two images (Liu and Laganière 2007). Kwitt et al. (2008) present an image similarity model by using Kullback-Leibler divergences between complex wavelet sub band statistics for texture retrieval. Sampat et al. (2009) put forward an image similarity method called the complex wavelet structural similarity. The theory behind it is that consistent phase changes in the local wavelet coefficients may arise owing to certain image distortions. Image similarity techniques are popular and have made some progress in web page similarity, for example, Saar et al. (2015) proposed a classification model for cross-browser testing based on image similarity. However, we found that a specified web page is an object embedded with a variety of elements and these elements can interact (such as overlap or partly overlap) with each other. Image similarity cannot reveal this interaction among elements. It is, therefore, a different problem from pure image similarity assessment.

In the other category, a web page is regarded as tree structured data, and thus web page similarity is studied through investigating tree similarity. With respect to tree structured data, a handful of tree distance functions are applied, such as tree edit distance (Shahbazi and Miller et al. 2014), multisets distance (Müller-Molina et al. 2009), entropy distance (Connor, et al. 2011), and path distance (Buttler 2004). The tree edit distance is defined as the minimum cost of operations for transferring one tree to another (Cording and Lyngby 2011). Tree edit distances can be further divided into different sub-categories in terms of distinct mapping constraints including top-down, bottom-up, isolated subtree, etc. (Zhai and Liu 2006). Müller-Molina et al. (2009) propose a tree distance function with multisets, which are sets that allow repetitive elements. Based on multiset operations, they define a similarity measure for multisets. They achieve this by converting a tree into two multisets, with one multiset including complete subtrees and another consisting of all the nodes without children. Connor et al. (2011) develop a bounded distance measurement for comparing tree structure based on Shannon's entropy equations. Buttler (2004) analyses the drawbacks of tree edit distance similarity, tag similarity, and Fourier transform similarity. Then he proposes path similarity to measure the similarity of the document tree between two distinct documents. Although the above achievements on tree similarity are significant, the theory cannot be used directly on web page similarity research. The main reason is that the theme of tree similarity has always been structural similarity. However, our focus is on content similarity, in spite the obvious connection between structural and content similarity.

Web page classification is an important topic relevant to web page similarity analysis. Hernández et al. (2014) explore a classification method based on URLs and develop an algorithm to produce URL-based web page classifiers that are used to perform enterprise web page classification. Onan (2015) combine various classifiers to enhance existing classification models by investigating different feature selection algorithms, ensemble approaches, and classification methods. Lee et al. (2015) introduced a simplified swarm optimization (SSO) algorithm for the purpose of obtaining the best weights for each feature in their data training process such that they can use the best weights in classifying the new web pages.

3 The Block Tree

Two major ways to represent a web page for visual similarity evaluation are the screen shot image and the DOM tree. The former holds all visible details, but fails to preserve the hierarchical clues. Although the later contains both visible and invisible details, the invisible details have no contribution to visual similarity. This chapter combines the advantages of the above two methods and proposes a new web page representation method, which is referred to as the block tree. It extracts only visible DOM elements and merges these elements into separate groups according to their semantic meanings.

Definition 1 (Block Tree): Given a web page WP, the *block tree* BT of WP is a finite set of nodes, where each node n (that is, the *block*) indicates a group of semantically related visible elements E from the DOM tree DT of WP ($BT = \{n|n \leftarrow E, E \subset DT\}$) and all the blocks follow the visual hierarchy of WP.

To construct blocks, we merge separate *render objects* into semantically related groups based on the Gestalt laws of grouping (Koffka 1955).

Definition 2 (Render Object): Given a web page WP, the *render object* maps to a visible DOM element e of the DOM tree DT of WP. The object contains all visible CSS properties of e as the *visual features* and serves as the merging candidates to build the blocks of the block tree BT.

According to the above definitions, only the visible DOM elements are considered and the invisible DOM elements are ignored during the construction of the blocks. The visual features of a render object refer to its geometric properties (left, top, width, and height) and all visible CSS properties. Note that invisible CSS properties, such as "`margin`" or "`padding`", are not included. This is because they do not include any visual information of the web page. In addition, the semantic meaning of the text is not included, owing to their weak effect on the web page visual similarity. For example, two pieces of text with the same meaning but written in different languages will be recognised as different text by way of comparing textual strings, but will be regarded as the same text if using the semantic meaning as the criteria.

3.1 Construction of Blocks by Gestalt Laws of Grouping

The Gestalt laws of grouping explain a human's mechanism for perception. To construct each block for the block tree, these laws need to be translated into computer compatible rules (Stevenson 2012; Xu and Miller 2015).

- The Gestalt law of simplicity indicates that humans tend to organise objects into the simplest representation. In a web page, the simplest representation of content are the DOM elements. Taking "google.ca" as an example, **Figure 3.1** shows its home page. In the figure, the middle image above the search box contains multiple elements (i.e., the text "GOOGLE" is the title and the three columns are the texts, images, and animations, respectively). However, when we read the whole web page, we treat it as one entire image rather than several separated ones. As such, to interpret this law, we consider the render object which maps to the DOM element as the smallest unit, and it cannot be further split.

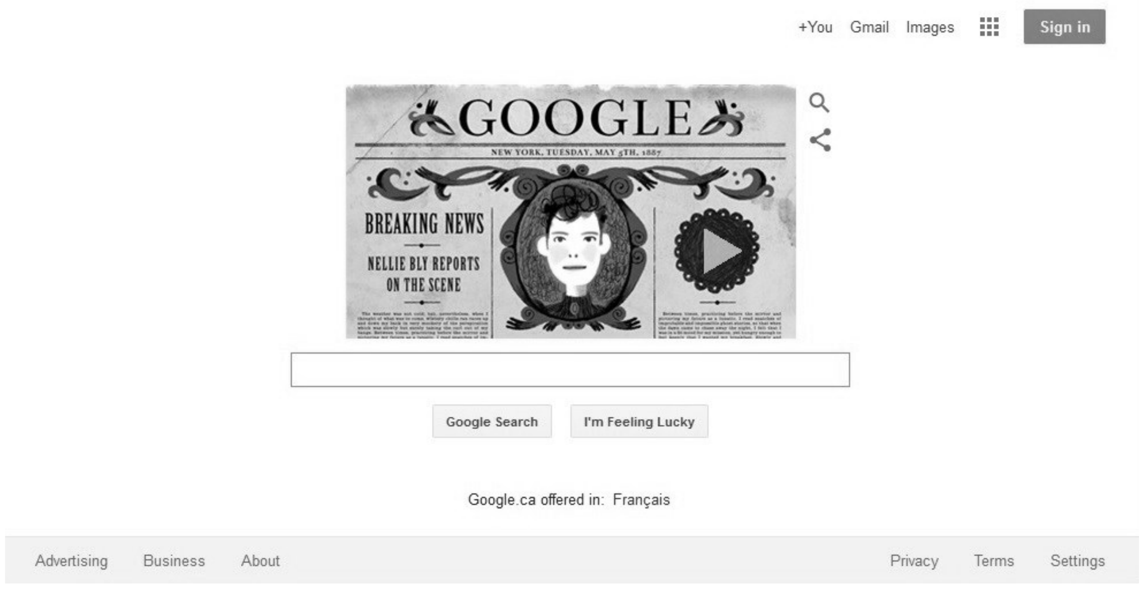

Figure 3.1 Home Page of "Google.ca"

- The Gestalt law of closure states that humans tend to perceive incomplete shapes as complete ones. Because child DOM elements overlap their parent elements, many of the render objects are not completely shown in the final web page. For example, in **Figure 3.2** (the home page of "twitter.com"), the upper right part of the background image is covered by two log-in boxes, but they are not regarded as two holes. Instead, our minds still believe the background image is complete. That is, the render object remains as a complete rectangle. Herein, we construct all render objects as complete rectangles rather than irregular shapes according to this law.

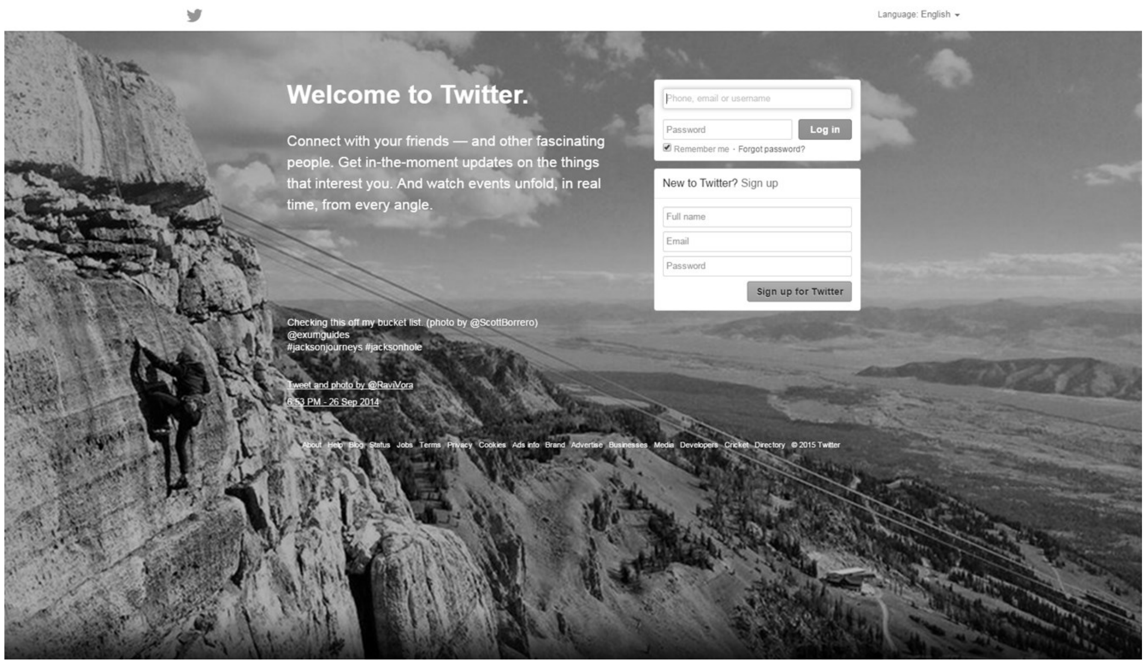
Welcome to Twitter.

Connect with your friends — and other fascinating people. Get in-the-moment updates on the things that interest you. And watch events unfold, in real time, from every angle.

Checking this off my bucket list. (photo by @ScottBorrero) @exumguides #jacksonjourneys #jacksonhole

Tweet and photo by @RaviVora

6:53 PM - 26 Sep 2014

Language: English
Phone, email or username
Password
Log in
Remember me · Forgot password?
New to Twitter? Sign up
Full name
Email
Password
Sign up for Twitter
About Help Blog Status Jobs Terms Privacy Cookies Ads info Brand Advertise Businesses Media Developers Cricket Directory © 2015 Twitter

Figure 3.2 Home Page of "Twitter.com"

- The Gestalt law of proximity illustrates that humans tend to group close objects together while separate distant objects apart. Based on this law, we merge render objects into different blocks by distance. In a series of render objects, if any pair of siblings have a larger distance than others, they should be put into separate groups. For example, as shown in **Figure 3.3**a, the top two objects are grouped together, the third and the fourth objects from the top are put into a second group, and the bottom object belongs to a third group. The dimensions of the render objects, compared with the gap, are commonly significant in web pages, so it cannot be ignored in calculating the proximity. The Hausdorff distance (HD) (Huttenlocher 1993; Dubuisson and Jain 1994; Chaudhuri and Rosenfeld 1999) takes the dimensions into consideration, but it is not precise enough. Therefore, the normalised Hausdorff distance (NHD), a variant of HD, is proposed. The details are discussed in Section 3.3.

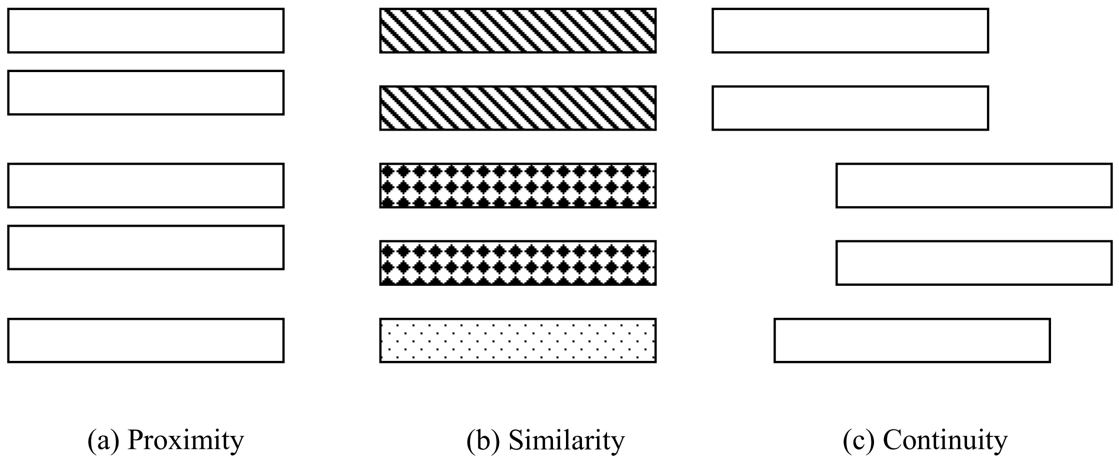

Figure 3.3 Gestalt Laws of Proximity, Similarity and Continuity

- The Gestalt law of similarity describes that humans perceive similar objects as a single group. Similarity among render objects includes background similarity, foreground similarity (text similarity) and size similarity. Meanwhile, it is evaluated by the visual features. Note that shape similarity is not considered because all the render objects are complete rectangles. In a series of render objects, if anyone has a different similarity value, then it belongs to a different group from the others. As shown in **Figure 3.3**b, the five objects are grouped into three groups in terms of styles. Specifically, the top two objects are in one group, the next two objects are included in a second group, and the bottom one belongs to a third group. In colour and image similarity comparison, it is not correct to simply compare the CSS value string. Instead, we compare the actual colour and image difference. The details are discussed in Section 3.4 and 3.5.
- The Gestalt law of continuity indicates that humans tend to group together objects that are aligned. This law is straightforward during the translation: if any render

object is not aligned with its siblings, then it belongs to a different group. So according to **Figure 3.3**c, the five objects are split into three groups, namely the top two, the next two, and the bottom one.

- The Gestalt law of common fate argues that humans are prone to include the objects with the same motion trend in the same group. However, once a web page is fully loaded, the major factor that causes web page motion is the "scrolling behaviour". As such, we only consider the scrolling behaviour as the motion trend. When the user scrolls the page, all the content will scroll accordingly. If any render object does not scroll in the same way with its siblings, then it belongs to a different group. For example, the lower banner marked by the black ellipse in **Figure 3.4**(the home page of "ubuntu.com") always hangs at the bottom even when the use scrolls the page, so its scrolling behaviour is not consistent with others. This kind of behaviour can be verified by the CSS property "position".
- The Gestalt law of symmetry illustrates humans' tendency of perceiving symmetric objects as a single group, even when they are far from each other. This law rarely appears in web pages; hence we will omit it from the discussion in the chapter.
- The Gestalt law of past experience indicates that humans tend to interpret objects according to the past experience. This law requires a higher level of cognations which does not belong to the field of web page analysis, so we will omit this law as well.

Among all the above six Gestalt laws, the first two shows us how to extract render objects from the DOM tree, and the remaining four regulates the way of merging the extracted render objects into groups (that is, the blocks in the block tree) by the visual features.

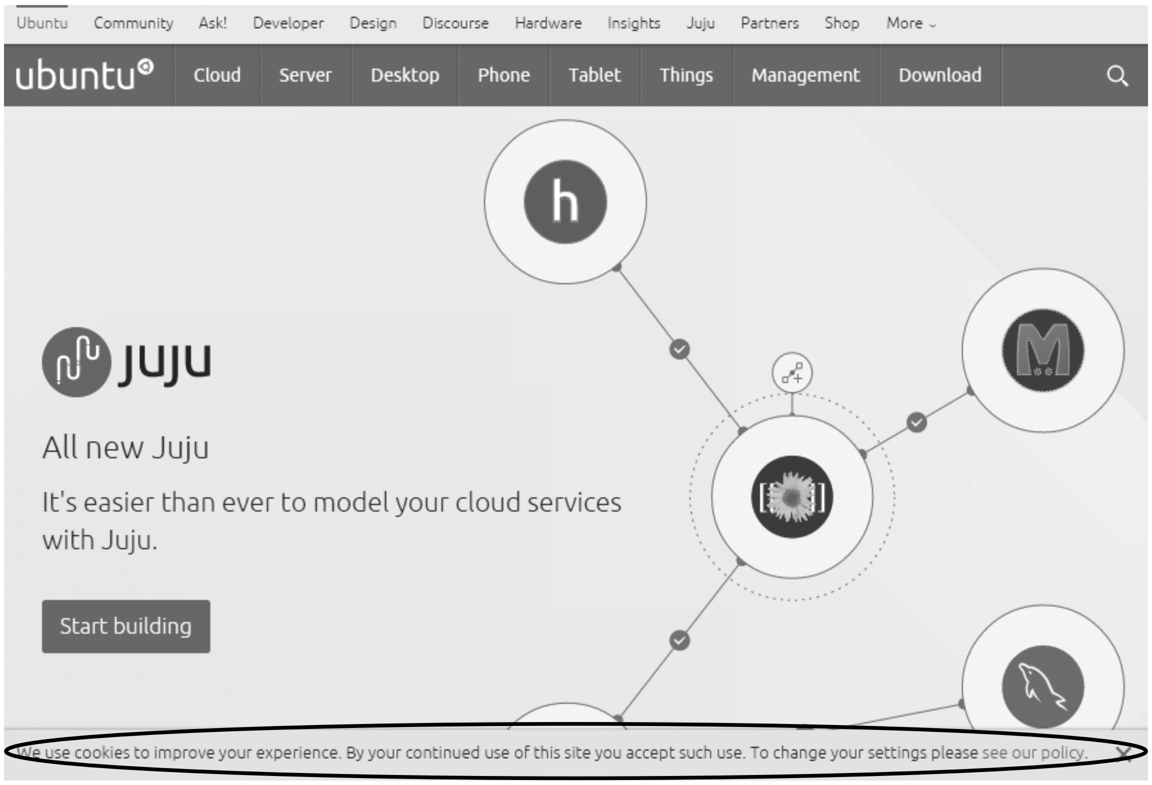
Ubuntu
Community
Ask!
Developer
Design
Discourse
Hardware
Insights
Juju
Partners
Shop
More
ubuntu
Cloud
Server
Desktop
Phone
Tablet
Things
Management
Download
juju
All new Juju
It's easier than ever to model your cloud services with Juju.
Start building
We use cookies to improve your experience. By your continued use of this site you accept such use. To change your settings please see our policy.

Figure 3.4 Home Page of “Ubuntu.com”

3.2 Construction of the Block Tree

The block tree takes the previously merged blocks as tree nodes, and follows the DOM tree’s hierarchy to organise these nodes. At the beginning, the first visible DOM element is the “BODY”, so the root node of the block tree will be a block that holds it. Although sometimes a BODY is invisible, the page will still be drawn by the browser on a white background, leaving the transparent BODY visible. Next, we follow the bottom up rule. From the root block onwards, all the direct child render objects of a block are evaluated by the Gestalt laws and split into one or more groups. Each of the laws are then applied to create a block. These blocks will maintain their hierarchy in the DOM tree.

However, if a DOM element is invisible but its direct children are visible, then the parent of the children's corresponding blocks will all point to the parent block of the invisible DOM element.

3.3 Hausdorff Distance and Normalised Hausdorff Distance

The HD between two render objects R_1 and R_2 can be calculated by (3-1) and (3-2) following the two steps.

1) Hausdorff distance from R_1 to R_2 refers to the maximum value of all distances from any point r_1 in R_1 to its nearest point in R_2:

$$hd(R_1, R_2) = \sup_{r_1 \in R_1} \inf_{r_2 \in R_2} \|r_1 - r_2\| \,, \tag{3-1}$$

   where, R_1 and R_2 are the two render objects; r_1 and r_2 refer to any points in R_1 and R_2, respectively; sup and inf calculate the maximum and minimum value of a given set, respectively; and $\|r_1 - r_2\|$ calculates the Euclidian distance between r_1 and r_2.

2) Hausdorff distance between R_1 and R_2 refers to the maximum value of all distances from any point in a render object to its nearest point in the other render object:

$$HD(R_1, R_2) = \max\{hd(R_1, R_2), hd(R_2, R_1)\} \,. \tag{3-2}$$

As shown in **Figure 3.5**, R_1 and R_2 are two squares both of the size 50×50 and share a same vertical side; R_3 and R_4 are another two squares both of the sized 10×10, and their bottom sides are in the same line while the horizontal distance between their closest vertical sides are 40. According to (1), $hd(R_1, R_2)$ equals to 50, which is the distance between a_1 and its nearest point in R_2 (that is, a_2). Similarly, $hd(R_2, R_1)$, $hd(R_3, R_4)$ and $hd(R_4, R_3)$ equals to the distance between d_2 and d_1, a_3 and a_4, d_4 and d_3, respectively. Therefore, according to (2), both $HD(R_1, R_2)$ and $HD(R_3, R_4)$ are 50.

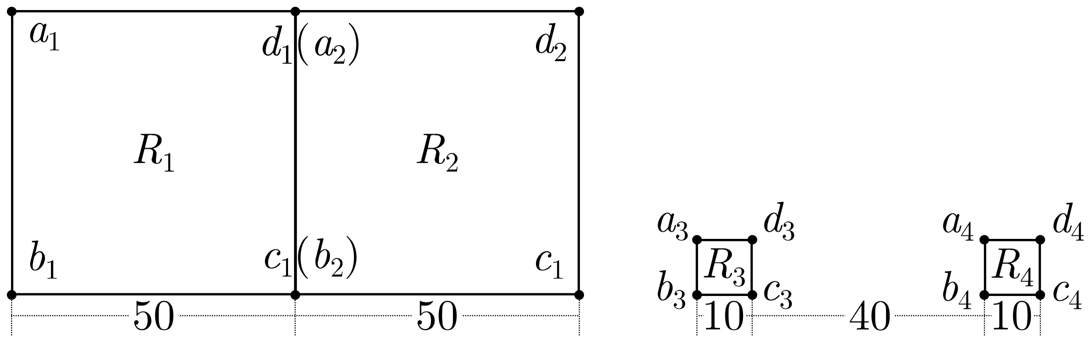

Figure 3.5 HD Inconsistency

In the above example, it seems that the first pair of squares looks closer to each other than the second pair. However, their HDs are the same. Therefore, using HD as the proximity measurement will cause contradictions and inaccuracies. In fact, this paradox is caused by the dimensions of the render objects. Hence, it can be eliminated by normalising the value of HD. By doing this, we obtain the *normalised HD*, which is denoted by NHD. When a render object is located inside of another render objects, its NHD is 0; otherwise it is the maximum of the normalised hd, as shown in (3-3):

$$NHD(R_1, R_2) = \max\left\{\frac{hd(R_1,R_2)}{d_{R_1}}, \frac{hd(R_2,R_1)}{d_{R_2}}\right\}, \tag{3-3}$$

where, d_{R_1} is the dimension of render object R_1, and $d_{R_2}$is the dimension of render object R_2.

The dimension varies according to the relative position of the two render objects. An example is illustrated in **Figure 3.6**. To determine d_{R_0} , we split the surrounding region of R_0 by the dashed lines. R_1 is inside of R_0, while R_2, R_3 and R_4 cover the north, west, and corner regions of R_0, respectively. In this circumstance, $NHD(R_0, R_1)$ is equal to 0; when calculating the values of $hd(R_0, R_2)$, $hd(R_0, R_3)$, and $hd(R_0, R_4)$, d_{R_0} represents the height, width, and diagonal of R_0, respectively.

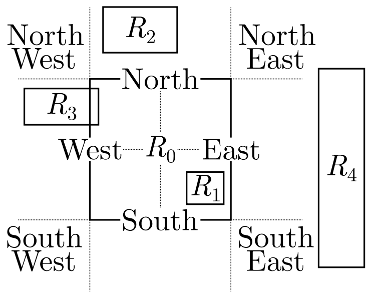

Figure 3.6 NHD Dimensions

3.4 Colour Translation and Colour Difference

In spite of RGB colour space being adopted by most web pages, it is difficult to define a universally acceptable RGB colour difference. On the other hand, the CIE-Lab colour space has provided a standard colour difference solution – the ΔE_{00} (Luo et al. 2001; Sharma, et al. 2005), as shown in (3-4):

$$\Delta E_{00} = \sqrt{\left(\frac{\Delta L^*}{k_L S_L}\right)^2 + \left(\frac{\Delta C^*}{k_C S_C}\right)^2 + \left(\frac{\Delta H^*}{k_H S_H}\right)^2 + R_T \left(\frac{\Delta C^*}{k_C S_C}\right)\left(\frac{\Delta H^*}{k_H S_H}\right)}\,, \qquad (3\text{-}4)$$

where, ΔL^*, ΔC^* and ΔH^* are the lightness, chroma and hue differences, respectively; S_L, S_C and S_H are the weighting functions of the lightness, chroma and hue components, respectively; k_L, k_C and k_H are the parametric factors; and R_T is the interactive term between the hue and chroma differences.

Colours can be converted from RGB space to CIE-Lab space. Once the conversion is completed, a threshold for distinguishing the two colours is necessary. Liu et al. have studied the concept of what constitutes two different colours via extensive experimentation; they have concluded that a threshold can be set to 3.30 (2013) to distinguish between two colour samples. Therefore, we use their value to identify our colour similarity.

3.5 Image Similarity Comparison

The browser parses the HTML and CSS before applying them in a web page, but it draws and displays images directly without parsing the content. This leaves the extracting of images' visual features from the page impossible. Hence, to compare image similarity, we take the raw (CIE-Lab) images as the direct input. A measurement for evaluating the similarity/difference of arbitrary objects is the normalised information distance (NID) (Bennett, et al., 1998). However, it is not computable (Terwijn, et al. 2011) because an "ideal" compressor (i.e., the compressor which provides the same result as the single object when compressing two identical objects) does not exist.

A potential replacement of NID is the normalised compression distance (NCD), where the compressor must be lossless. The NCD is calculated by (3-5) (Li, etc. 2004):

$$NCD(X,Y) = \frac{C(XY) - \min\{C(X),C(Y)\}}{\max\{C(X),C(Y)\}}, \qquad (3\text{-}5)$$

where, X and Y are the two images; XY is the concatenation of X and Y; and $C(q)$ calculates the length of the lossless compression of q.

The value of NCD is 0.0 if two images are identical, and 1.0 if they are completely different. Similar with ΔE_{00} in representing colour difference, a proper threshold is necessary to decide the image similarity. Roshabin and Miller (2011) have undertaken studies on the empirical threshold, and we adopt their findings in this chapter: the compression should be implemented by a LZMA compressor, and a threshold of 0.25 provides an adequate decision point.

4 Visual Similarity between Two Web Pages

After web pages being represented by the block trees, the similarity of a pair of web pages can be determined by the similarity of their block trees. This similarity can be determined by the tree edit distance (TED) (Tai, K. C. 1979) because the block trees are labelled and ordered. The order of the block tree nodes follows the appearance of them, which is essentially follow the appearance of the render objects, and the label of a block is its visual feature set.

4.1 Block Tree Edit Distance

Let T be a block tree, $|T|$ be the size (that is, number of nodes), t_i be the ith node in the post-order traversal, and T^p and T^q be two different block trees, respectively. TED of T^p and T^q is then defined as the minimum cost of edit operations when shifting from T^p to T^q. In this chapter, we assume costs of all the edit operations are the same and take the value of 1. In this case, the TED reflects the number of edit operations.

The edit operations include insertion, deletion, and relabel. When transferring T^p to T^q, if a node t_i^p in T^p has no corresponding node t_j^q in T^q, then the edit operation is deletion. If t_j^q has no corresponding node t_i^p, then it is insertion. If a pair of corresponding nodes t_i^p and t_j^q exist but their labels are different, then it is a relabel operation. The mapping of the corresponding nodes, denoted by $m(t_i^p, t_j^q)$, is not arbitrary. Rather, it should follow a series of rules (Shahbazi and Miller 2014). Considering two mappings $m(t_{i_1}^p, t_{j_1}^q)$ and $m(t_{i_2}^p, t_{j_2}^q)$, the rules include:

- the one-to-one rule – a node of the first tree can only map to one node of the second tree: $j_1 = j_2 \Leftrightarrow i_1 = i_2$;
- the horizontal-order-preserving rule – $t_{j_1}^q$ locates before $t_{j_2}^q \Leftrightarrow t_{i_1}^p$ locates before $t_{i_2}^p$.
- the vertical-order-preserving rule – $t_{j_1}^q$ is an ancestor of $t_{j_2}^q \Leftrightarrow t_{i_1}^p$ is an ancestor of $t_{i_2}^p$.

By default, TED calculates the structural similarity of two trees. However, what we concern about is the visual similarity induced by the visual features. Hence, in the block tree, we encode the visual features into the labels, and consequently, during the block tree edit distance (B-TED) calculation, the relabel operation will compare the blocks "visually". For instance, when mapping one block in a block tree to another block in a second block tree, if the first block has different visual features with the second block, then it is relabelled after mapping with a relabel operation; it remains the same otherwise. The model of block tree construction and visual similarity calculation is illustrated by **Figure 3.7**.

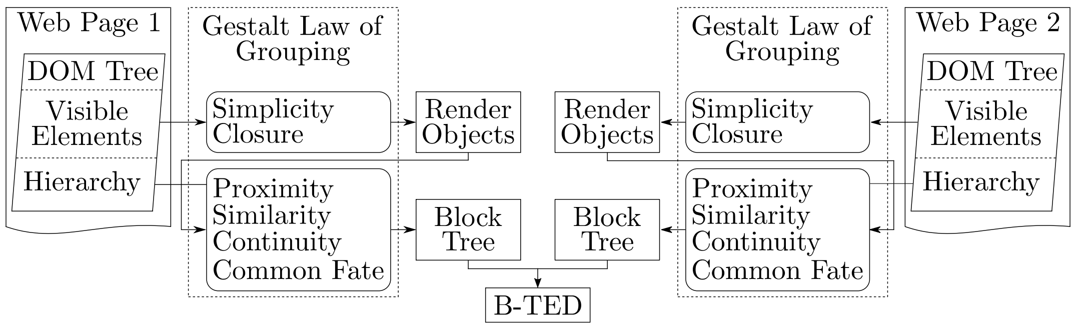

Figure 3.7 The Calculation Model

4.2 Case Study

This section investigates the block tree and visual similarity model through a series of test cases. The first test case is the home page of the electrical and computer engineering department from the university of Alberta (ECE, http://www.ece.engineering.ualberta.ca/). The original page, shown in **Figure 3.8**, includes various blocks, such as the left navigation menu, the big image under the department banner, the three columns of "news and events", and the footer. **Figure 3.9** illustrates the page after merging. Different background colours and boarder shadows are utilized to indicate different blocks. For example, if two render objects are marked with the same colour, they belong to the same block.

Two conclusions can be made from **Figure 3.8** and **Figure 3.9**. Fist, most of the render objects are merged into blocks. For example, the background of the menu items (i.e., the objects framed with the white-edged rectangle) above the department banner are marked with green, and that of all the footer content is marked with light pink. Second, some render objects are not identified correctly, such as the left navigation menu (i.e., the object framed with the red-edged round rectangle). It is obvious that the menu should go to the same block, but they are marked in different colours. This is because each menu item is a link (an "A" DOM element) under a list item (a "LI" DOM element) according to the hierarchy, under which each A has the same size and position with its parent "LI". Therefore, each "LI" and "A" are marked with the background colour, resulting in invisible LI block from the final screenshot image. In fact, content in the right of the three columns (the right red rounded rectangle) are in the same case, but the margins (i.e., the uncovered background by the three columns) eliminate this display issue by showing the content covered by the paragraphs. In fact, this problem happens whenever the foreground text and the background colours/images are displayed in different DOM elements and is a limitation of the current model.

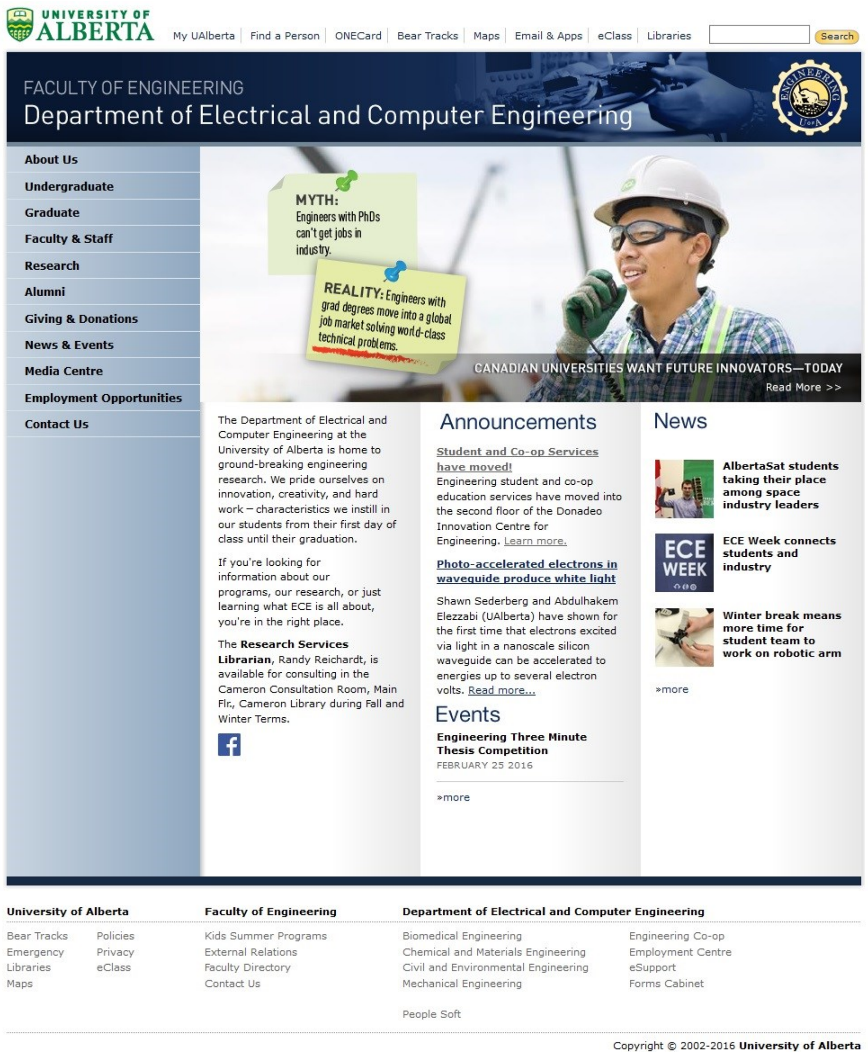
UNIVERSITY OF ALBERTA
My UAlberta | Find a Person | ONECard | Bear Tracks | Maps | Email & Apps | eClass | Libraries
Search
FACULTY OF ENGINEERING
Department of Electrical and Computer Engineering
About Us
Undergraduate
Graduate
Faculty & Staff
Research
Alumni
Giving & Donations
News & Events
Media Centre
Employment Opportunities
Contact Us
MYTH: Engineers with PhDs can't get jobs in industry.
REALITY: Engineers with grad degrees move into a global job market solving world-class technical problems.
CANADIAN UNIVERSITIES WANT FUTURE INNOVATORS—TODAY
Read More >>

The Department of Electrical and Computer Engineering at the University of Alberta is home to ground-breaking engineering research. We pride ourselves on innovation, creativity, and hard work – characteristics we instill in our students from their first day of class until their graduation.

If you're looking for information about our programs, our research, or just learning what ECE is all about, you're in the right place.

The **Research Services Librarian**, Randy Reichardt, is available for consulting in the Cameron Consultation Room, Main Flr., Cameron Library during Fall and Winter Terms.

Announcements

Student and Co-op Services have moved!
Engineering student and co-op education services have moved into the second floor of the Donadeo Innovation Centre for Engineering. Learn more.

Photo-accelerated electrons in waveguide produce white light

Shawn Sederberg and Abdulhakem Elezzabi (UAlberta) have shown for the first time that electrons excited via light in a nanoscale silicon waveguide can be accelerated to energies up to several electron volts. Read more...

Events

Engineering Three Minute Thesis Competition
FEBRUARY 25 2016

»more

News

AlbertaSat students taking their place among space industry leaders

ECE Week connects students and industry

Winter break means more time for student team to work on robotic arm

»more

University of Alberta		Faculty of Engineering	Department of Electrical and Computer Engineering	
Bear Tracks	Policies	Kids Summer Programs	Biomedical Engineering	Engineering Co-op
Emergency	Privacy	External Relations	Chemical and Materials Engineering	Employment Centre
Libraries	eClass	Faculty Directory	Civil and Environmental Engineering	eSupport
Maps		Contact Us	Mechanical Engineering	Forms Cabinet
			People Soft	

Copyright © 2002-2016 **University of Alberta**

Figure 3.8 Case Study: The Home Page of ECE

The block tree of the above web page is partly shown in **Figure 3.10**. Each line in the figure indicates a single block, where the full visual features are saved for visual similarity evaluation. Different indentions reflect the hierarchy.

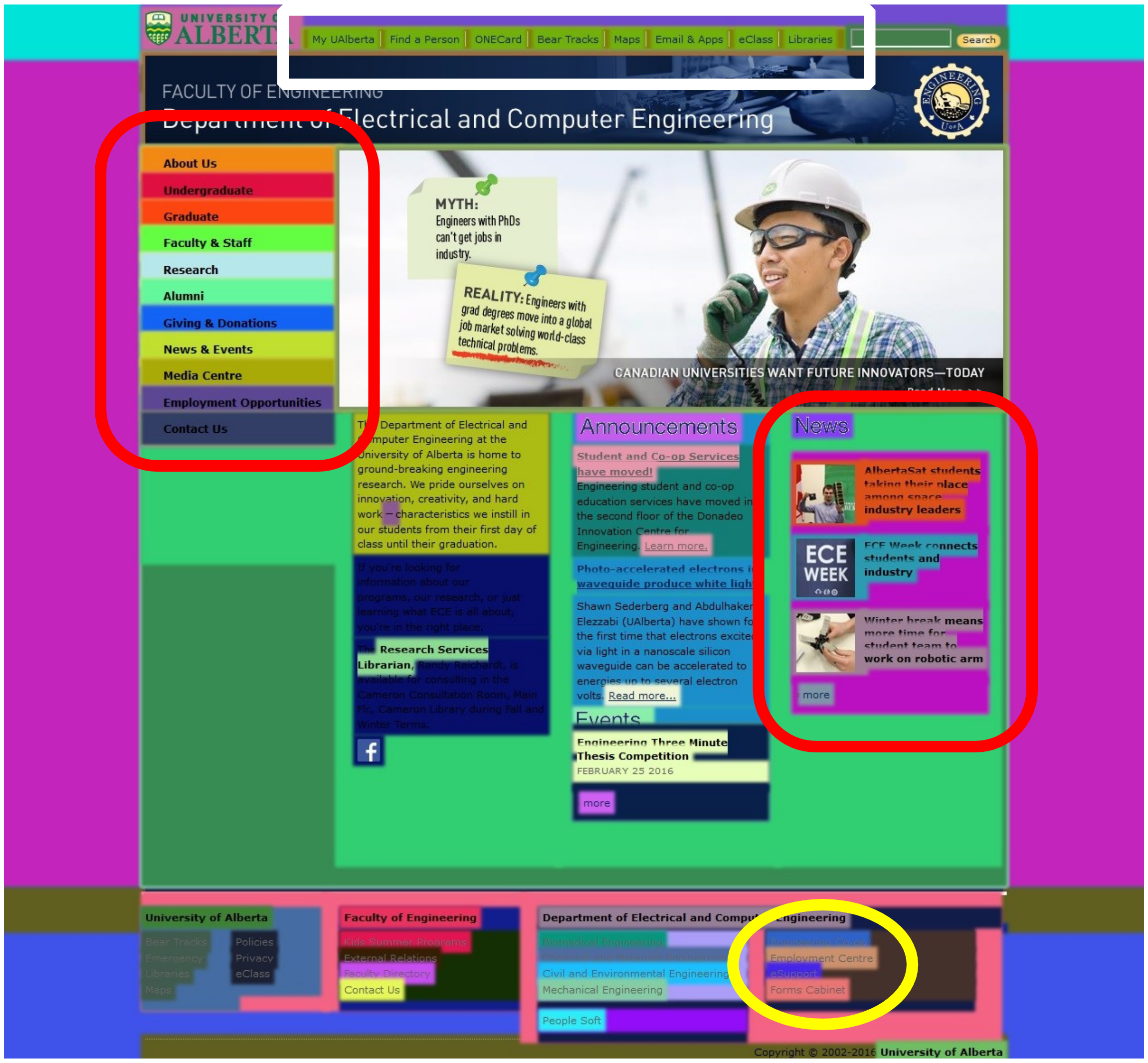

The Department of Electrical and Computer Engineering at the University of Alberta is home to ground-breaking engineering research. We pride ourselves on innovation, creativity, and hard work – characteristics we instill in our students from their first day of class until their graduation.

If you're looking for information about our programs, our research, or just learning what ECE is all about, you're in the right place.

The Research Services Librarian, Randy Reichardt, is available for consulting in the Cameron Consultation Room, Main Flr., Cameron Library during Fall and Winter Terms.

Student and Co-op Services have moved!
Engineering student and co-op education services have moved in the second floor of the Donadeo Innovation Centre for Engineering. Learn more.

Photo-accelerated electrons in waveguide produce white light
Shawn Sederberg and Abdulhakem Elezzabi (UAlberta) have shown for the first time that electrons excited via light in a nanoscale silicon waveguide can be accelerated to energies up to several electron volts. Read more...

Engineering Three Minute Thesis Competition
FEBRUARY 25 2016

AlbertaSat students taking their place among space industry leaders

ECE Week connects students and industry

Winter break means more time for student team to work on robotic arm

Copyright © 2002-2016 University of Alberta

Figure 3.9 Case Study: The Home Page of ECE (marked)

```
[BODY]: left=0,top=0,  # visual features are partly shown
 |- [FORM]: left=0,top=0, #...
 |    |- [DIV,FOOTER]: left=0,top=0, #...
 |    |    |- [HEADER,SECTION]: left=0,top=0, #...
 |    |    |    |- [DIV,DIV]: left=0,top=0, #...
 |    |    |    |    |- [DIV]: left=157,top=0, #...
 |    |    |    |    |    |- [A]: left=157,top=10, #...
 |    |    |    |    |    |    |- [SPAN]: left=-99833,top=9, #...
 |    |    |    |    |    |- [NAV,DIV]: left=336,top=35, #...
 |    |    |    |    |    |    |- [DIV]: left=336,top=34, #...
 |    |    |    |    |    |    |    |- [UL]: left=336,top=34, #...
# ... ...
```
Figure 3.10 Part of the Block Tree

Another two web pages are analysed to evaluate the visual similarity, including the home pages of the University of Alberta (UA, http://ualberta.ca/), and that of the faculty of graduate studies and research (FGSR, https://uofa.ualberta.ca/graduate-studies), as shown in **Figure 3.11** and **Figure 3.12**, respectively.

Among the three web pages, the last two pages are more similar with each other in both theme (such as the colours, fonts, and image styles) and layout settings. More specifically, they both have function menus and green banner images at the top; navigation menu below the green banner, and green footer at the bottom; the central pages are mixed with images and paragraphs; the news and events sections have three columns, where the left columns are the wildest and the right columns are the narrowest. In comparison, the first page owns a blue theme, a navigation menu locating at the left, and a central page with image and texts separated. **Table 3.1** shows the sizes of the "BODY" sub DOM tree, the visual tree (that is, the DOM tree of visible elements) and the block.

Table 3.1 Tree Sizes of the Three Web Pages

Web Page	DOM Tree	Visual Tree	Block Tree
1	235	157	88
2	420	278	128
3	831	233	114

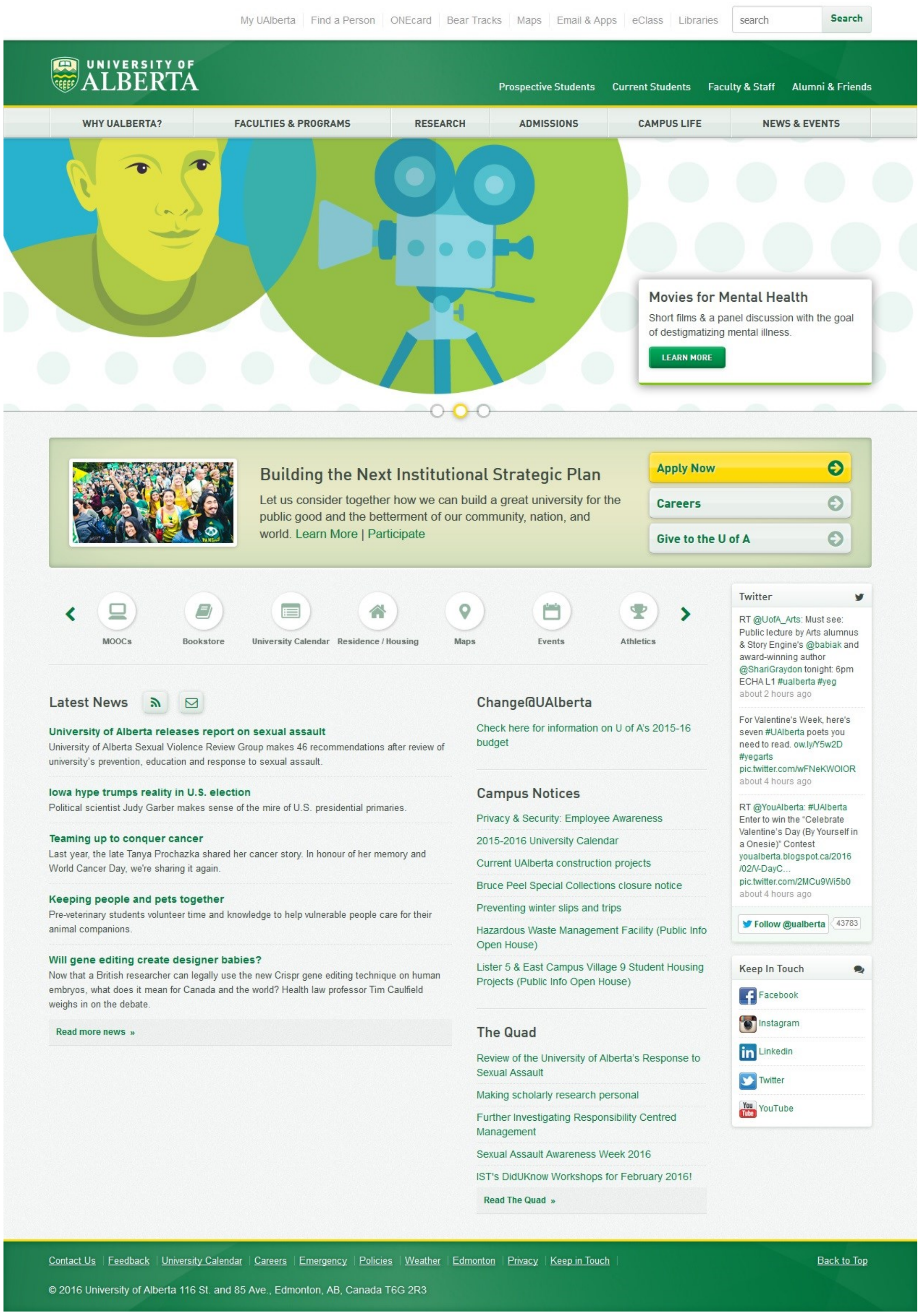
My UAlberta | Find a Person | ONEcard | Bear Tracks | Maps | Email & Apps | eClass | Libraries | search | Search

UNIVERSITY OF ALBERTA

Prospective Students | Current Students | Faculty & Staff | Alumni & Friends

WHY UALBERTA? | FACULTIES & PROGRAMS | RESEARCH | ADMISSIONS | CAMPUS LIFE | NEWS & EVENTS

Movies for Mental Health

Short films & a panel discussion with the goal of destigmatizing mental illness.

LEARN MORE

Building the Next Institutional Strategic Plan

Let us consider together how we can build a great university for the public good and the betterment of our community, nation, and world. Learn More | Participate

Apply Now

Careers

Give to the U of A

MOOCs | Bookstore | University Calendar | Residence / Housing | Maps | Events | Athletics

Latest News

University of Alberta releases report on sexual assault
University of Alberta Sexual Violence Review Group makes 46 recommendations after review of university's prevention, education and response to sexual assault.

Iowa hype trumps reality in U.S. election
Political scientist Judy Garber makes sense of the mire of U.S. presidential primaries.

Teaming up to conquer cancer
Last year, the late Tanya Prochazka shared her cancer story. In honour of her memory and World Cancer Day, we're sharing it again.

Keeping people and pets together
Pre-veterinary students volunteer time and knowledge to help vulnerable people care for their animal companions.

Will gene editing create designer babies?
Now that a British researcher can legally use the new Crispr gene editing technique on human embryos, what does it mean for Canada and the world? Health law professor Tim Caulfield weighs in on the debate.

Read more news »

Change@UAlberta

Check here for information on U of A's 2015-16 budget

Campus Notices

Privacy & Security: Employee Awareness
2015-2016 University Calendar
Current UAlberta construction projects
Bruce Peel Special Collections closure notice
Preventing winter slips and trips
Hazardous Waste Management Facility (Public Info Open House)
Lister 5 & East Campus Village 9 Student Housing Projects (Public Info Open House)

The Quad

Review of the University of Alberta's Response to Sexual Assault
Making scholarly research personal
Further Investigating Responsibility Centred Management
Sexual Assault Awareness Week 2016
IST's DidUKnow Workshops for February 2016!

Read The Quad »

Twitter

RT @UofA_Arts: Must see: Public lecture by Arts alumnus & Story Engine's @babiak and award-winning author @ShariGraydon tonight: 6pm ECHA L1 #ualberta #yeg
about 2 hours ago

For Valentine's Week, here's seven #UAlberta poets you need to read. ow.ly/Y5w2D #yegarts pic.twitter.com/wFNeKWOIOR
about 4 hours ago

RT @YouAlberta: #UAlberta Enter to win the "Celebrate Valentine's Day (By Yourself in a Onesie)" Contest youalberta.blogspot.ca/2016/02/V-DayC... pic.twitter.com/2MCu9Wi5b0
about 4 hours ago

Follow @ualberta 43783

Keep In Touch

Facebook
Instagram
Linkedin
Twitter
YouTube

Contact Us | Feedback | University Calendar | Careers | Emergency | Policies | Weather | Edmonton | Privacy | Keep in Touch | Back to Top

© 2016 University of Alberta 116 St. and 85 Ave., Edmonton, AB, Canada T6G 2R3

Figure 3.11 Case Study: The Home Page of UA

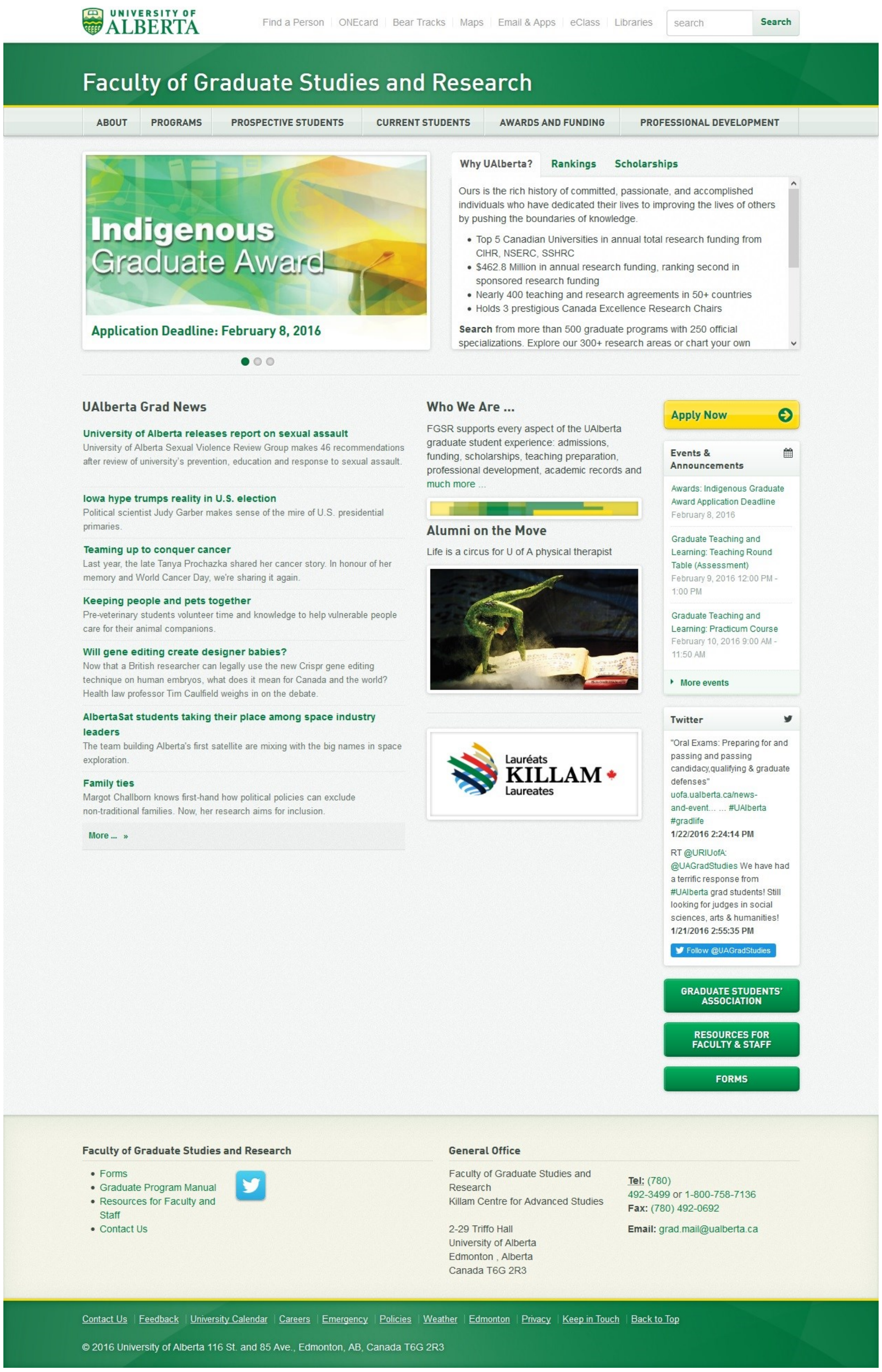

UNIVERSITY OF ALBERTA

Find a Person | ONEcard | Bear Tracks | Maps | Email & Apps | eClass | Libraries

search Search

Faculty of Graduate Studies and Research

ABOUT | PROGRAMS | PROSPECTIVE STUDENTS | CURRENT STUDENTS | AWARDS AND FUNDING | PROFESSIONAL DEVELOPMENT

Indigenous Graduate Award

Application Deadline: February 8, 2016

Why UAlberta? | Rankings | Scholarships

Ours is the rich history of committed, passionate, and accomplished individuals who have dedicated their lives to improving the lives of others by pushing the boundaries of knowledge.

- Top 5 Canadian Universities in annual total research funding from CIHR, NSERC, SSHRC
- $462.8 Million in annual research funding, ranking second in sponsored research funding
- Nearly 400 teaching and research agreements in 50+ countries
- Holds 3 prestigious Canada Excellence Research Chairs

Search from more than 500 graduate programs with 250 official specializations. Explore our 300+ research areas or chart your own

UAlberta Grad News

University of Alberta releases report on sexual assault
University of Alberta Sexual Violence Review Group makes 46 recommendations after review of university's prevention, education and response to sexual assault.

Iowa hype trumps reality in U.S. election
Political scientist Judy Garber makes sense of the mire of U.S. presidential primaries.

Teaming up to conquer cancer
Last year, the late Tanya Prochazka shared her cancer story. In honour of her memory and World Cancer Day, we're sharing it again.

Keeping people and pets together
Pre-veterinary students volunteer time and knowledge to help vulnerable people care for their animal companions.

Will gene editing create designer babies?
Now that a British researcher can legally use the new Crispr gene editing technique on human embryos, what does it mean for Canada and the world? Health law professor Tim Caulfield weighs in on the debate.

AlbertaSat students taking their place among space industry leaders
The team building Alberta's first satellite are mixing with the big names in space exploration.

Family ties
Margot Challborn knows first-hand how political policies can exclude non-traditional families. Now, her research aims for inclusion.

More ... »

Who We Are ...

FGSR supports every aspect of the UAlberta graduate student experience: admissions, funding, scholarships, teaching preparation, professional development, academic records and much more ...

Alumni on the Move

Life is a circus for U of A physical therapist

Lauréats KILLAM Laureates

Apply Now

Events & Announcements

Awards: Indigenous Graduate Award Application Deadline
February 8, 2016

Graduate Teaching and Learning: Teaching Round Table (Assessment)
February 9, 2016 12:00 PM - 1:00 PM

Graduate Teaching and Learning: Practicum Course
February 10, 2016 9:00 AM - 11:50 AM

More events

Twitter

"Oral Exams: Preparing for and passing and passing candidacy,qualifying & graduate defenses" uofa.ualberta.ca/news-and-event... ... #UAlberta #gradlife
1/22/2016 2:24:14 PM

RT @URIUofA: @UAGradStudies We have had a terrific response from #UAlberta grad students! Still looking for judges in social sciences, arts & humanities!
1/21/2016 2:55:35 PM

Follow @UAGradStudies

GRADUATE STUDENTS' ASSOCIATION

RESOURCES FOR FACULTY & STAFF

FORMS

Faculty of Graduate Studies and Research

- Forms
- Graduate Program Manual
- Resources for Faculty and Staff
- Contact Us

General Office

Faculty of Graduate Studies and Research
Killam Centre for Advanced Studies

2-29 Triffo Hall
University of Alberta
Edmonton , Alberta
Canada T6G 2R3

Tel: (780) 492-3499 or 1-800-758-7136
Fax: (780) 492-0692

Email: grad.mail@ualberta.ca

Contact Us | Feedback | University Calendar | Careers | Emergency | Policies | Weather | Edmonton | Privacy | Keep in Touch | Back to Top

© 2016 University of Alberta 116 St. and 85 Ave., Edmonton, AB, Canada T6G 2R3

Figure 3.12 Case Study: The Home Page of FGSR

From the table, although the second two pages are similar, the size difference between their DOM trees is larger than that between the first two DOM trees. Also, the size difference between the second two pages' visual trees is smaller than that between the rest pairs. These two facts prove again that only the visible content of a web page contributes to the visual similarity. Hence, the DOM tree is not suitable for visual similarity evaluation, owing to abundant invisible elements it contains. In addition, the block tree size difference between the last two pages is smaller than that between the first and the second as well as that between the first and the third, which indicates the block tree reflects visual similarity.

Calculated by the three block trees, B-TEDs are: 121 between web page 1 and 2, 128 between page 1 and 3, and 108 between page 2 and 3. None of these values is 0, which represents that the three block trees are different from each other. Due to the smallest B-TED being witnessed, page 2 and 3 are most similar. Meanwhile, B-TED between page 1 and 2 is smaller than that between page 1 and 3, indicating that page 2 is more similar with page 1 compared to page 3.

5 Experiments

The experiments are designed to evaluate whether B-TED is an effective measurement for web page visual similarity analysis. First, a set of web pages are crawled as the test cases and split into subsets randomly. Then the aforementioned model is applied to all pairs of test cases within each subset to calculate the B-TEDs. The values of B-TEDs indicate the similarity between web pages; and the pre-classified results are exploited to obtain the values of precision, recall, and accuracy rates.

5.1 Test Set

The test cases are generated from the global top sites of Alexa (http://www.alexa.com/, these top sites and links were retrieved on March 27, 2015). With the home pages of the world's top 500 websites as the initial pool, we crawl all direct links to generate a final test case pool, which includes 78298 links. All these links are unique in terms of the identifying URL, and are currently active. Different URLs, however, may have similar content. For example, the pages of "Gmail" and "Blogger" are almost the same except one word, because both of the two links are redirected to the login page of a Google account. Asian websites tend to contain lots of links in a single page (sometimes even more than 1000 links, such as "163.com"), leading to a high probability of domain sharing among Asian web pages in the test pool. Many western websites' home pages, on the other hand, are very concise and contain fewer links.

Cross-comparing each pair of all the test cases requires approximately 6.13 billion comparisons, resulting in infeasible experiment. Therefore, we choose 500 test cases from the pool randomly. **Figure 3.13** describes the distribution of the 500 test cases, with the x-axis representing the web sites and the y-axis illustrating the number of selected pages for each web site. As shown in the figure, these test cases cover 109 web sites, and some of them contain more web pages than others, with an average of 4.59 pages per web site. For instance, the 88th web site ("bitauto.com") includes the most pages, which is 66; and 47 web sites only possess one page each.

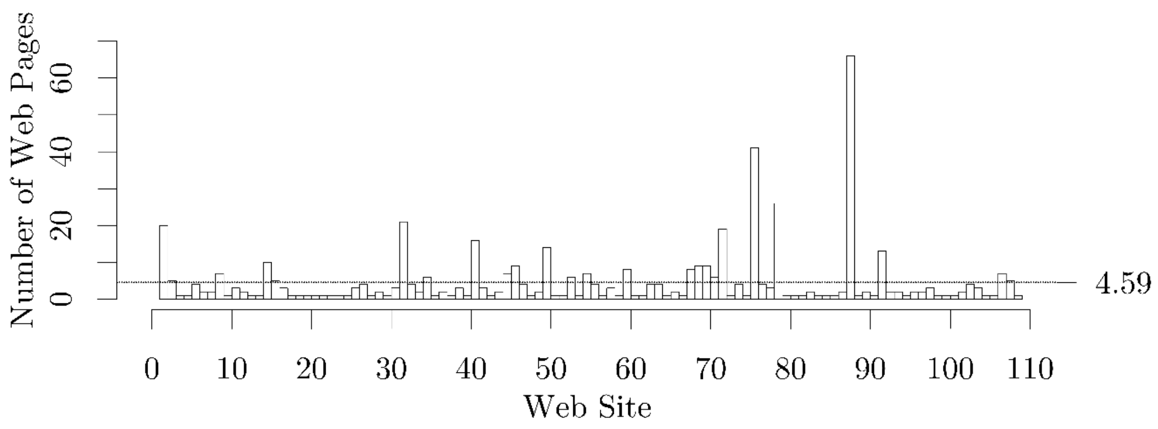

Figure 3.13 The Distribution of Randomly Selected Web Pages per Web Site

Figure 3.14 illustrates the sizes of all the block trees (i.e., the number of nodes per block tree). Among them, the largest block tree has 1237 nodes, and the smallest contains only 4 nodes. The mean size of all the block trees is 346.38.

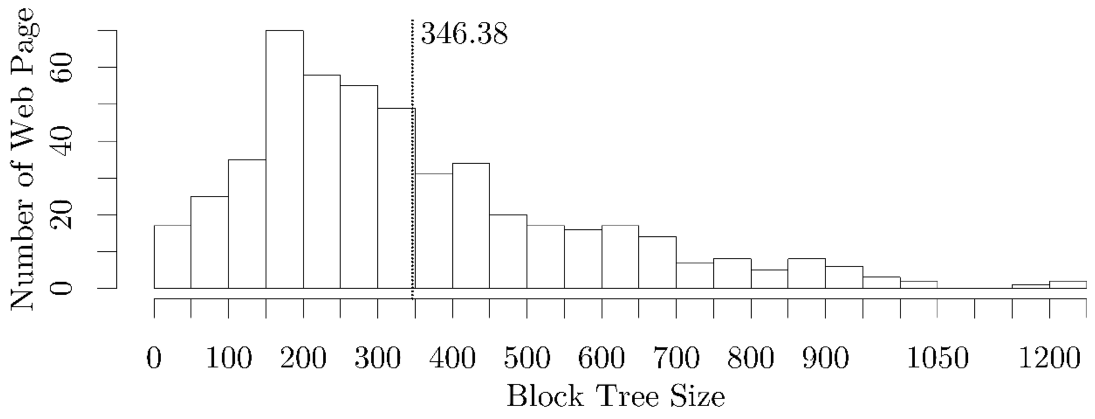

Figure 3.14 The Distribution of Block Tree Size

5.2 Experimental Methodology

It is infeasible to cross-compare the visual similarity between web pages manually, this is because there will be $\binom{500}{2} = 142750$ pairs of pages. Therefore, in the experiment, we build a web classification model to identify the visual similarity automatically. This classification model runs a naive Bayes classifier (McCallum and Nigam 1998) and follows a 10-fold cross-validation (Refaeilzadeh et al. 2009) routine. Specifically, in the experimental preparation, the test set is first divided into 10 subsets randomly and equally. The next step is to prepare the feature set for the classifier. For each subset, there are $\binom{50}{2}$ = 1225 pairs of web pages, so the feature vector contains 1225 records, each of which includes the block trees of the two web pages as well as the B-TED values between them. Also, we set the category variable as a Boolean with "YES" denoting similar and "NO" representing different.

The category variable is determined manually. In each subset, all the web pages are read by five people and then split into several groups, where visually similar pages are put in the same group, while different pages are placed into different groups. The split decisions are made purely by the comprehensive understanding of the five people, so we can use it to evaluate how well the algorithm simulates human perception. For example, the home pages of "google.ca" and "google.fr" are similar so they are put in the same group; and conversely, the home page of "google.ca" is visually different from that of "yahoo.com", so they are sorted into different groups. During manual classification, it is not reasonable to make the five people identify web page similarity following rules, because any given rule will affect people's way of thinking, leading to the inaccurate judgement and thus disrupting the manual classification. After pre-classification, if two web pages are in the same group, then the corresponding category of this feature record will be "YES"; and vice versa. Inter rater reliability of the five people are evaluated by Cohen's Kappa, where the results are shown in **Table 3.2**. According to the table and **Table 2.4**, κ of each two of the five raters are all within the "substantial" range (and higher) for all the 10 subsets, indicating the five people all agree with each other.

Table 3.2 κ of Each Two Raters' Evaluations

Raters		**Subsets**									
A	**B**	**1**	**2**	**3**	**4**	**5**	**6**	**7**	**8**	**9**	**10**
1	2	0.6938	0.7628	0.7736	0.7720	0.7092	0.8147	0.7963	0.7792	0.7369	0.7620
1	3	0.8034	0.7460	0.8099	0.7386	0.7501	0.7127	0.7797	0.7763	0.7690	0.7764
1	4	0.7202	0.7679	0.8091	0.7172	0.8083	0.7070	0.7806	0.7675	0.8028	0.7113
1	5	0.7523	0.8067	0.7784	0.8043	0.8075	0.7954	0.7702	0.7454	0.7648	0.7785
2	3	0.7692	0.8139	0.8075	0.7561	0.7737	0.8099	0.7797	0.7766	0.7723	0.8099
2	4	0.7460	0.7188	0.7990	0.6973	0.7741	0.7675	0.7927	0.6959	0.7684	0.7794
2	5	0.8138	0.7160	0.6974	0.8155	0.7669	0.7999	0.7187	0.7706	0.7943	0.7742
3	4	0.8059	0.8083	0.8116	0.7708	0.7785	0.7266	0.7728	0.7684	0.8052	0.7444
3	5	0.7714	0.7775	0.7074	0.7556	0.8115	0.6987	0.7657	0.8067	0.7999	0.7468
4	5	0.7613	0.8067	0.7000	0.8115	0.7396	0.7999	0.8139	0.7710	0.8025	0.8099

10 rounds are involved in the cross-validation process of the experiment. In each round, nine subsets are selected as the training sets, and the last subset serves as the validation set. The naive Bayes classifier is first trained by all the feature records and the corresponding categories from the training set. Then it reads the feature vector of the validation set and makes the prediction of a category vector. Finally, efficiency is obtained by comparing the prediction result with the pre-classification result. The experimental methodology is illustrated in **Figure 3.15**.

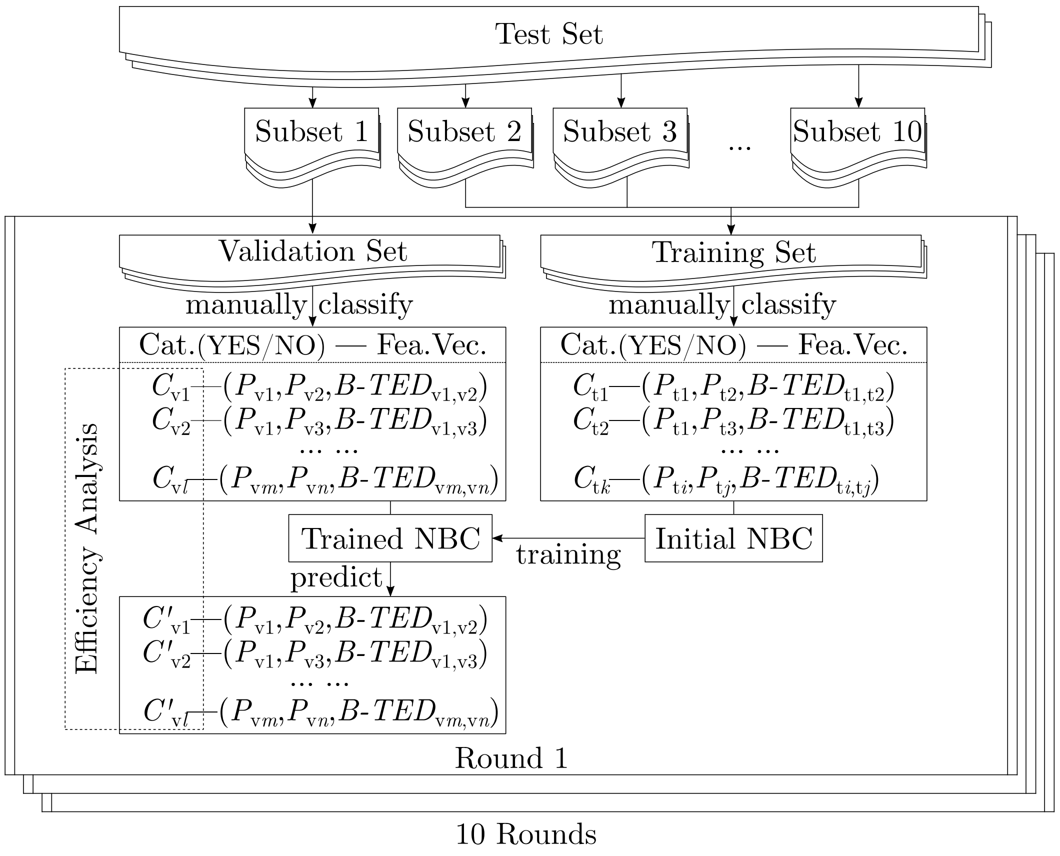
Test Set
Subset 1
Subset 2
Subset 3
...
Subset 10
Validation Set
Training Set
manually classify
manually classify
Cat.(YES/NO) — Fea.Vec.
Cat.(YES/NO) — Fea.Vec.
C_{v1}—(P_{v1},P_{v2},$B\text{-}TED_{v1,v2}$)
C_{v2}—(P_{v1},P_{v3},$B\text{-}TED_{v1,v3}$)
C_{vl}—(P_{vm},P_{vn},$B\text{-}TED_{vm,vn}$)
C_{t1}—(P_{t1},P_{t2},$B\text{-}TED_{t1,t2}$)
C_{t2}—(P_{t1},P_{t3},$B\text{-}TED_{t1,t3}$)
C_{tk}—(P_{ti},P_{tj},$B\text{-}TED_{ti,tj}$)
Trained NBC
training
Initial NBC
predict
Efficiency Analysis
C'_{v1}—(P_{v1},P_{v2},$B\text{-}TED_{v1,v2}$)
C'_{v2}—(P_{v1},P_{v3},$B\text{-}TED_{v1,v3}$)
C'_{vl}—(P_{vm},P_{vn},$B\text{-}TED_{vm,vn}$)
Round 1
10 Rounds

Figure 3.15 Experimental Methodology

5.3 Experimental Results

The B-TED distribution of the 1225 records in subset 1 is displayed in **Figure 3.16**. Two findings can be concluded from this figure. First, B-TED can be used as a visual similarity measurement, owing to the fact its different values towards with similar pages and different pages. To be specific, B-TED values between similar web pages (the “YES” category) are smaller than that between different web pages (the “NO” category). Second, the threshold to determine web page similarity does not exist, because there is no clear gap between the two categories Distributions of the remaining nine subsets are similar, which reveals the above findings as well.

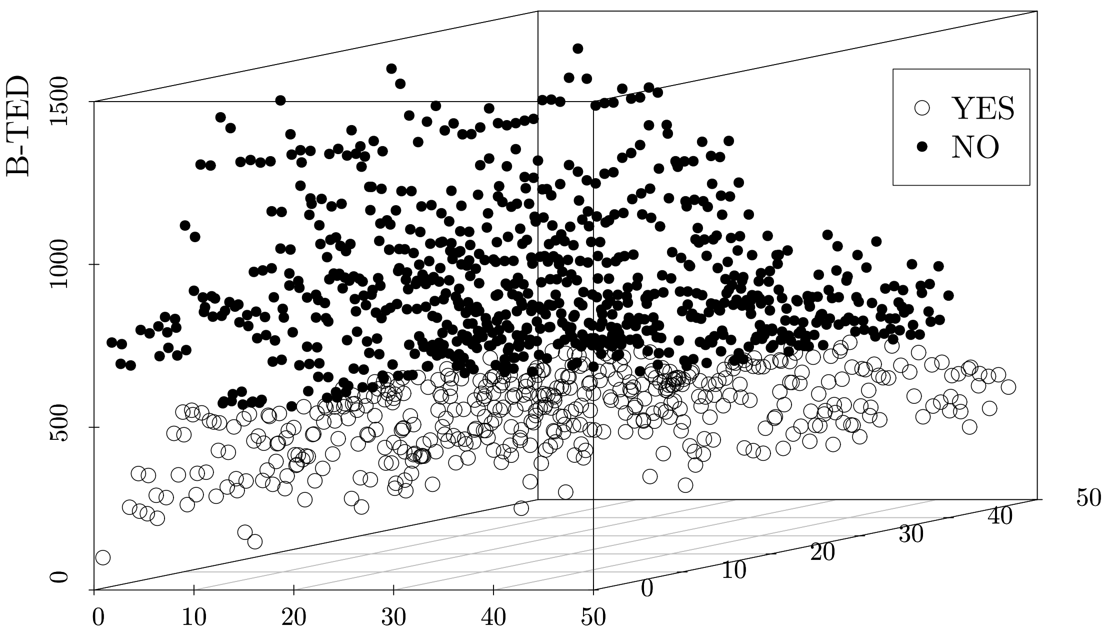

Figure 3.16 B-TED Distributions of Subset 1

Table 3.3 depicts more details about the B-TED values. The maximum B-TED of each subset ranges from 1037 to 1542, and the minimum value is between 24 and 112. With respect to the mean values, the "YES" cases have values from 662.90 to 811.89, and the "NO" test cases take the values from 309.35 to 357.09. The latter is approximately 300 smaller than the former, indicating that although the obvious threshold does not exist, the visual similarity can still be identified by the B-TED.

Table 3.3 B-TED Value Details

Subset	Maximum	Minimum	Mean of "YES" cases	Mean of "NO" cases
1	1490	54	764.24	355.03
2	1233	42	758.12	309.35
3	1292	32	736.67	352.26
4	1174	78	731.92	312.45
5	1373	68	811.89	333.61
6	1037	112	690.02	348.86
7	1093	27	662.90	343.56
8	1085	24	666.78	317.45
9	1052	80	663.64	357.09
10	1542	82	799.02	346.90

To evaluate the model's performance, the precision, recall, and accuracy of the classification are collected by (3-6).

$$\begin{aligned} P_i &= \frac{TP_i}{TP_i + FP_i} \\ R_i &= \frac{TP_i}{TP_i + FN_i} \\ A_i &= \frac{TP_i + TN_i}{TP_i + TN_i + FP_i + FN_i} \end{aligned} \quad , \tag{3-6}$$

where, i denotes the subset number; P_i, R_i, and A_i are the precision, recall, and accuracy of the classification, respectively; TP_i, TN_i, FP_i, and FN_i are the numbers of "true positive", "true negative", "false positive", and "false negative" classifications, respectively:

- if two web pages are similar and correctly identified by the classifier, then they are referred to as true positive (TP);
- if two web pages are different and correctly identified, then they are referred to as true negative (TN);
- if two web pages are different but incorrectly identified as similar, then they are referred to as false positive (FP);
- if two web pages are similar but incorrectly identified as different, then they are referred to as false negative (FN).

From the experimental results shown in **Table 3.4**, it can be seen that round 6 demonstrates the best performance with precision of 94.72% and accuracy of 98.29%. Conversely, the first trial demonstrates the poorest performance with a precision of 74.38%, and an accuracy of 87.27%. This is caused by the high FP rate of the corresponding predictions. This problem also appears in round 10. There are more TPs and TNs than FPs and FNs in each of the 10 rounds. Also, the overall accuracy is 94.43%, which proves that B-TED is an effective measurement for visual similarity. Meanwhile, FPs are non-zero, showing that some pairs of different pages are incorrectly identified as similar. Conversely, FNs are all zero, which reveals that there are no pairs of similar pages identified as different. The probably reason for this is that people tend to focus on the overall sketch when looking for similarity, and pay attention to details when searching for differences. Therefore, if two pages are similar, the probability that they are identified as different is very low; conversely, if they are different, there is possibility that they are judged as similar.

Table 3.4 Experimental Results

Round	**TP**	**TN**	**FP**	**FN**	**Precisio n**	**Recall**	**Accurac y**
1	453	616	156	0	74.38%	100.00%	87.27%
2	619	528	78	0	88.81%	100.00%	93.63%
3	592	554	79	0	88.23%	100.00%	93.55%
4	682	505	38	0	94.72%	100.00%	96.90%
5	732	432	61	0	92.31%	100.00%	95.02%
6	786	418	21	0	97.40%	100.00%	98.29%
7	810	390	25	0	97.01%	100.00%	97.96%
8	659	530	36	0	94.82%	100.00%	97.06%
9	734	460	31	0	95.95%	100.00%	97.47%
10	593	475	157	0	79.07%	100.00%	87.18%
Average	666.00	490.80	68.20	0	90.27%	100.00%	94.43%

6 Conclusion

Modern web pages are embedded with abundant information, such as images and streaming media. Hence, traditional text-based similarity evaluation methods are problematic; however, similarity based on visual information is a promising orientation for modern web pages.

In this chapter, a novel approach to this problem is proposed. The “block tree” model is introduced to represent a web page visually. This is done by retrieving visual information from the web page and interpreting the Gestalt laws of grouping to merge related content. A normalised Hausdorff distance is introduced to evaluate proximities; the CIE-Lab colour space and its colour difference are used to find the colour similarities; and the normalised compression distance is used to calculate image similarities. A page similarity classification model is then built based on the block tree edit distance (B-TED). When calculating B-TED, we label each block tree node with all its visual features, and compare the corresponding nodes by them.

An experiment is preformed utilizing a test set built from randomly crawling popular web sites. To evaluate the correctness of B-TED as a measurement for visual similarity, a 10-fold cross-validation is conducted. The overall precision, recall, and accuracy in the experiment are 90.27%, 100%, and 94.43%, respectively. This implies that B-TED is a promising measurement for web page similarity evaluation, and provides satisfactory identification results.

In spite of the contributions, limitation still exists for the proposed methodology. That is, the hierarchy of the block tree does not precisely reflect the visual layout when foreground text and background colours/images are separated. In the future work, a proper solution for this limitation will be the first task.

To the best of our knowledge, this is the first time that the Gestalt laws of grouping have been used to investigate web page similarity. Therefore, no similar study exists in the literature. In the future, we plan to investigate and validity our interpretation of these laws via experiments which explored the effectiveness of each law independently.

Acknowledgement

The authors would like to thank China Scholarship Council (CSC) and Natural Sciences and Engineering Research Council of Canada (NSERC) for their financial support.

References

Bennett, C. H., G´acs, P., Li, M., Vit´anyi, P. M., Zurek, W. H., 1998. Information distance. IEEE Transactions on information theory 44 (4), 1407–1423.

Buttler, D., 2004. A short survey of document structure similarity algorithms. Tech. rep., Lawrence Livermore National Laboratory (LLNL), Livermore, CA.

Chaudhuri, B. B., Rosenfeld, A., 1999. A modified hausdorff distance between fuzzy sets. Information Sciences 118 (1), 159–171.

Chechik, G., Sharma, V., Shalit, U., Bengio, S., 2010. Large scale online learning of image similarity through ranking. Journal of Machine Learning Research 11 (Mar), 1109–1135.

Connor, R., Simeoni, F., Iakovos, M., Moss, R., 2011. A bounded distance metric for comparing tree structure. Information Systems 36 (4), 748–764.

Cording, P. H., Lyngby, K., 2011. Algorithms for web scraping. PDF] Available: http://www2. imm. dtu. dk/pubdb/views/publicationdetails. php.

Dorner, D., 1996. The logic of failure: Recognizing and avoiding error in complex situations. Basic Books.

Dubuisson, M.-P., Jain, A. K., 1994. A modified hausdorff distance for object matching. In: Pattern Recognition, 1994. Vol. 1-Conference A: Computer Vision & Image Processing., Proceedings of the 12th IAPR International Conference on. Vol. 1. IEEE, pp. 566–568.

Hern´andez, I., Rivero, C. R., Ruiz, D., Corchuelo, R., 2014. Cala: An unsupervised url-based web page classification system. Knowledge-Based Systems 57, 168–180.

Huttenlocher, D. P., Klanderman, G. A., Rucklidge, W. J., 1993. Comparing images using the hausdorff distance. IEEE Transactions on pattern analysis and machine intelligence 15 (9), 850–863.

Koffka, K., 2013. Principles of Gestalt psychology. Vol. 44. Routledge.

Kwitt, R., Uhl, A., 2008. Image similarity measurement by kullback-leibler divergences between complex wavelet subband statistics for texture retrieval. In: Image Processing, 2008. ICIP 2008. 15th IEEE International Conference on. IEEE, pp. 933–936.

Lee, J.-H., Yeh,W.-C., Chuang, M.-C., 2015.Web page classification based on a simplified swarm optimization. Applied Mathematics and Computation 270, 13–24.

Li, M., Chen, X., Li, X., Ma, B., Vit´anyi, P. M., 2004. The similarity metric. IEEE transactions on Information Theory 50 (12), 3250–3264.

Liu, H. X.,Wu, B., Liu, Y., Huang, M., Xu, Y. F., 2013. A discussion on printing color difference tolerance by ciede2000 color difference formula. In: Applied Mechanics and Materials. Vol. 262. Trans Tech Publ, pp. 96–99.

Liu, Z., Lagani`ere, R., 2007. Phase congruence measurement for image similarity assessment. Pattern Recognition Letters 28 (1), 166–172.

Luo, M. R., Cui, G., Rigg, B., 2001. The development of the cie 2000 colour-difference formula: Ciede2000. Color Research & Application 26 (5), 340–350.

McCallum, A., Nigam, K., et al., 1998. A comparison of event models for naive bayes text classification. In: AAAI-98 workshop on learning for text categorization. Vol. 752. Madison, WI, pp. 41–48.

M¨uller-Molina, A. J., Hirata, K., Shinohara, T., 2008. A tree distance function based on multi-sets. In: Pacific-Asia Conference on Knowledge Discovery and Data Mining. Springer, pp. 87–98.

Onan, A., 2016. Classifier and feature set ensembles for web page classification. Journal of Information Science 42 (2), 150–165.

Refaeilzadeh, P., Tang, L., Liu, H., 2009. Cross-validation. In: Encyclopedia of database systems. Springer, pp. 532–538.

Rohlfing, T., 2012. Image similarity and tissue overlaps as surrogates for image registration accuracy: widely used but unreliable. IEEE transactions on medical imaging 31 (2), 153–163.

Roshanbin, N., Miller, J., 2011. Finding homoglyphs-a step towards detecting unicode-based visual spoofing attacks. Web Information System Engineering–WISE 2011, 1–14.

Saar, T., Dumas, M., Kaljuve, M., Semenenko, N., 2016. Browserbite: cross-browser testing via image processing.

Software: Practice and Experience 46 (11), 1459–1477.

Sampat, M. P., Wang, Z., Gupta, S., Bovik, A. C., Markey, M. K., 2009. Complex wavelet structural similarity: A new image similarity index. IEEE transactions on image processing 18 (11), 2385–2401.

Shahbazi, A., Miller, J., 2014. Extended subtree: a new similarity function for tree structured data. IEEE Transactions on knowledge and Data Engineering 26 (4), 864–877.

Sharma, G., Wu, W., Dalal, E. N., 2005. The ciede2000 color-difference formula: Implementation notes, supplementary test data, and mathematical observations. Color Research & Application 30 (1), 21–30.

Stevenson, H., 2012. Emergence: The gestalt approach to change. Unleashing Executive and Orzanizational Potential. Retrieved 7.

Tai, K.-C., 1979. The tree-to-tree correction problem. Journal of the ACM (JACM) 26 (3), 422–433.

Terwijn, S. A., Torenvliet, L., Vit´anyi, P. M., 2011. Nonapproximability of the normalized information distance. Journal of Computer and System Sciences 77 (4), 738–742.

Wei, Y., Wang, B., Liu, Y., Lv, F., 2014. Research on webpage similarity computing technology based on visual blocks. In: Chinese National Conference on Social Media Processing. Springer, pp. 187–197.

Xu, Z., Miller, J., 2016. Identifying semantic blocks in web pages using gestalt laws of grouping. World Wide Web. 19 (5), 957–978.

Zhai, Y., Liu, B., 2006. Structured data extraction from the web based on partial tree alignment. IEEE Transactions on Knowledge and Data Engineering 18 (12), 1614–1628. 12

CHAPTER 4 Cross-Browser Differences Detection based on an Empirical Measurement for Web Page Visual Similarity[6]

Abstract

This chapter aims to develop a method to detect visual differences introduced into web pages when they are rendered in different browsers. To achieve this goal, we propose an empirical visual similarity measurement by mimicking human mechanisms of perception. The Gestalt laws of grouping are translated into a computer compatible rule set. A block tree is then parsed by the rules for similarity calculation. During the translation of the Gestalt laws, experiments are performed to obtain measurements for proximity, color similarity, and image similarity. After a validation experiment, the empirical measurement is employed to detect cross-browser differences. Experiments and case studies on the world's most popular web pages provide positive results for this methodology.

Keywords: Block Tree; Extended Subtree; Gestalt Laws of Grouping; Web Page Visual Similarity; Cross-Browser Differences Detection.

1 Introduction

Web applications, with web browsers as their carriers, have become an indispensable part of our life today. While we enjoy the convenience that different web

6 Xu, Zhen, and James Miller. "Cross-Browser Differences Detection based on an Empirical Measurement for Web Page Visual Similarity". ACM Transactions on Internet Technology (in review).

browsers bring to us, we also face the problems that web pages are rendered differently across different web browsers. Cross-browser visualization issues, therefore, become prevalent, which affects user experience. In addition, they also cause maintenance issues for web designers.

Cross-browser issues refer to cross-browser incompatibilities, which are differences in a web page's appearances (i.e., visual features) or behaviors, or both, when it is displayed on different browsers (Choudhary, et al. 2013). This chapter will focus on the appearances of web pages. The first step (details can be found at Xu and Miller, 2015b) is to remove the invisible elements and CSS attributes of the web page from its DOM tree. The remaining visible elements are then grouped into different blocks by the Gestalt laws of grouping to finally construct "the block tree". The Gestalt laws of grouping are originally used in psychology to account for people's tendency of perceiving various objects as organized together (Wolfe et al. 2009; Banerjee 1994). In the second step, we propose an empirical visual similarity measurement to detect how similar (or different) a specified web page is, when it is rendered in two different browsers. The major contributions of this chapter include:

1) it provides a numerical mechanism to translate the Gestalt laws of grouping into a set of computer-compatible rules;
2) it presents a novel data structure to represent web page visual information;
3) it develops an empirical measurement to evaluate web page visual similarity; and
4) it applies the empirical measurement to detect cross-browser differences.

The remainder of this chapter is organized as follows: Section 2 investigates the empirical translation of the Gestalt laws of grouping; Section 3 introduces an empirical measurement for evaluating the visual similarity between web pages; Section 4 conducts experiments on detecting cross-browser differences. Section 5 reviews recent work; and Section 6 draws conclusions from the presented work.

2 Translating Algorithm of the Gestalt Laws of Grouping

2.1 Motivations and Goals

The Gestalt laws of Grouping illustrate how people perceive objects. In this section, we attempt to translate these laws into a format that a computer can process within the domain of web pages. It should be noted that this task is significantly different from, and easier than, parallel efforts to translate these laws for general image processing applications. Analyzing the screenshot image of a web page will contain significant noise components, whereas using the DOM tree is effectively noise free. This is because the DOM tree stores actual content (such as text or videos) while screenshot image stores color values of each pixel. Also, the DOM tree includes the hierarchical information, thus relationships among different content components is preserved. It is argued that utilizing the actual content components and their relationships is essential to producing an accurate solution.

The original Gestalt laws of grouping include eight items (each item represents a single law), i.e., the Gestalt laws of (a) simplicity, (b) closure, (c) proximity, (d) similarity, (e) continuity, (f) common fate, (g) symmetry, and (h) past experience (Stevenson 2012; Koffka 2013). In the context of web page similarity, the Gestalt laws of symmetry and the Gestalt laws of past experience are not employed. This is because the former considers symmetric elements that are in widely scattered locations (which are very rare in web pages), and the latter refers to higher level of human perceptions (i.e., it requires knowledge that is beyond the scope of web page analysis). Hence, we focus here on the remaining six laws.

2.2 Translating the Gestalt Law of Simplicity

The Gestalt law of simplicity states that people tend to break down content into the simplest units when reading a web page. Although a web page can be split as small as a single pixel, we will not follow this method. This is because when we read the page, we focus on useful information such as a single image or a piece of text instead of pixels. The useful information corresponds to the DOM elements of a web page.

Taking the home page of the IEEE (https://www.ieee.org/index.html) as an example, the logo contains three parts: the diamond figure, the big bold "IEEE", and the phrase under them. Despite having different types and styles, they are considered as a single group rather than three unrelated items; this simplifies the process of reading and understanding. Based on this observation, we define DOM elements as the smallest units that cannot be further split during the process of web page analysis.

2.3 Translating the Gestalt Law of Closure

The Gestalt law of closure indicates that upper elements of a web page will cover lower elements, however, humans are prone to regard the lower elements as complete rectangles even if they are partially covered. Our brain fills the hole that is blocked by the upper elements. Use the home page of Facebook (https://www.facebook.com/) as the example, the login boxes cover the right part of the top ribbon, which makes the latter incomplete. Even though, we still perceive the ribbon as complete. According to this observation, we treat each element as a full rectangle during the process of web page analysis. This also makes the representation much easier and thus is consistent with the Gestalt law of simplicity and human visual systems.

2.4 Translating the Gestalt Law of Proximity

The Gestalt law of proximity argues that we tend to put close elements of a web page into the same group and assign distant elements into different groups. Considering the home page of Facebook again, we perceive the two login boxes as related (regarded as a group), the five boxes regarding signup are related (regarded as a second group), and the three boxes under the "Birthday" are also related (regarded as a third group). However, any two elements in different groups are not related according to their distance relationships. (The words proximity and distance are used interchangeable in this chapter.) For a series of sibling elements, we calculate the proximity between every two adjacent elements. Then we group the adjacent elements together if their proximities are the same and split them into different groups otherwise. In order to find an appropriate mechanism to calculate the proximity of elements, we will investigate and compare available proximity calculation candidates documented in the literature.

2.4.1 Proximity Candidates

Two intuitive measurements for the proximity of rectangular objects are the *centroid distance* (CD) and the *gap distance* (GD). CD is the Euclidean distance between the centroids of the two rectangles; and GD denotes the distinct orthogonal distance between the four sides of them.

$$CD(N_1, N_2) = \sqrt{(x_1 - x_2)^2 + (y_1 - y_2)^2}\ , \qquad (4\text{-}1)$$

$$GD(N_1, N_2) = \max\{SGN_{1,2}^{\mathrm{h}} \times dist_{1,2}^{\mathrm{h}}, SGN_{1,2}^{\mathrm{v}} \times dist_{1,2}^{\mathrm{v}}\}\,, \qquad (4\text{-}2)$$

where N_1 and N_2 are the two rectangles; (x_1, y_1), and (x_2, y_2) are the respective coordinates of the centroids of N_1 and N_2; $dist_{1,2}^{\mathrm{v}}$ and $dist_{1,2}^{\mathrm{h}}$ represent the distance between the closest vertical and horizontal sides of N_1 and N_2, respectively; and $SGN_{1,2}^{\mathrm{v}}$ and $SGN_{1,2}^{\mathrm{h}}$ represent the corresponding signs. The parameters of GD are calculated through:

$$SGN_{1,2}^{\mathrm{h}} = \begin{cases} 1, & |x_1 - x_2| > (width_1 + width_2)/2 \\ -1, & \text{otherwise} \end{cases};$$

$$SGN_{1,2}^{\mathrm{v}} = \begin{cases} 1, & |y_1 - y_2| > (height_1 + height_2)/2 \\ -1, & \text{otherwise} \end{cases};$$

$$dist_{1,2}^{\mathrm{h}} = \min\{|left_1 - left_2|, |left_1 - right_2|, |right_1 - left_2|, |right_1 - right_2|\}\,;$$

$$dist_{1,2}^{\mathrm{v}} = \min\{|top_1 - top_2|, |top_1 - bottom_2|, |bottom_1 - top_2|, |bottom_1 - bottom_2|\}\,.$$

However, these two distance measurements may lead to an inconsistent situation. For example, as shown in **Figure 4.1**a, the left two large rectangles are close to each other, and the right two small ones are more distant in the perceptual perspective. However, the calculated CDs of the two pairs are actually the same. Similar problem happens for GD, as shown in **Figure 4.1**b.

This issue is owing to the dimensions of the two nodes being ignored. Therefore, an appropriate measurement should take size (i.e. width and height of the rectangle) into account. The *Hausdorff distance* (HD) satisfies this requirement (Huttenlocher et al. 1993). It denotes the maximum value of all distances from any point in one node to its nearest point in the other node, as shown in (4-3):

$$HD(N_1, N_2) = \max\{hd_{1,2}, hd_{2,1}\} = \max\left\{\sup_{n_1 \in N_1} \inf_{n_2 \in N_2} \|n_1 - n_2\|, \sup_{n_2 \in N_2} \inf_{n_1 \in N_1} \|n_2 - n_1\|\right\}, \quad (4\text{-}3)$$

where $HD(N_1, N_2)$ is the HD between N_1 and N_2; $hd_{1,2}$ is the HD from N_1 to N_2; $\|n_1 - n_2\|$ calculates the Euclidean distance between two points n_1 and n_2; sup and inf calculate the maximum and minimum value of a given set, respectively.

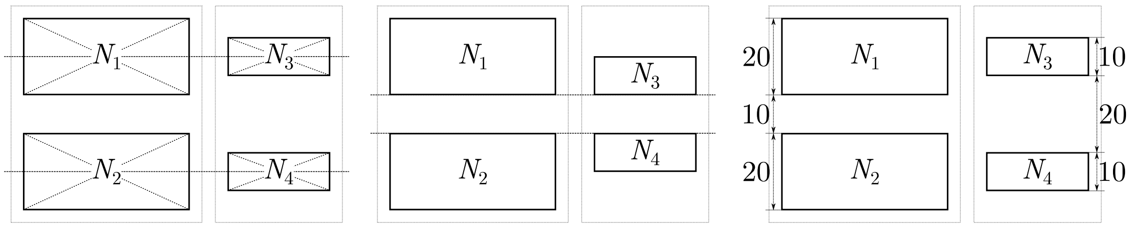

(a) Centroid Distance (b) Gap Distance (c) Hausdorff

Figure 4.1 Contradictions between Calculation Distances and Perceptual Distances

As shown in **Figure 4.1**c, although HD reflects size of rectangles, it fails to eliminate the inconsistency issues of CD and GD, Therefore, we choose the fourth candidate, which is the normalized version of HD – the *relative Hausdorff distance* (RHD). It is calculated by (4-4):

$$RHD(N_1, N_2) = \max\left\{\frac{hd_{1,2}}{rd_1}, \frac{hd_{2,1}}{rd_2}\right\}, \quad (4\text{-}4)$$

where rd_1 and rd_2 are the relative dimensions that act as normalizing factors. The detail of calculation can be found at (Xu and Miller 2015a).

2.4.2 Experiment and Discussion

The experiment focuses on proximity's influence on people's visual perception, so we minimize other influencing factors (such as similarity and continuity) by controlling these parameters. Specifically, we create eight rectangles, the sizes and content of which are randomly generated but kept the same. Meanwhile, the rectangles are evenly distributed and kept close to each other, so that the edge distances between adjacent rectangles are smaller than their dimensions. Consequently, all of them can be considered as one group. Second, the edge distance between the fourth and the fifth elements increases continuously while those of the remaining adjacent elements remain unchanged. Five volunteers were requested to observe the changing scenario, and to record when the eight rectangles were split into two groups, specifically between the fourth and the fifth rectangles, based on their perception. The values of the four proximity candidates are calculated and logged.

Each volunteer repeated the above test 100 times. The difference between the increased and the original values of a good proximity measurement should reflect the threshold of the volunteer's visual perception, i.e., it needs to be constant during the 100 tests. The differences of the four proximity candidates (ΔCD, ΔGD, ΔHD and ΔRHD) are illustrated in **Figure 4.2**. In the experiment, ΔCD, ΔGD and ΔHD are exactly the same according to their formulas, because all the rectangles are exactly the same in dimension and left-aligned. Therefore, in **Figure 4.2**, their corresponding curves coincide.

Table 4.1 shows the details of the comparison results. In the table, ΔCD, ΔGD, ΔHD, and ΔRHD are denoted as 1, 2, 3, and 4, respectively. The variances of ΔCD, ΔGD and ΔHD from all the 100 tests are all above 0.06, while the variances of ΔRHD are all bellow 0.002. Consequently, we conclude that RHD provides the best performance as a proximity estimation.

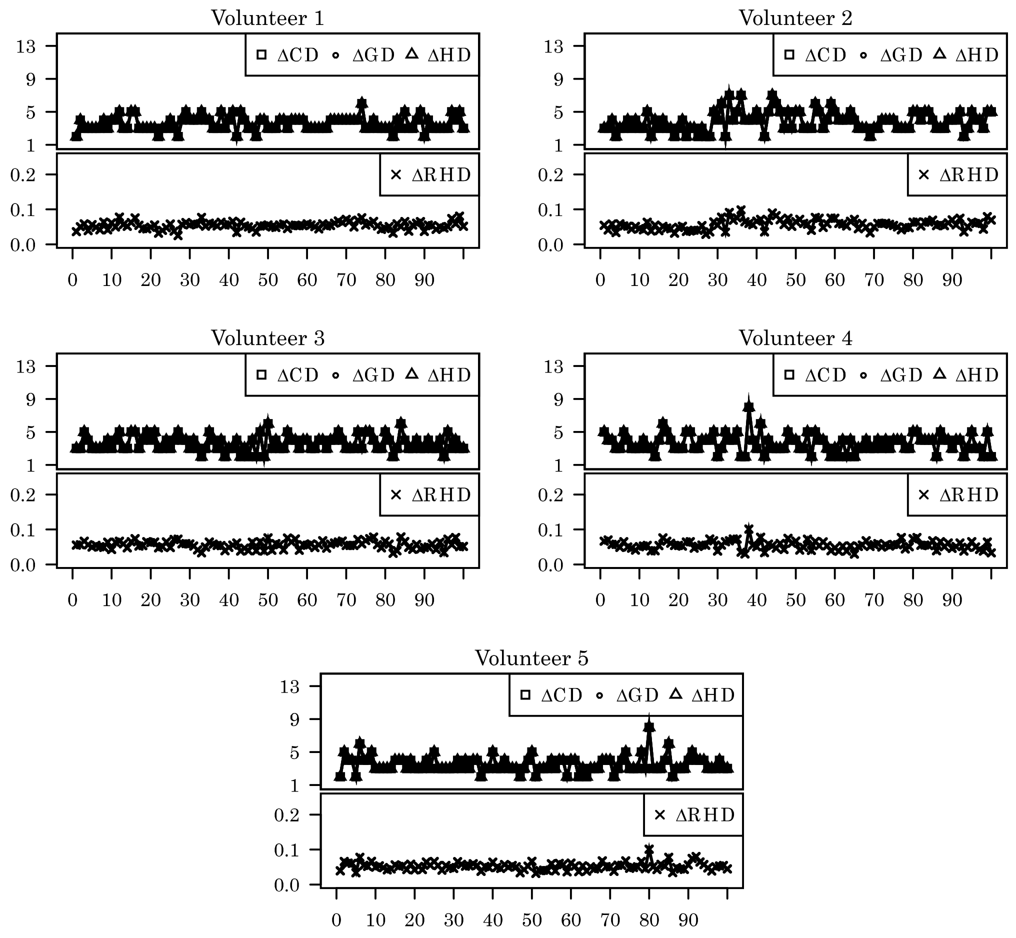

Figure 4.2 The Distribution of Proximity Candidate Comparison Results

As is stated above, the translation of the Gestalt law of proximity aims to group elements together if their distances with adjacent elements are exactly the same. However, the experimental results show that the mean of all the RHD values from the five volunteers is approximately 0.05. Therefore, during the translation, we define "same" as $\Delta RHD < 0.05$, i.e., if the value of ΔRHD is less than 0.05, we regard the two proximities as the same.

Table 4.1 Proximity Candidate Comparison Results

Volunteer	**1**		**2**		**3**		**4**		**5**	
	1, 2, 3	**4**	**1, 2, 3**	**4**	**1, 2, 3**	**4**	**1, 2, 3**	**4**	**1, 2, 3**	**4**
Maximum	6	0.0806	7	0.0986	6	0.0789	8	0.1012	8	0.1012
Minimum	2	0.0253	2	0.0290	2	0.0322	2	0.0298	2	0.0322
Mean	3.54	0.0541	3.81	0.0568	3.61	0.0562	3.62	0.0552	3.47	0.0524
Variance	0.6884	0.0001	1.3739	0.0002	0.8379	0.0001	1.1556	0.0002	0.9291	0.0001

2.5 Translating the Gestalt Law of Similarity

Different elements in a web page are displayed in various styles; however, the Gestalt law of similarity reveals that we tend to perceive similar elements as related. This law compares elements by all their visual features such as background colors/images, textual styles and paragraph styles, which are represented by a series of CSS properties. Generally, most CSS properties can be compared directly by their values. For example, two textual elements with "`font-style`" both being "`italic`" are considered as similar and as different from a third textual element with the same CSS property being "`normal`". When a CSS property contains colors or images (e.g. "`background`", "`border-color`", "`list-style-image`"), it is not accurate for them to be compared in this way. This is because the value of a color can be either the RGB value (e.g. "`rgb(255, 255, 255)`" or "`#FFFFFF`") or the color name (e.g. "`white`"). Both of them can refer to the same color; however, the string values are not the same. For accuracy, we compare the actual colors and images directly.

2.5.1 Empirical Comparison of Colors.

Most web pages describe colors utilizing the RGB space, so the direct way for comparing two colors is by comparing their color difference under the RGB color space. Riemersma (2008) exploits the weighted Euclidean distance as the color difference for the RGB color space.

$$\Delta C(C_1, C_2) = \sqrt{\left(2 + \frac{\bar{r}}{256}\right)(r_1 - r_2)^2 + 4(g_1 - g_2)^2 + \left(2 + \frac{255-\bar{r}}{256}\right)(b_1 - b_2)^2} \text{ ,(4-5)}$$

where C_1 and C_2 are the two colors; r, g and b are the values of a color's red, green and blue channels, respectively; and $\bar{r} = (r_1 + r_2)/2$ is the mean value of the red channels.

An alternative color space is CIELAB, which has a wider gamut that covers all RGB colors. Meanwhile, compared with the RGB color model designed for display devices, the CIELAB model is designed to mimic human vision. Color differences in this space, the ΔE_{00}^{12}, are calculated by (4-6) (Luo et al. 2001). The parameter list is omitted in this chapter for brevity, but can be found in (Luo et al. 2001).

$$\Delta E_{00}^{12} = \sqrt{\left(\frac{\Delta L'}{k_L S_L}\right)^2 + \left(\frac{\Delta C'}{k_C S_C}\right)^2 + \left(\frac{\Delta H'}{k_H S_H}\right)^2 + R_T \left(\frac{\Delta C'}{k_C S_C}\right)\left(\frac{\Delta H'}{k_H S_H}\right)}\,. \qquad (4\text{-}6)$$

Due to the respective merits of the two color spaces, we design experiments to test which color space has a better color difference measurement in terms of distinguishing colors for human perception when utilized in web pages. The empirical threshold for the better color difference is determined by the experiments. The experiment consists of 50 rounds of tests with each round including two groups of comparison. In each group, 100 pairs of random colors are generated. The first group lists the 100 pairs by ΔC, and the second group lists them by ΔE_{00}^{12}. We record both: (a) the first pair of colors that is distinguishable (by a human test subject) in each group; and, (b) the corresponding color difference.

The experiment is repeated five times, and the results are shown in **Table 4.2** and **Figure 4.3**. As can be seen in this table that the values of ΔE_{00}^{12} vary from 4.03 to 5.35 with a variance being smaller than 0.1; and the values of ΔC fluctuate from 22.44 to 61.24 with a variance being at least 63.90. The variance of ΔE_{00}^{12} is smaller than 0.1 while that of ΔC is larger than 60, meaning that the former is more stable. Therefore, ΔE_{00}^{12} is more distinguishable than ΔC for our human volunteers, and thus we select ΔE_{00}^{12} as the color difference metric and set its mean value as the threshold, which is 4.65.

Table 4.2 Color Comparison Results

Repetition	**1**		**2**		**3**		**4**		**5**	
	ΔE_{00}^{12}	ΔC	ΔE_{00}^{12}	ΔC	ΔE_{00}^{12}	ΔC	ΔE_{00}^{12}	ΔC	ΔE_{00}^{12}	ΔC
Maximum	5.06	57.70	5.15	61.24	5.15	57.48	5.35	57.50	5.05	56.05
Minimum	4.06	23.31	4.04	25.05	4.03	22.44	4.05	24.09	4.16	24.60
Mean	4.56	41.80	4.62	43.82	4.65	39.66	4.73	36.68	4.69	39.49
Variance	0.07	72.44	0.09	75.37	0.08	63.90	0.05	81.70	0.06	94.09

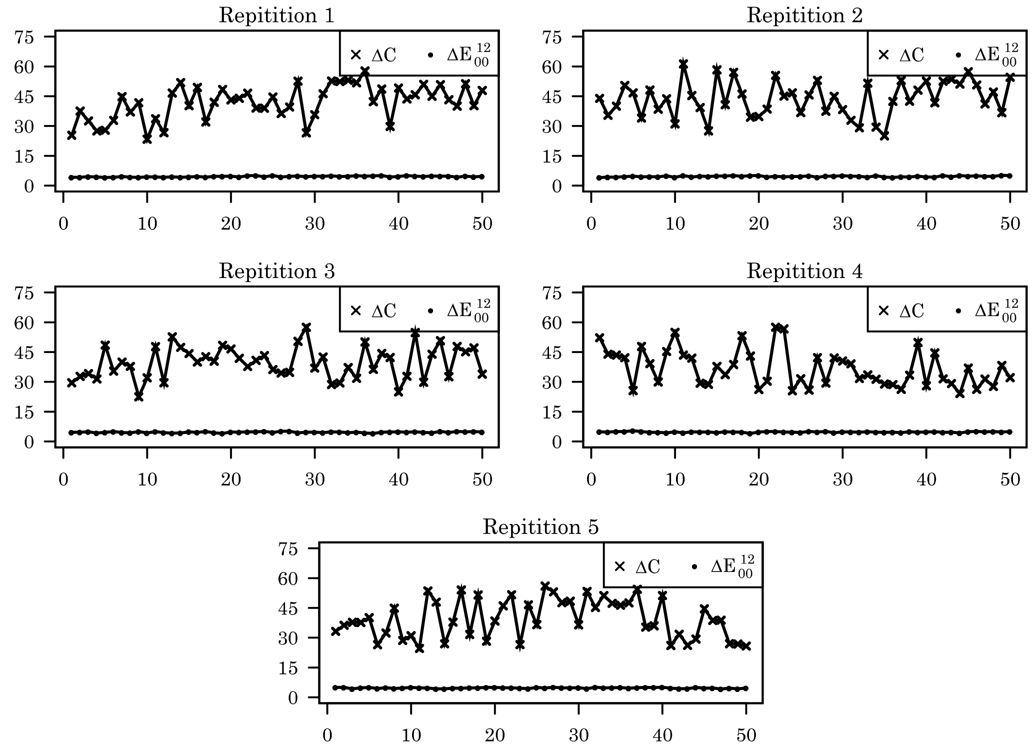

Figure 4.3 Distributions of Color Comparison Results

2.5.2 Empirical Comparison of Images

An image from a web page can be represented in several different ways: (a) a general file object that is a series of binaries; (b) a mathematical sample that is a series of numeric values; and (c) a general image that is a series of pixels.

When the image is treated as a file object, the similarity between two images can be estimated by the *normalized compression distance* (NCD), (Li et al. 2004),

$$NCD(I_1, I_2) = \frac{C(I_1 I_2) - \min\{C(I_1), C(I_2)\}}{\max\{C(I_1), C(I_2)\}}, \quad (4\text{-}7)$$

where, I_1 and I_2 are the two images, with are each represented as an array of pixel colors; $I_1 I_2$ is the concatenation of I_1 and I_2; and $C(x)$ calculates the compressed length of x. If the two images are the same, then their NCD is 0.0; and if they are completely different, the value is 1.0. Due to the performance of the current generation of compressors, errors are inevitable when calculating NCD. That is, NCD is sensitive to the selection of the compressor. The higher the performance of a compressor, the more accurate the result. Therefore, we adopt the LZMA algorithm as recommended in several previous papers (Chen et al. 2010; Claude et al. 2010). (Specifically, we utilized LZMA2, which is superior to LZMA when compressing already compressed data such as JPEG).

If we treat an image as a mathematical sample, then the similarity can be calculated mathematically as the *mean square error* (MSE) (Hore and Ziou 2010).

$$MSE(I_1, I_2) = \frac{1}{N}\sum_{x=1}^{N}(i_x^1 - i_x^2)^2, \quad (4\text{-}8)$$

where N equals to the size of I_1 and I_2 (that is, $width \times height$); i_x^1 and i_x^2 refer to the color values of pixels in I_1 and I_2, respectively.

To deal with a general image, the *structural similarity index* (SSIM) can be applied, which is designed for digital image comparison in order to imitate human perception

(Koffka 2013). The value of SSIM for two identical images is 1.0, and for two completely different images is -1.0. SSIM is calculated via (4-9),

$$SSIM(I_1, I_2) = \frac{(2\mu_1\mu_2+c)(2\sigma_{1,2}+d)}{({\mu_1}^2+{\mu_2}^2+c)({\sigma_1}^2+{\sigma_2}^2+d)}, \tag{4-9}$$

where μ_1 and μ_2 are the mean of I_1 and I_2, respectively; ${\sigma_1}^2$ and ${\sigma_2}^2$ are the variances of I_1 and I_2, respectively; and, c and d are two variables to stabilize the division with the denominator.

This experiment evaluates the aforementioned three measurements and aims at finding the best one for image similarity. We choose the McGill calibrated color image database (Olmos and Kingdom 2004) as the test pool to conduct a 10-round-comparison. This database provides over 1500 images. These images are colorful natural and manmade scenes – stored in tif format and 72 dpi resolution – such as animals, foliage, fruits, and land water, which cover almost all the themes we see in web pages. During each round, 10 pairs of similar images (i.e., 20 images) are randomly selected from the test pool to build up the test set. 20 images can make $\binom{20}{2} = 190$ pairs of images (i.e., 190 comparisons). Among them, the preselected 10 pairs of similar images are marked as the first 10 pairs, and the remaining 180 pairs are randomly marked as the 11 to 190 pairs (i.e., last 180 pairs). All the 190 pairs of images are evaluated by the three measurements respectively.

In **Figure 4.4**, two groups of box plots are drawn for each round, where group 1 shows the first 10 pairs and group 2 shows the remaining 180 pairs. All of the 10 rounds (each sub-figure represents a round) reveal similar result patterns. Qualitatively, the MSE values of group 1 in any round are not distinguishable from group 2, so it cannot be a useful measurement. Regarding the NCD results, although the values of the first 10 pairs are generally smaller than that of the last 180 pairs, they are too close to be distinguished, i.e. approximately 0.02 between the minimum and the maximum. Therefore, it is difficult to determine a threshold to divide the two groups apart. With respect to SSIM, there is a clear separation (i.e., the horizontal dashed line as shown) in each sub-figure to allow an accurate division between the two groups. As a result, among the three methods, only SSIM is capable of distinguishing between similar pages and dissimilar pages, and the empirical threshold is set to the overall mean value, which is 0.48.

Quantitatively, the minimal, maximal, and mean values of MSE, NCD, and SSIM are illustrated in **Table 4.3**. For MSE and NCD, the value range (i.e., the values between the minimum and the maximum) of the first 10 pairs crosses with that of the last 180 pairs. In contrast, there is no common part between the value ranges of SSIM's first 10 pairs and the last 180 pairs. This, again, proves that only SSIM among the three is able to distinguish the similar and the dissimilar of image pairs. Therefore, we select SSIM as the measurement to calculate web page similarity. Furthermore, for SSIM, the smallest value of the first 10 pairs is 0.5050, and the largest value of the last 180 pairs is 0.4504; therefore, we pick their overall mean (i.e., 0.4755) as the threshold to distinguish between similar and dissimilar images.

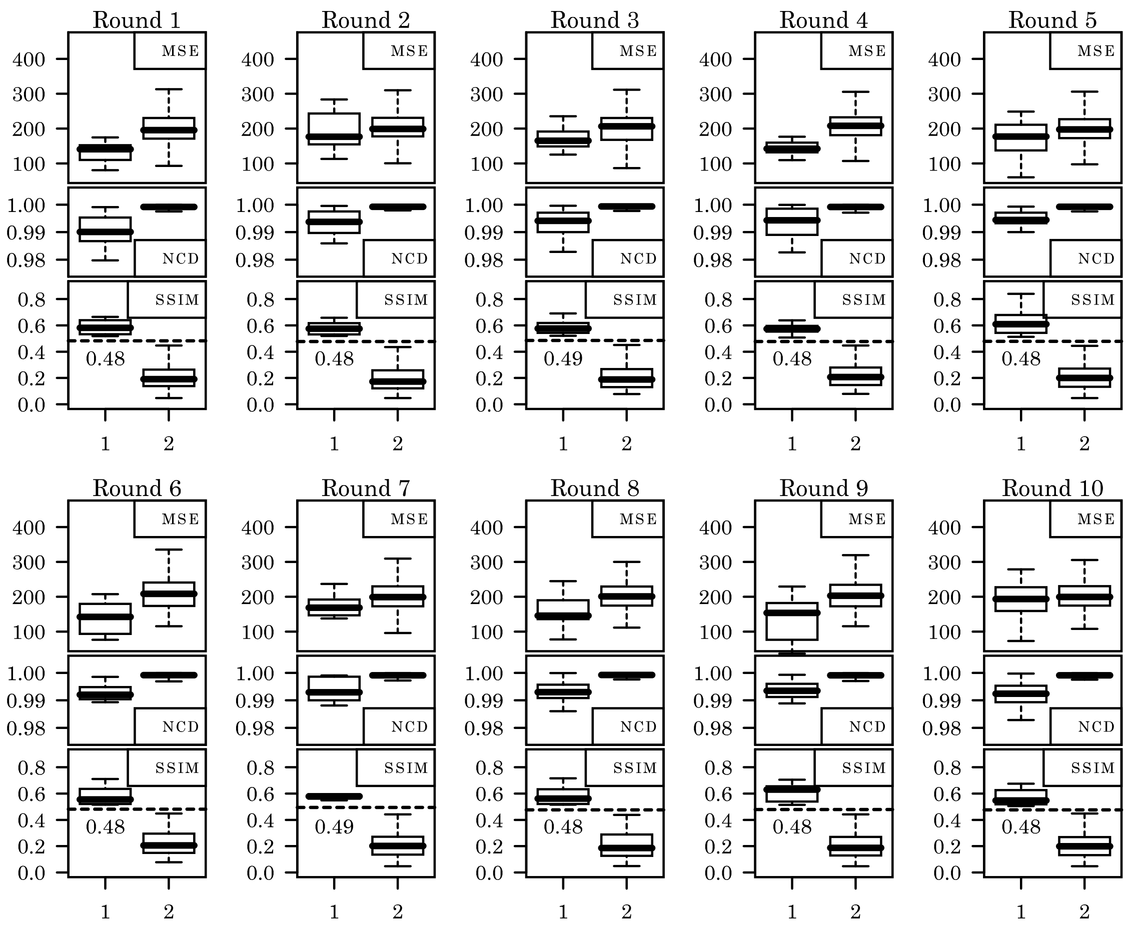

Figure 4.4 Distributions of Image Comparison Results

Table 4.3 Image Comparison Results

	MSE		**NCD**		**SSIM**	
	Group 1	**Group 2**	**Group 1**	**Group 2**	**Group 1**	**Group 2**
Minimum	36.8994	86.7609	0.9722	0.9894	0.5050	0.0476
Maximum	311.8292	421.2648	0.9999	0.9999	0.8397	0.4504
Mean	162.4931	206.7298	0.9927	0.9989	0.5920	0.2105

2.6 Translating the Gestalt Law of Continuity

The Gestalt law of continuity expresses that people tend to judge the elements on a web page as related in a situation where they are aligned, and as dissimilar when they are not aligned. In other words, this law refers to the geometrical alignment. By default, the browser places elements in a justified manner. If certain elements are not justified with others, it indicates that they are not related. In this case, the designers have separated them deliberately.

As shown in the example of Amazon's home page (**Figure 4.5**), the paragraphs in the blue rectangle ("Get to Know Us", "Careers", "About Amazon", etc.) are left aligned, indicating they are related content. In general, to evaluate continuity, we compare the left, top, right, and bottom coordinates of two elements. If any of the four coordinates of two elements are the same, we conclude that they are related; and that they are dissimilar otherwise.

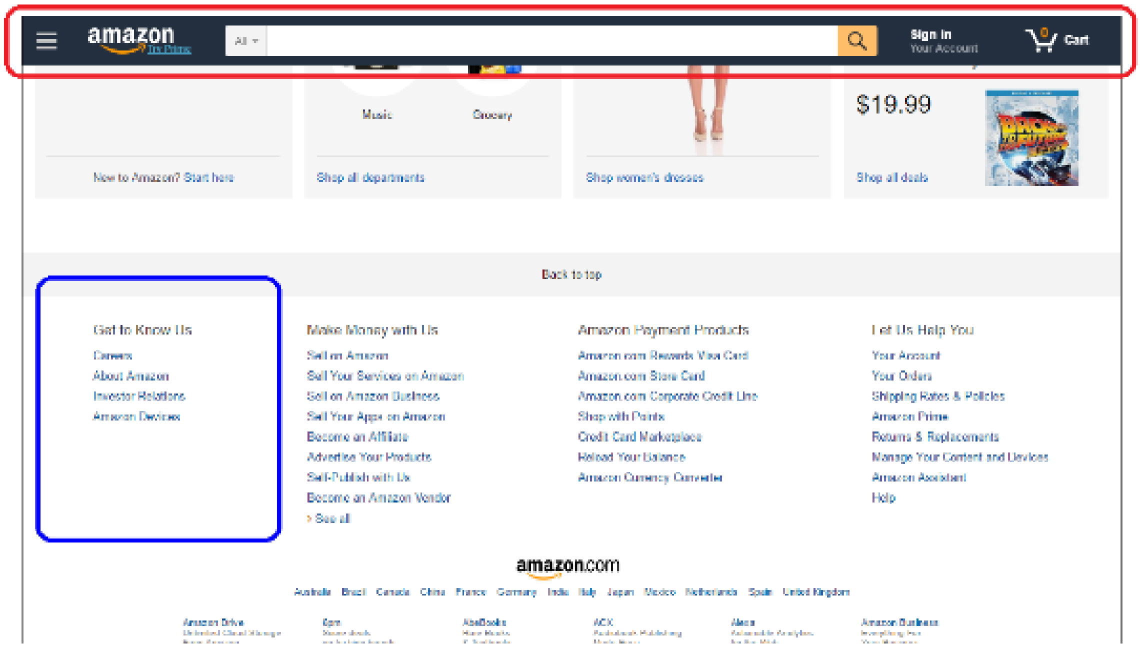

Figure 4.5 Home Page of Amazon

2.7 Translating the Gestalt Law of Common Fate

The Gestalt law of common fate describes that during the process of web page loading, elements in a web page can have different motion trends, and people's tendency is to regard elements with the same motion trend as related. When the page is loaded, most web page content does not move during the load operation. However, if the reader scrolls up and down the page, all nodes will move by default. In some situations, there are elements that do not move with scrolling pages, under this situation, we believe these elements have different motion trends and as such that we treat them as dissimilar. This motion trend is controlled by the CSS property "position", therefore translation of this law will compare the corresponding values of DOM elements for merging determination.

Taking the home page of Amazon in **Figure 4.5** again as the example, when the page is scrolled, the search bar (marked by the red rectangle) is always hanging at the top, but other content moves accordingly. Under this circumstance, we tend to think of the search bar and the other content as dissimilar.

With the DOM tree of a web page as the raw input, the translated Gestalt laws constructs the block tree by removing all invisible elements and merging semantically related elements into blocks, as shown in **Figure 4.6**. This data structure, the block tree that contains all visual information of a web page, is used for visual similarity evaluation and cross-browser difference detection. Efficiency of the block tree is discussed in (Xu and Miller, 2015a), where it is utilized as part of a web page segmentation algorithm empirically shown to outperform VIPS.

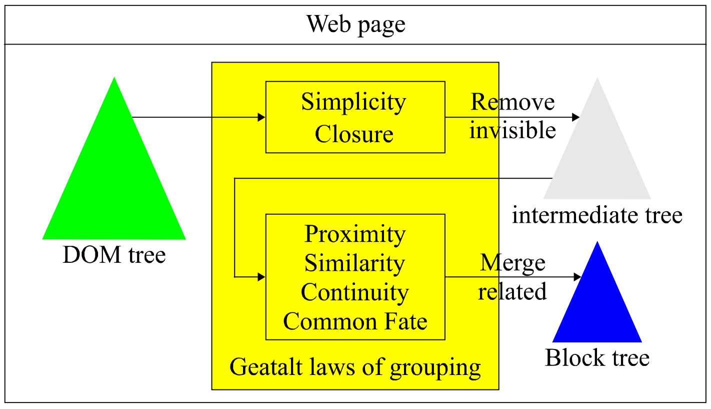

Figure 4.6 Translation of Gestalt Laws of Grouping

3 The Empirical Visual Similarity Measurement

The similarity between two block trees can be decided by the *tree edit distance* (TED) (Pawlik and Augsten 2015). To calculate TED, the first step is to determine their mapping relationship. If we post-order traverse all the nodes of a tree, then the mapping relationship between nodes of two trees is restricted to the following three rules:

1) *one-to-one* rule: any node in one tree can map to one and only one node in the other tree;
2) *horizontal-order preserving* rule: the (post-order-traversal) order of two sibling nodes in one tree is always the same with the order of the mapped nodes in the other tree;
3) *vertical-order preserving* rule: if two nodes are parent and child in one tree, then their mapped nodes in the other tree must still be parent and child.

Note that a node in one tree may not be mapped to any node in the other tree. After obtaining the mapping relationship, one of the following three types of edit operations is determined. (1) if a node from the first tree does not map to any node in the second tree, it is *removed* when the first tree is transformed to the second tree. (2) if a node from the second tree does not map to any node in the first tree, it is *added*. (3) if a node from the first tree maps to a node in the second tree, but the two mapped nodes have different content, then the node in the first tree is *relabeled*. If the two mapped nodes have the same content, then there is no edit operation during the transformational process. The value of TED between the two trees refers to the number of edit operations required to transform one tree to the other.

3.1 The Extended Subtree

The edit distance of the corresponding two block trees denotes the visual similarity between two web pages. However, directly using TED as the visual similarity measurement is not sufficient. First, it calculates the absolute distance between two trees, which is unable to precisely reveal the similarity of two trees. Consider the situation of two comparisons where one compares two 1000-node trees and the other compares two 10-node trees. If the TED values under the two comparisons are both 10, the proportions of changed nodes are 1% and 100%, respectively. It is obvious that the smaller the proportion, the more similar the two trees. Second, when we read web pages, we do not read only the detail of a single block. Instead, we read the sub tree of each block. This is because in a web page, all the descendants of a block (if exist) are placed above the block, thus the visible part of that block is actually the sub tree. Therefore, a TED measurement, which maps single nodes instead of sub trees, is not precise.

To solve these problems, we employ the *extended subtree similarity* (EST) (Shahbazi and Miller 2014) to reflect the visual similarity between two block trees. This model normalizes the TED, with similarity ranging from 0.0 to 1.0, regardless of the sizes of the two trees. Particularly, 1.0 and 0.0 denote if two trees are identical or completely different, respectively. Furthermore, the EST model maps sub trees instead of tree nodes, which can be achieved by the new mapping rules (Shahbazi and Miller 2014):

1) sub tree mapping: EST maps both sub trees and single nodes;
2) one-time mapping: once two sub trees are mapped, the common sub trees of them are not allowed to be mapped again;

3) sub tree weight assignment: the weight of a map equals to the mean value of the two mapped sub trees' weights, and a sub tree's weight equals to the number of nodes it has.

The EST similarity of two block trees X and Y is calculated by (4-10):

$$S^*(X,Y) = \frac{\sqrt[\alpha]{\sum_{m_k \in M} \beta_k \times W(m_k)^\alpha}}{max(|X|,|Y|)}, \tag{4-10}$$

where, $|X|$ and $|Y|$ represents the numbers of nodes in X and Y; $W(m_k)$ is the weight of a mapping m_k; α is a coefficient that adjusts the relation among mappings according to their sub tree sizes; and β_k is a geometrical parameter reflecting the importance of m_k with respect to the position of k in X and Y. $\beta_k = 1$ when the node x_k and y_k have the same depth in X and Y, otherwise $\beta_k = \beta_0$, which equals to a constant within the range of $(0,1)$.

Figure 4.7 shows an example of the method, with the visual incompatibility detection and similarity estimation between the two trees X and Y being conducted as follows.

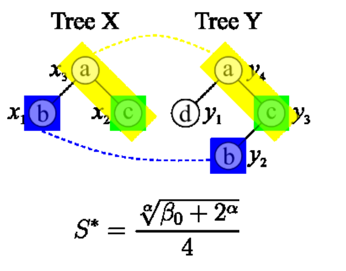

$$M_x = \begin{bmatrix} \emptyset & \{x_1\} & \emptyset & \emptyset \\ \emptyset & \emptyset & \{x_2\} & \emptyset \\ \emptyset & \emptyset & \emptyset & \{x_2, x_3\} \end{bmatrix} \qquad M_y = \begin{bmatrix} \emptyset & \emptyset & \emptyset \\ \{y_2\} & \emptyset & \emptyset \\ \emptyset & \{y_3\} & \emptyset \\ \emptyset & \emptyset & \{y_3, y_4\} \end{bmatrix}$$

$$LS_x = \begin{bmatrix} \binom{1}{2} & \binom{3}{4} & \binom{3}{4} \end{bmatrix} \qquad LS_y = \begin{bmatrix} \emptyset & \binom{1}{2} & \binom{3}{4} & \binom{3}{4} \end{bmatrix}$$

$$W_x = \begin{bmatrix} 0 & 1 & 0 & 0 \\ 0 & 0 & 0 & 0 \\ 0 & 0 & 0 & 2 \end{bmatrix} \qquad W_y = \begin{bmatrix} 0 & 0 & 0 \\ 1 & 0 & 0 \\ 0 & 0 & 0 \\ 0 & 0 & 2 \end{bmatrix}$$

Figure 4.7 Example of the Visual Incompatibility Detection and Similarity Estimation

1) All the nodes from the two trees need to be attached with numbers. This numbering scheme is done by post-order traversal. Therefore, the nodes b, c, a in Tree X are denoted as x_1, x_2 and x_3, and nodes d, b, c, a in Tree Y are denoted as y_1, y_2, y_3 and y_4, respectively.

2) All possible mapping relationship need to be located before further analysis. As mentioned above, the mapping scheme considers subtrees instead of nodes, and therefore, the final mapping results include $m_1 = \{x_1\} \leftrightarrow \{y_2\}$ (subtree of b, marked by the blue rectangle), $m_2 = \{x_2\} \leftrightarrow \{y_3\}$ (subtree of c, marked by the green rectangle), and $m_3 = \{x_2, x_3\} \leftrightarrow \{y_3, y_4\}$ (subtree of a-c, marked by the yellow rectangle).

3) The mapping results are saved in two matrices M_x and M_y, where each cell of the matrices records the mapping relationship between the corresponding nodes. For example, the subtree of a-c has the root node a, which is the 3rd node in X and the 4th node in Y. Hence, the grid in the 3rd row and 4th column of M_x stores $\{x_2, x_3\}$, and the grid in 4th row and 3rd column of M_y stores $\{y_3, y_4\}$. If the corresponding nodes does not map, then the grid is an empty set.

4) Now the complement set of nodes from the mapping results indicates the visual incompatibilities. In this case, the node d in Y – the corresponding content only appears in the web page instance Y but not in X.

5) According to the one-time mapping rule, common subtrees are to be avoided in order to construct the largest subtree mapping. Of all the mapped subtrees, x_1 only belongs to m_1. Therefore, the first element of LS_x stores this mapping relationship, denoted as $\binom{1}{2}$. y_1 does not belong to any mapping relationship, so the first element of LS_y stores an empty set. Both x_2 and x_3 in X (also y_3 and y_4 in Y) belong to m_3, and herein, the 2nd and 3rd elements of LS_x (and the 3rd and 4th elements of LS_y) store this mapping relationship.

6) Weights of each node in X and Y are assigned by comparing M_x with LS_x, and M_y with LS_y. LS_x has 1 of $\binom{1}{2}$, 0 of $\binom{2}{3}$, and 2 of $\binom{3}{4}$. As such, the weight matrix W_x has the weights of $\{x_1\}$, $\{x_2\}$ and $\{x_2, x_3\}$ as 1, 0 and 2, respectively. Similarly, the weight matrix W_y has the weights of $\{y_2\}$, $\{y_3\}$ and $\{y_3, y_4\}$ as 1, 0 and 2, too.

7) $\beta_1 = 1$ as the depth of node b in X and Y are not the same. However, the depth of node a in X and Y are the same, and accordingly, we can get $\beta_3 = \beta_0$. α and β_0 are set to 1.6 and 0.5 respectively following the recommendations in (Shahbazi and Miller 2014), hence, the similarity between X and Y equals to 0.55.

3.2 The Validity Experiment

This experiment is to evaluate the validity of the empirical measurement. It is repeated for 15 rounds. During the initialization of each round, 100 different web pages are randomly retrieved from Alexa's statistics of worldwide top sites (http://www.alexa.com/topsites, the web pages were crawled on January 14, 2016) and manually classified by human volunteers according to their visual appearance. Cross-comparing each pair of the web pages produces $\binom{100}{2} = 4950$ EST records. As shown in **Figure 4.8**, these records are displayed in two boxplots, where the first plot illustrates EST values between two similar pages and the second plot denotes those between two different pages.

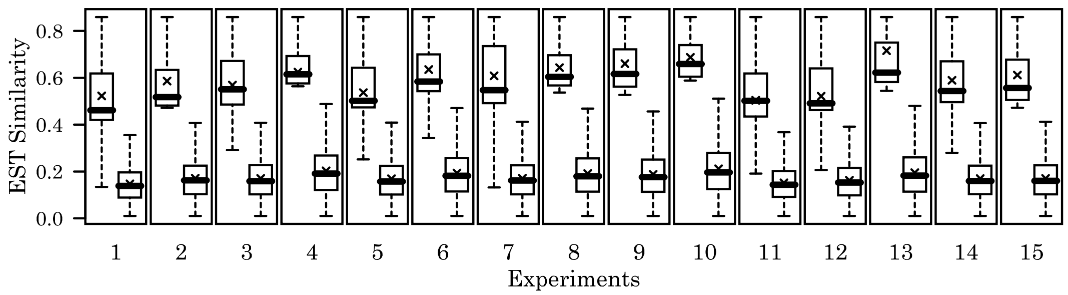

Figure 4.8 EST Similarity of All 15 Rounds

According to the boxplots, group 1 in each round demonstrates larger values than group 2. The Mann–Whitney U test and the Cliff's Delta effect size estimation are conducted to quantitatively analyze the EST records. Both of the two tests are conducted with a confidence level of 0.95. According to the results in **Table 4.4**, all the p-values are smaller than 0.05, and all the delta estimate values are categorized as "large" (Romano et al. 2006). This concludes that the EST similarities between similar web page pairs are higher than those between different pairs, indicating this measurement is able to identify web page visual similarity.

Table 4.4 Results of Mann–Whitney U Test and Cliff's Delta Effect Size Estimation

Experiment	**1**	**2**	**3**	**4**	**5**
p-value	1.64E-28	3.26E-26	7.09E-19	2.28E-24	3.88E-24
Delta Estimate	0.9276	0.8368	0.8817	0.8531	0.8007
Experiment	**6**	**7**	**8**	**9**	**10**
p-value	4.76E-26	1.18E-18	1.53E-17	1.64E-23	1.19E-32
Delta Estimate	0.8664	0.8515	0.8730	0.8737	0.8712
Experiment	**11**	**12**	**13**	**14**	**15**
p-value	2.70E-19	2.99E-17	4.25E-13	1.11E-24	2.22E-17
Delta Estimate	0.8132	0.7942	0.9619	0.9070	0.8824

We categorize the EST records, of the 15 rounds, into the following four categories:

- *true positive* (TP): two similar pages are identified as similar correctly;
- *true negative* (TN): two different pages are identified as different correctly;

- *false positive* (FP): the situation where two different pages are identified as similar incorrectly; and
- *false negative* (FN): two similar pages are identified as different incorrectly.

Five metrics based on the above four categories are investigated to find out the optimal threshold, namely: *precision* (*positive predictive value*, PPV), *negative predictive value* (NPV); *recall* (*true positive rate*, TPR), *true negative rate* (TNR), and *accuracy* (Olson and Delen 2008). To be specific, PPV represents the ratio of similar page pairs being correctly identified over all similar page pairs; while NPV reflects the proportion of different page pairs being identified as different. Similarly, TPR denotes the ratio of similar page pairs being correctly identified over all page pairs identified as similar; while TNR refers to the fraction of different page pairs over all the identified different page pairs. Accuracy is the ratio of correct identification to all identifications.

Figure 4.9 shows how the metrics vary according to the shift of the threshold. From the left side figure, we can find that with the increase of the threshold, 0.40 is a turning point of TP, FP, FN, and TN. Prior to this turning point, FP decreases significantly and TN increases quickly; while after this point, TP has a sharp decrease and FP has a dramatic increase. A similar pattern can be seen from the right side figure, too. This indicates that 0.40 is a best point for a threshold.

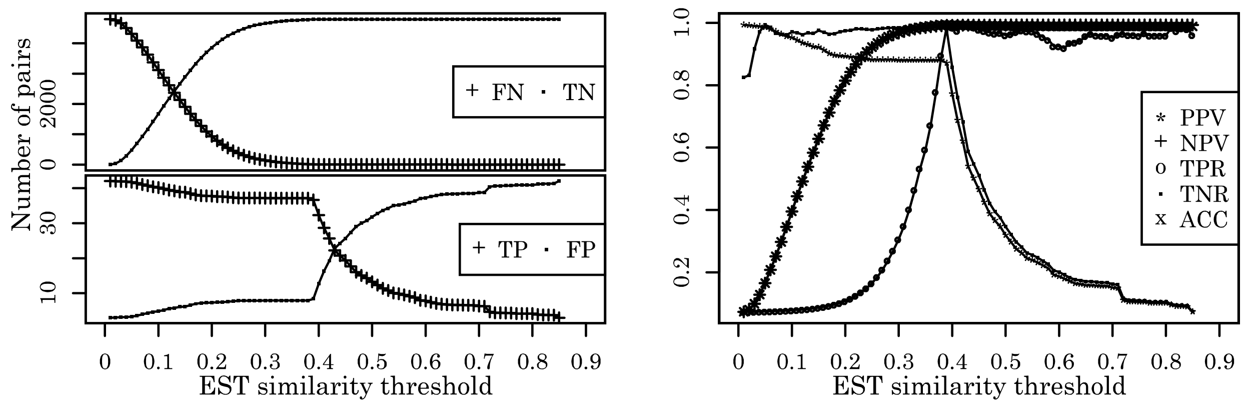

(a) TP, FP, FN and TN (b) PPV, NPV, TPR, TNR and Accuracy

Figure 4.9 Performance of the Empirical Measurement on Different Thresholds

4 Detection of Cross-Browser Differences

The differences are detected by a series of experiments, where the EST similarity value of each web page pair is calculated by comparing the corresponding block trees. A static web page contains the same content for every loading, so the potential cross-browser differences refer only to rendering style differences. However, due to many modern pages having dynamic content, they change during every refreshing. Therefore, this dynamic content should also be part of the detection targets.

In fact, there are two types of dynamic content: *page-related content* (for example, weather status in a weather report page, or breaking news items in a newspaper page) and *advertisements*. Although the first type is determined by the server side and cannot be controlled by browsers, the second type is able to be filtered. Consequently, the experiments are designed to proceed twice, where the first time is to evaluate the original version of the web pages, and the second time is to test the ad-free version. During the advertisement filtering in the second experiment, we employ “Adblock Plus” and maximize its filter by enabling all its supported languages. We do not add any customized filters.

4.1 Experimental Setups

The test sets of the two experiments use the same URL pool, which contains 1000 different records retrieved from Alexa's top web sites (crawled on August 20th, 2016). These web pages covered 360 different web sites, and the average number of pages per site is 2.78. "bitauto.com" contains 31 pages in the pool, which is the largest number. 191 of the 360 sites contribute only one page. The distribution is shown in **Figure 4.10**.

The first step of each experiment is the data retrieval. Two of the most popular browsers, Google Chrome and Mozilla Firefox, are selected for cross-browser difference detection, and they are further tested on both Linux and Windows platforms. Therefore, there are four scenarios in each experiment, Chrome in Linux (CL), Chrome in Windows (CW), Firefox in Linux (FL), and Firefox in Windows (FW). During the retrieval of each scenario, we compose extensions compatible for the two browsers to parse the 1000 web pages into a set of block trees. Specially, we set the browser's inner window size to 1024×768 to eliminate potential side effects to the difference detection. Additionally, Adblock Plus is enabled in the second experiment to filter any possible advertisements from the original web pages. The four scenarios finally collect four sets of block trees for each experiment.

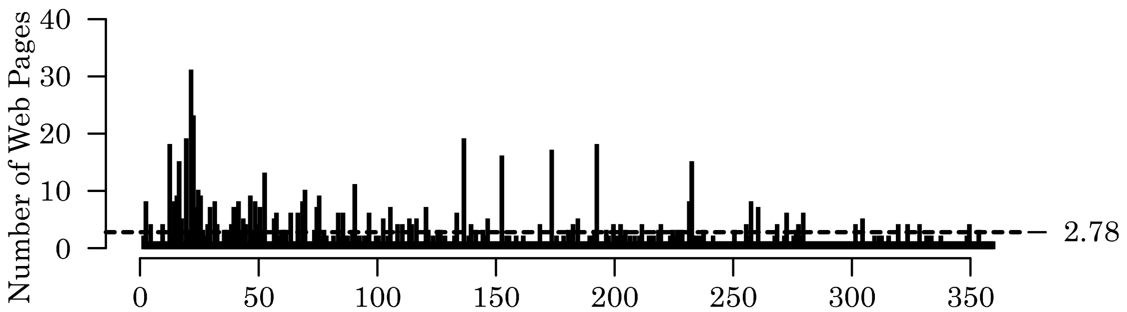

Figure 4.10 Distribution of Test Cases

The second step is tree comparison. We cross-compare the corresponding block trees of a web page by fixing either the browser or the platform. That is, by fixing the browser, we will compare results in different platforms (i.e., CL vs. CW and FL vs. FW); and by fixing the platform, we compare results in different browsers (i.e., CL vs. FL and CW vs. FW).

Finally, we select the WebCompare algorithm (Alpuente and Romero 2009) as the benchmark to test the performance of the proposed algorithm. This is because the WebCompare algorithm (1) provides a compatible output; and, (2) can be considered as the current state of the art. Many other algorithms were also considered as one of the comparisons, but are finally removed from the experiments; the rationale for this decision is discussed in Section 5.

4.2 Experimental Results

Figure 4.11 shows the distribution of EST and WebCompare similarity values for each comparison scenario. Each bar in the histograms indicates the number of records that is greater than or equal to the corresponding value as indicated in the x-axis, and each curve shows the accumulate number of records that are less than the next value. For example, the highest bar in the first chart shows that there are 450 EST values equal to "1.0", and the corresponding dot (the second dot from the right side) of the curve is 550 – the summation of the two numbers is exactly 1000.

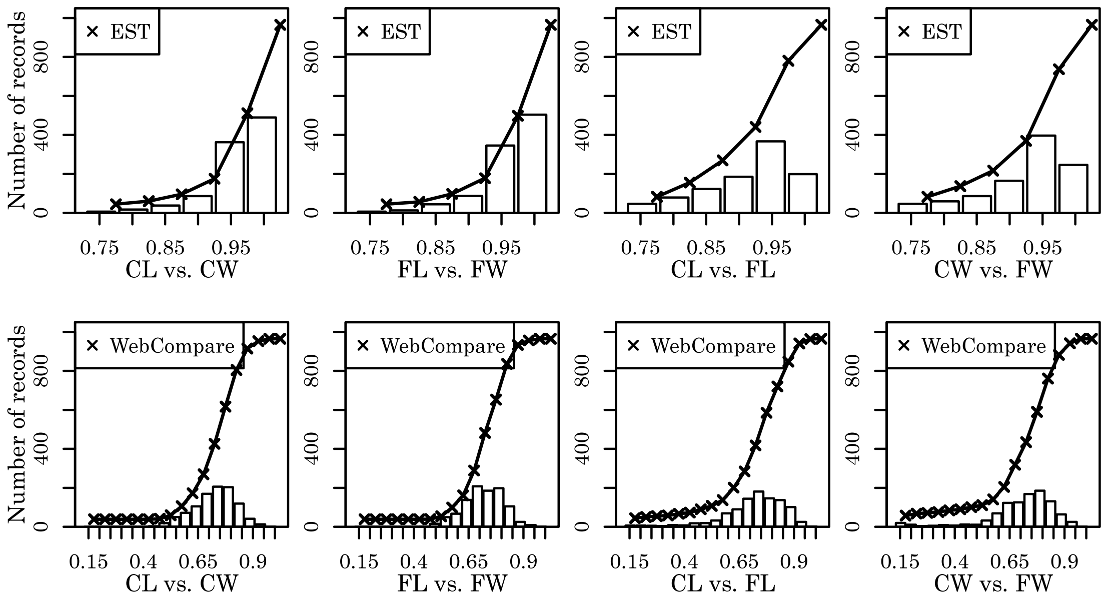

Figure 4.11 Distributions of the Experimental Results for Original Web Pages

According to the figure, the distribution of the four scenarios reveals the following patterns: (a) All of the EST similarity values are greater than or equal to 0.75, and most of them are greater than or equal to 0.9, indicating that the web pages are renderer similarly by the two browsers on the two platforms. (b) Less than 60% of all the 1000 EST values are 1.0, meaning that the cross-browser visual differences exist in the test cases and are detected by the measurement. (c) The same-browser-comparisons generally produce higher similarity estimates than same-platform-comparisons. And, (d) the EST similarity shows higher values than the WebCompare similarity: most of the WebCompare values are between 0.5 to 0.9, with the lowest value of 0.1095 and only one value of 1.0. That is WebCompare only believes that in one situation is a web page rendered identically across two browsers.

To figure out whether the two measurements are consistent with human perceptions, we asked five volunteers to view the screenshot images of all the previous test cases and then make further comparisons. They were required to mark "same" or "different" for each pair of web pages. The identification results from all of the volunteers were identical. This is because it is possible for a human to assert whether two screenshot images are identical or not, but it is difficult for humans to assert numerically how much dissimilar they are (this is exactly the reason why we need a numeric measurement to evaluate the similarity of web pages). By comparing the previous (EST/WebCompare) values with the volunteers' identifications, a confusion matrix can be built for the following scenarios: "both EST/WebCompare value and the volunteer identification of the two pages are same", "EST/WebCompare value of two web pages shows different but the volunteer identifies as same", "both EST/WebCompare value and the volunteer identification of the two pages are different", and "EST/WebCompare value of the pages shows same but volunteer identifies as different". As shown in **Table 4.5**, the EST similarity can identify the web page differences with the precision and accuracy over 90% and 70%, respectively. As the comparison, WebCompare's precision and accuracy are all below 50%. This is because the WebCompare identifies very few identical comparisons, leading to the low TP rate.

Table 4.5 Comparison of Human Perceptions and Calculation Results (Original Web Pages)

		TP	FP	TN	FN	Precision	Accuracy
EST	**CL vs. CW**	256	5	505	234	0.9808	0.7610
	FL vs. FW	263	2	494	241	0.9925	0.7570
	CL vs. FL	97	2	799	102	0.9798	0.8960
	CW vs. FW	137	1	753	109	0.9928	0.8900
WebCompare	**CL vs. CW**	13	486	479	22	0.0261	0.4920
	FL vs. FW	9	575	400	16	0.0154	0.4090
	CL vs. FL	26	444	456	74	0.0553	0.4820
	CW vs. FW	25	534	363	78	0.0447	0.3880

As mentioned in the previous subsection, two types of dynamic content affect the results, and the advertisements can be controlled in the experiment. The distribution of the Ad-free version of the 1000 web pages is illustrated in **Figure 4.12**. By comparison, **Figure 4.11** and **Figure 4.12** reveal similar patterns as discussed above. Furthermore, after removing the advertisements, the EST similarity values become higher. For example, the number of EST records with value 1.0 in **Figure 4.11** is 450, but it increases to 490 in **Figure 4.12**. The precisions and accuracies are listed in **Table 4.6**, which shows similar pattern with **Table 4.5**, indicating the efficiency evaluation using TP, FP, TN, FN is consistent and stable.

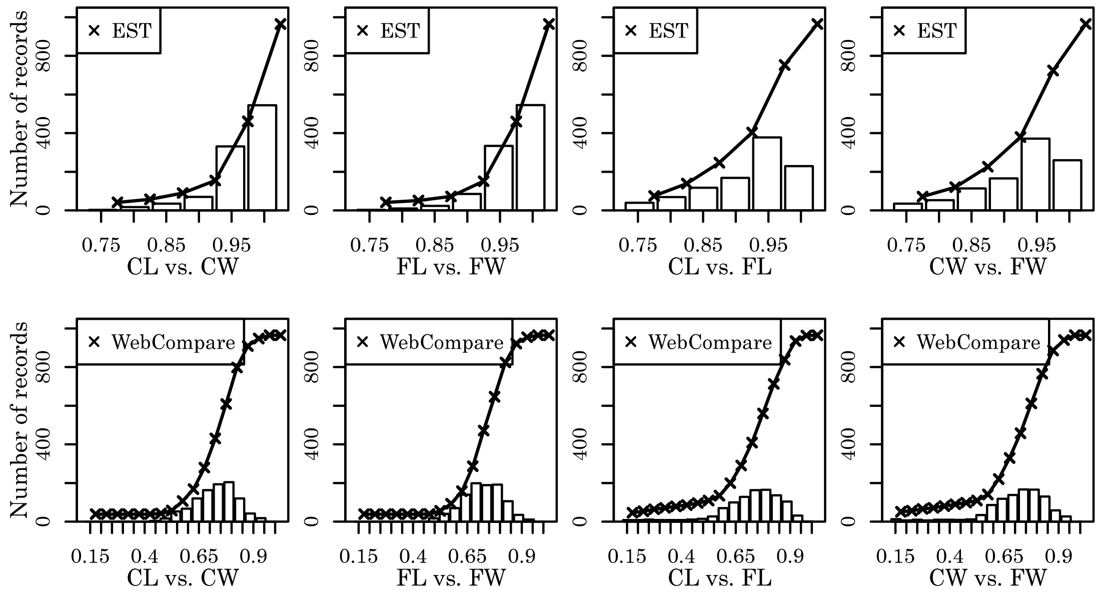

Figure 4.12 Distributions of the Experimental Results for Ad-Free Web Pages

Table 4.6 Comparison of Human Perceptions and Calculation Results (Ad-Free Web Pages)

		TP	**FP**	**TN**	**FN**	**Precision**	**Accuracy**
EST	**CL vs. CW**	270	7	449	274	0.9747	0.7190
	FL vs. FW	277	5	450	268	0.9823	0.7270
	CL vs. FL	121	1	770	108	0.9918	0.8910
	CW vs. FW	139	2	738	121	0.9858	0.8770
WebCompare	**CL vs. CW**	18	416	546	20	0.0415	0.5640
	FL vs. FW	11	409	562	18	0.0262	0.5730
	CL vs. FL	32	549	343	76	0.0551	0.3750
	CW vs. FW	27	375	522	76	0.0672	0.5490

4.3 Case Studies

Figure 4.13 shows the home page of Google.ca in different browsers and platforms. It is evident that the two pages in the same browser are rendered identically, but it shows noticeable differences between the Chrome version and the Firefox version. Both Chrome versions have a microphone icon at the right side of the search bar (i.e., the icon marked by the blue rectangle); and both Firefox versions have an extra popup message window (i.e., the top right block marked by the red rectangle). By parsing the sources of the four pages, the results are illustrated in **Table 4.7**, where the "visual tree size" refers to the number of visible elements in the original DOM tree. Quantitatively, the sizes of the three types of trees are all the same for pages rendered by the same browsers, but the sizes between Chrome version and Firefox version are different. The EST values of the first two comparisons are both the highest possible values (i.e. 1.0000), and the values of the second comparisons are both 0.8134, which is relatively low. Interpretations of these values are consistent with **Figure 4.13**. As the comparison, however, the WebCompare similarity approach provides lower results; in addition, the same-browser-comparisons fail to reflect the identicalness.

Table 4.7 Case Study of Google.ca

	CL	**CW**	**FL**	**FW**
DOM Tree	343	343	299	299
Visual Tree	30	30	34	34
Block Tree	14	14	16	16
	CL vs. CW	**FL vs. FW**	**CL vs. FL**	**CW vs. FW**
EST	1.0000	1.0000	0.8134	0.8134
WebCompare	0.8167	0.8382	0.7188	0.7188

The next case, the home page of JSON tutorials from w3schools (http://www.w3schools.com/json/default.asp), illustrates how the advertisements cause cross-browser differences. In **Figure 4.14**, the screenshots of the original pages are partially cropped and only the differences are the four pieces of advertisements marked in red rectangles. Due to this dynamic content, the EST values of the four comparison scenarios are 0.9368, 0.9343, 0.8988, and 0.8948, respectively; and after the removal of the advertisements, all the EST values are 1.0000, as shown in **Table 4.8**. The WebCompare results show slight increment after the advertisement filtering, however are still lower than the EST.

Table 4.8 Case Study of W3schools' JSON Home Page

	CL vs. CW	**FL vs. FW**	**CL vs. FL**	**CW vs. FW**
EST (Original)	0.9368	0.9343	0.8988	0.8948
WebCompare (Original)	0.6877	0.6442	0.7470	0.5731
EST (Ad-Free)	1.0000	1.0000	1.0000	1.0000
WebCompare (Ad-Free)	0.6950	0.6467	0.7490	0.5772

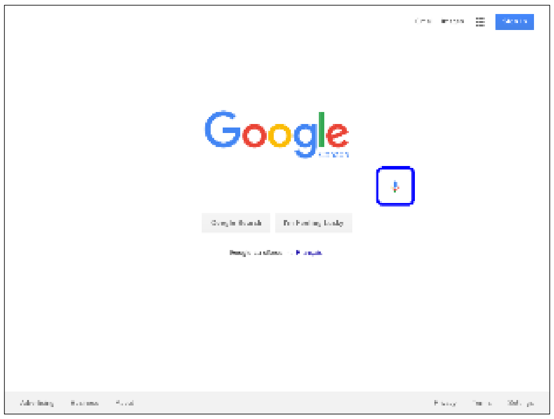

(a) Chrome in Linux

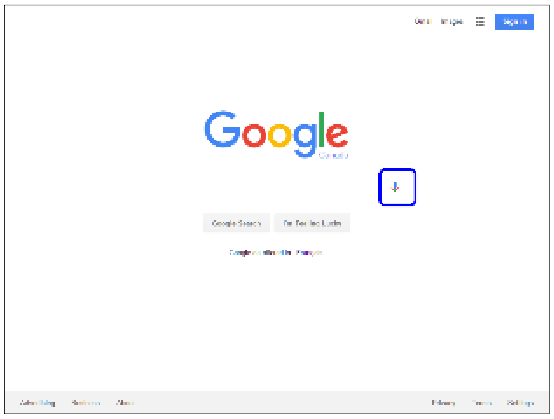

(b) Chrome in Windows

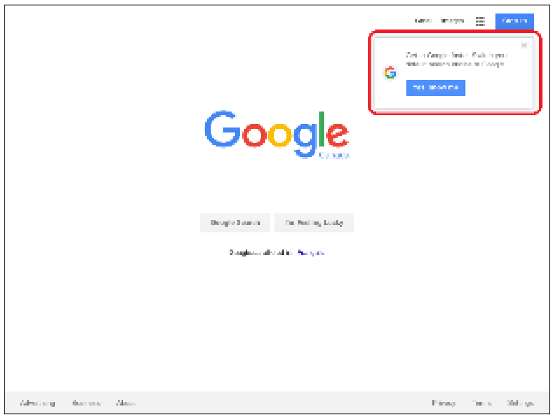

(c) Firefox in Linux

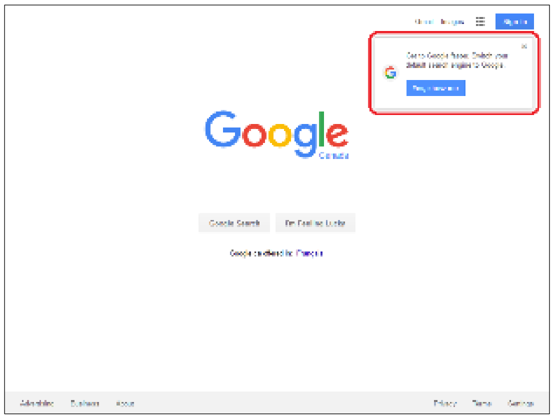

(d) Firefox in Windows

Figure 4.13 Screenshots of Google.ca in the Four Browser Scenarios

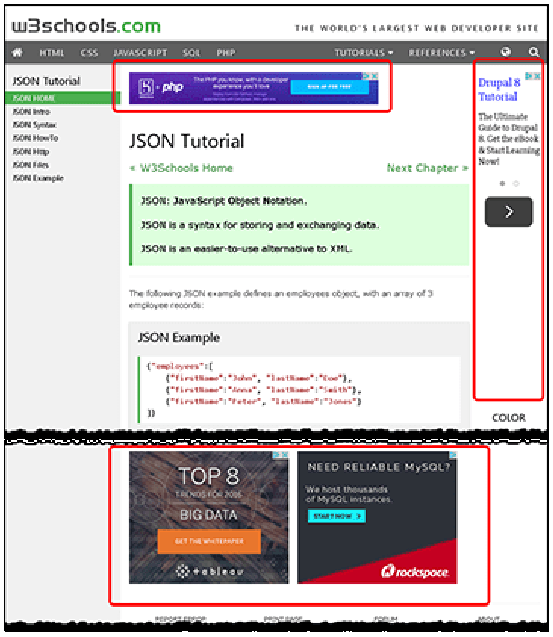

JSON Tutorial

JSON: JavaScript Object Notation.

JSON is a syntax for storing and exchanging data.

JSON is an easier-to-use alternative to XML.

The following JSON example defines an employees object, with an array of 3 employee records:

JSON Example

```
{"employees":[
    {"firstName":"John", "lastName":"Doe"},
    {"firstName":"Anna", "lastName":"Smith"},
    {"firstName":"Peter", "lastName":"Jones"}
]}
```

(a) Chrome in Linux

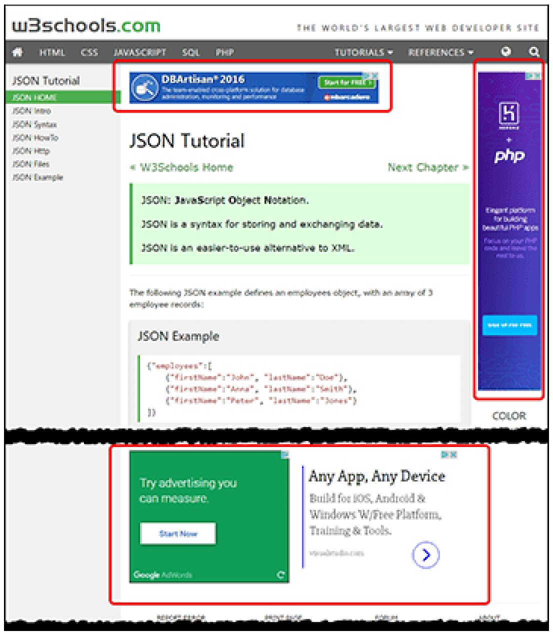
w3schools.com
THE WORLD'S LARGEST WEB DEVELOPER SITE
HTML CSS JAVASCRIPT SQL PHP TUTORIALS REFERENCES
JSON Tutorial
JSON HOME
JSON Intro
JSON Syntax
JSON HowTo
JSON Http
JSON Files
JSON Example
« W3Schools Home
Next Chapter »
COLOR

JSON Tutorial

JSON: JavaScript Object Notation.

JSON is a syntax for storing and exchanging data.

JSON is an easier-to-use alternative to XML.

The following JSON example defines an employees object, with an array of 3 employee records:

JSON Example

```
{"employees":[
    {"firstName":"John", "lastName":"Doe"},
    {"firstName":"Anna", "lastName":"Smith"},
    {"firstName":"Peter", "lastName":"Jones"}
]}
```

DBArtisan® 2016
Start for FREE
embarcadero
php
Elegant platform for building beautiful PHP apps
Try advertising you can measure.
Start Now
Google AdWords
Any App, Any Device
Build for iOS, Android & Windows W/Free Platform, Training & Tools.

(b) Chrome in Windows

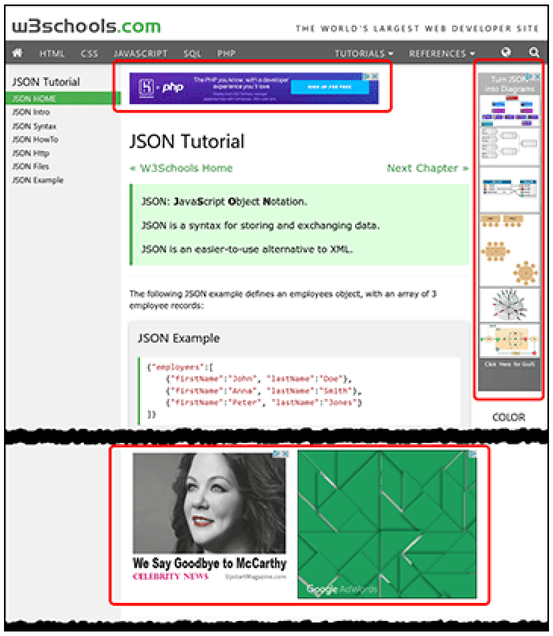

JSON Tutorial

JSON: JavaScript Object Notation.

JSON is a syntax for storing and exchanging data.

JSON is an easier-to-use alternative to XML.

The following JSON example defines an employees object, with an array of 3 employee records:

JSON Example

```
{"employees":[
    {"firstName":"John", "lastName":"Doe"},
    {"firstName":"Anna", "lastName":"Smith"},
    {"firstName":"Peter", "lastName":"Jones"}
]}
```

(c) Firefox in Linux

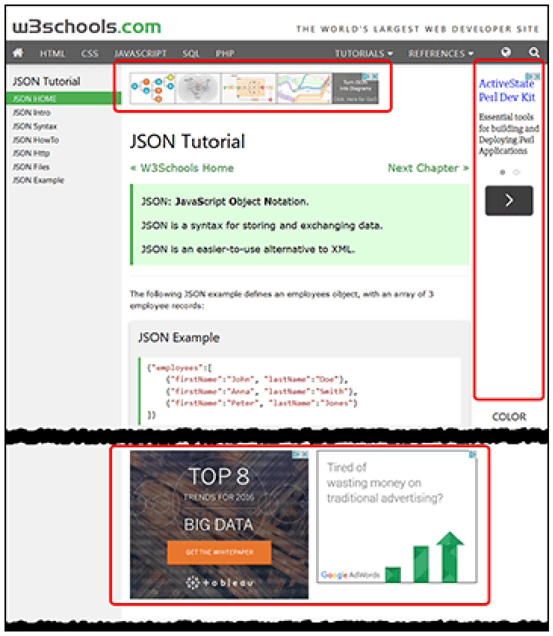

JSON Tutorial

JSON: JavaScript Object Notation.

JSON is a syntax for storing and exchanging data.

JSON is an easier-to-use alternative to XML.

The following JSON example defines an employees object, with an array of 3 employee records:

JSON Example

```
{"employees":[
    {"firstName":"John", "lastName":"Doe"},
    {"firstName":"Anna", "lastName":"Smith"},
    {"firstName":"Peter", "lastName":"Jones"}
]}
```

ActiveState Perl Dev Kit
Essential tools for building and Deploying Perl Applications
TOP 8
TRENDS FOR 2016
BIG DATA
GET THE WHITEPAPER
tableau
Tired of wasting money on traditional advertising?
Google AdWords

(d) Firefox in Windows

Figure 4.14 Screenshots of W3schools' JSON Home Page in the Four Browser Scenarios

The third case is the home page of Amazon.ca, which reveals the effects of the page-related dynamic content. The top search bar, the big poster and the footer sections of the four versions are exactly the same, so they are cropped in **Figure 4.15**. However, the rest of the pages are different. For simplicity, we name the different blocks with unique numbers, where identical blocks have the same value. As shown in the figure, there are totally 21 different blocks in the four pages. Through comparing each pair of pages, it is concluded that the pages on the same platforms are most similar. That is, subfigure (a) and (c) are the first similar pair, and subfigure (b) and (d) are the second similar pair. For example, subfigure (a) has blocks 1 through 13, and subfigure (c) also has these blocks except block 9. The EST similarity values reveal the same results as well. Specifically, the EST values are 0.8765, 0.8734, 0.9788 and 0.9156, respectively. The WebCompare results are 0.6494, 0.7016, 0.6153 and 0.8207, indicating that it is able to identify the differences. However, it provides a lower similarity value than EST. In addition, the third scenario (CL vs. FL) is considered as the most similar comparison, however, the corresponding WebCompare value is smaller than the fourth one, which is viewed as an inconsistency.

The fourth case is the home page of FedEx.com, as shown in **Figure 4.16Error! Reference source not found.**. The only visual difference of the four versions is the select box in the middle: the two Windows versions have a solid white background while the two Linux versions are gradient gray; besides, the Firefox version in Linux has a larger height than the other three. The values of EST similarity further reflect the above observations. More specifically, the value between CL and CW is 0.9003; the values between FL and FW, CL and FL are both 0.8188; and the value between CW and FW is 1.0. In comparison, the values of the WebCompare similarity are more than 30% lower than the EST similarity, namely 0.5345, 0.5079, 0.1767 and 0.1095 for each comparison scenario, respectively.

Note that the two browsers in Windows render the web page identically, however WebCompare shows only 10% of the similarity.

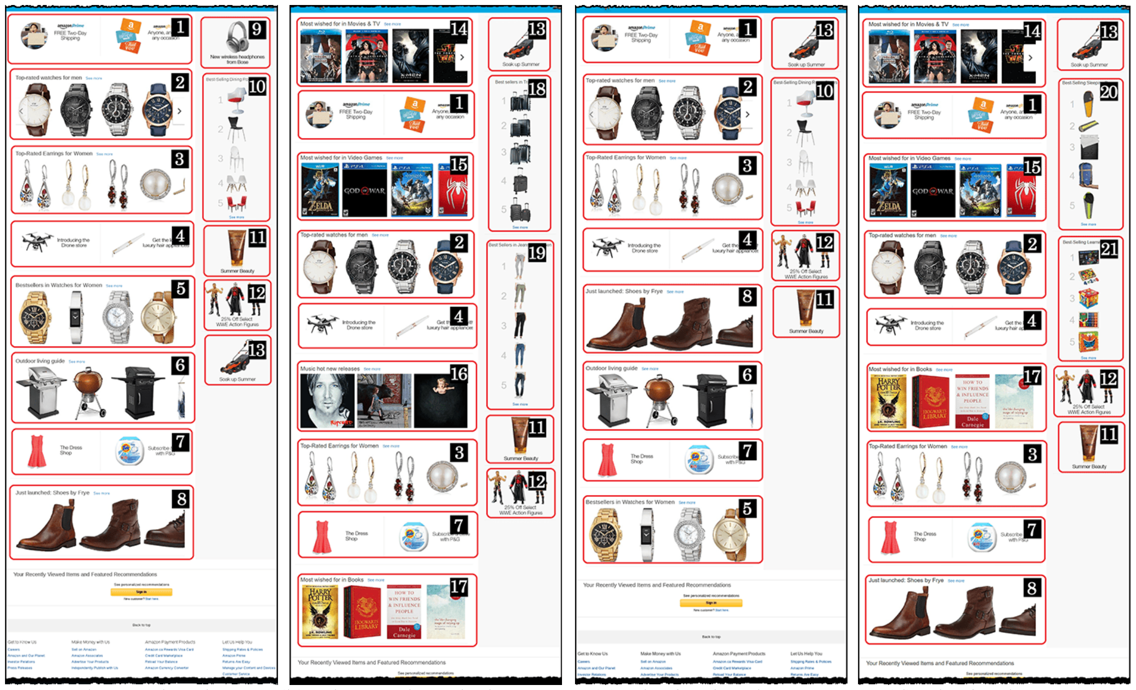

(a) Chrome in Linux (b) Chrome in Windows (c) Firefox in Linux (d) Firefox in Windows

Figure 4.15 Screenshots of Amazon.ca in the Four Browser Scenarios

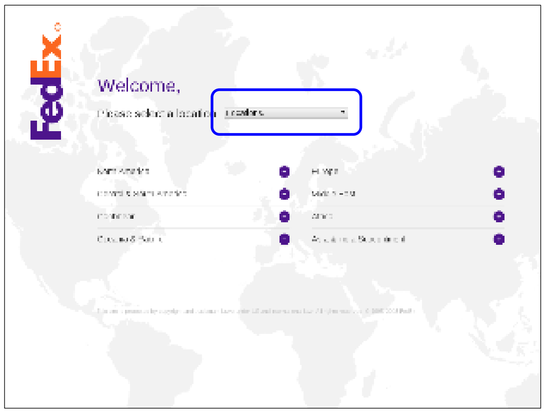

(a) Chrome in Linux

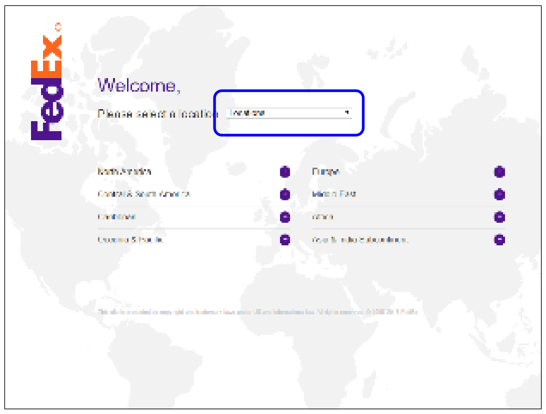

(b) Chrome in Windows

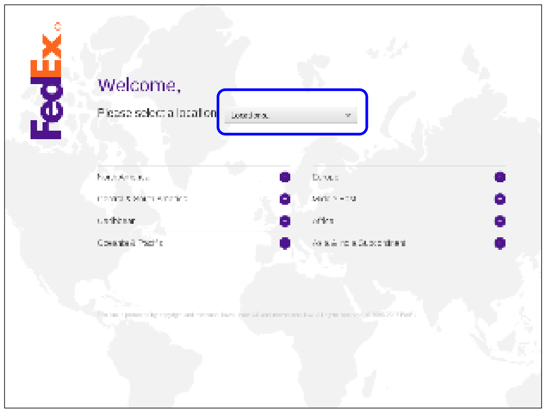

(c) Firefox in Linux

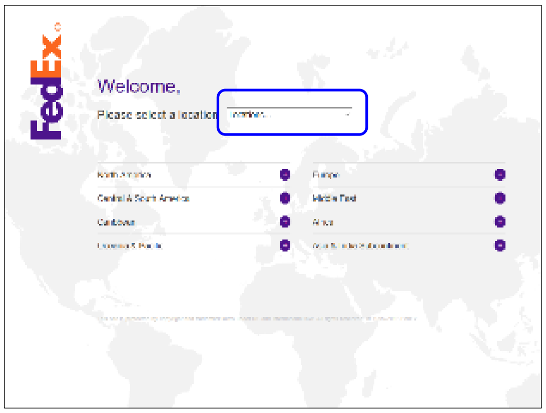

(d) Firefox in Windows

Figure 4.16 Screenshots of FedEx.com in the Four Browser Scenarios

5 Related Work

The area of web page visual analysis is widely adopted by researchers. Michailidou et al. (2008) investigated the user perception of visual complexity and aesthetic appearance of web pages. They further proposed the definition of visual complexity for web pages by empirical experiment using card sorting and triadic elicitation (Harper, et al. 2009). Eraslan et al. (2016) performed Scanpath trend analysis by clustering users' eye tracking scanpaths according to visual elements of a web page. Wu et al. (2016) used the structural SVM and a multitask fusion learning model to conduct multimodal web aesthetics assessment. These researchers analyzed web page visual elements to determine whether the visualization a web page is clear and easy to read. Similarly, in this chapter, we analyze the visual elements of web pages. However, as stated in the introduction section, we focus on cross-browser issues from the angle of web page visual similarity. Therefore, we will mainly investigate the work in the literature related to web page visual similarity, and pay less attention on behavioral incompatibilities. A number of papers have focussed on the detection of visual cross-browser issues.

Fu et al. (2006) evaluated web page similarity by using the Earth Mover's Distance (EMD) metric. They treated different web pages as pure images, normalized them into squares with the same size, downgraded the pixel colors with different granularities as the signature, and finally determined similarity by the signatures. The size matrices in the chapter included 100*100 and 10*10, which potentially downgraded the precision of the screenshot images. In our research, we retrieve all visual features while keeping the web pages in their original resolution, in order to prevent precision loss.

Saar et al. (2014) proposed another detection methodology purely base on image processing, the Browserbite. The original web pages were first rendered in different browsers and operating systems so that the precise screenshot images can be retrieved. The images were then split into segments by pixel-level visual features such as discontinuity or color changes. Pairwise comparisons were finally conducted among the segments for cross-browser incompatibility detection. Treating web pages as images ultimately reflects how people seeing and processing the pages, however it ignores all the structural information and thus may introduce false identifications. For example, if a logo image of a web site has both texts and figures, then image processing could split the two components apart. In our research, we determined to preserve the structural information in order to improve the accuracy of segmentation.

Mesbah and Prasad (2011) proposed an automated testing framework to detect cross-browser incompatibilities in both visual and behavioral aspects. They defined and limited the cross-browser compatibility issues in a novel aspect that both human users and the client-side browsers can find, and conducted detections within this aspect.

Rao and Ali (2015) exploit the speed up robust features (SURF) detector, a computer vison technique, to extract discriminative feature points of images, to compare the similarity of suspicious and legitimate web pages. They first create a list of legitimate web pages as the base pool, compare the suspicious web pages with the web pages in the base pool, and then updated the base pool based upon the results of the comparison. When comparing images, the similarity score is calculated for the screenshots of both the suspicious and legitimate web pages by the SURF algorithm, and a threshold score is used as a judging standard. This is an interesting method for computing web page similarity, but the determination of a threshold score is difficult.

Takama and Mitsuhashi (2005) investigate web page visual features, and develop a method to calculate visual similarity between the top pages of two web sites. In web page layout processing, they divide each web page into several regions and labeled them as text, image, or mixture. In the next procedure, they perform graph matching based upon a layout processing procedure. Finally, visual similarity is calculated according to the graph matching results. Their primary contribution is considering visual features when comparing web page similarity and their proposed method works well for this purpose.

Unfortunately, they only focus on static images and do not take into account other multimedia elements found in web pages.

Shi, et al. (2008) investigate text similarity computation and extended the concept of similarity computation into multimedia elements. They put forward a multi-layer semantic model by describing each multimedia type in a single layer according to its characteristics and user demands. A limitation of this model is that it ignores the relationship among different multi-media content and may lead to inaccuracies of similarity computation. The image in terms of visual similarity analysis is difficult to handle.

Choudhary et al. (2010) investigated cross-browser issues by the WebDiff algorithm. They further improved their research by combining the WebDiff with CrossT to propose new algorithms, namely CrossCheck and X-Pert (2012, 2013). Detection of the visual incompatibilities from these algorithms were all the same. They identified the content by cropping the screenshot image with DOM coordinates, and then compared the similarity based on the color histogram of the cropped sub-images. Screenshots reflect the final representation of web pages; however, they will potentially raise false positive results. For example, when a web page defines its text style with a font family such as “serif” instead of the concrete font, different browsers will interpret this with their own standards (and actually this standard can also be customized by the user). The users are not concern with the actual font at all, and many times they do not recognize such differences. In our research, we avoid using the screenshots of web pages. On contrary, we evaluated all the CSS values supported by different browsers, which consists of the comparison candidates of cross-browser visualization incompatibilities.

Alpuente and Romero (2009) developed the theory that first extracted web page content to different categories, namely “grp”, “row”, “col”, and “text”, and then merged and compressed the DOM tree. The visual similarity was then determined by the normalized version of the tree edit distance.

6 Conclusion and Future Work

Web applications have pervaded into almost every aspect of our daily life. However, with the advent of various versions of web browsers, issues abound, i.e., different web browsers cannot always render web pages and applications correctly. In order to detect whether web pages and applications are rendered the same across different web browsers, this chapter starts from the perspective of visual similarity, and develops a visual similarity measurement to evaluate the visual similarity of a web page or application across different web browsers.

We notice that the Gestalt laws of grouping are capable of revealing human’s mechanisms of visual processing; hence, we introduce these laws into the study of web page visual similarity by translating them into a computer compatible version. During this process, the measurements of proximity, color similarity, and image similarity are obtained through experimentation. To represent web pages correctly, we substitute the block tree from the DOM tree by extracting visual features and combining visible elements through the Gestalt laws of grouping (the code is available at https://github.com/MarcoXZh/GestaltBlockTree). The block tree is then employed to calculate web page visual similarity by the EST model. An experiment is conducted and a case is studied to use this measurement to detect cross-browser differences among a test set of 1000 web pages. The experimental data concludes positive results for this solution.

Acknowledgment

The authors thank China Scholarship Council (CSC) for financial supports.

References

María Alpuente and Daniel Romero. 2009. A visual technique for web pages comparison. Electronic Notes in Theoretical Computer Science 235 (2009), 3–18.

Jyotish Chandra Banerjee. 1994. Encyclopaedic Dictionary of psychological terms. MD Publications Pvt. Ltd., New Delhi.

Teh-Chung Chen, Scott Dick, and James Miller. 2010. Detecting visually similar web pages: Application to phishing detection. ACM Transactions on Internet Technology (TOIT) 10, 2 (2010), 5.

Shauvik Roy Choudhary, Mukul R Prasad, and Alessandro Orso. 2012. Crosscheck: Combining crawling and differencing to better detect cross-browser incompatibilities in web applications. In 2012 IEEE Fifth International Conference on Software Testing, Verification and Validation. IEEE, 171–180.

Shauvik Roy Choudhary, Mukul R Prasad, and Alessandro Orso. 2013. X-PERT: accurate identification of cross-browser issues in web applications. In Proceedings of the 2013 International Conference on Software Engineering. IEEE Press, 702–711.

Shauvik Roy Choudhary, Husayn Versee, and Alessandro Orso. 2010. WEBDIFF: Automated identification of cross-browser issues in web applications. In Software Maintenance (ICSM), 2010 IEEE International Conference on. IEEE, 1–10.

Francisco Claude, Antonio Farina, Miguel A. Mart´ınez-Prieto, and Gonzalo Navarro. 2010. Compressed qgram indexing for highly repetitive biological sequences. In BioInformatics and BioEngineering (BIBE), 2010 IEEE International Conference on. IEEE, 86–91.

Sukru Eraslan, Yeliz Yesilada, and Simon Harper. 2016. Scanpath Trend Analysis on Web Pag-es: Clustering Eye Tracking Scanpaths. ACM Transactions on the Web (TWEB) 10, 4 (2016), 20.

Anthony Y Fu, Wenyin Liu, and Xiaotie Deng. 2006. Detecting phishing web pages with visual similarity assessment based on earth mover's distance (EMD). IEEE transactions on dependable and secure computing 3, 4 (2006), 301–311.

Simon Harper, Eleni Michailidou, and Robert Stevens. 2009. Toward a definition of visual complexity as an implicit measure of cognitive load. ACM Transactions on Applied Perception (TAP) 6, 2 (2009), 10.

Alain Hore and Djemel Ziou. 2010. Image quality metrics: PSNR vs. SSIM. In Pattern Recognition (ICPR), 2010 20th International Conference on. IEEE, 2366–2369.

Daniel P. Huttenlocher, Gregory A. Klanderman, and William J. Rucklidge. 1993. Comparing images using the Hausdorff distance. Pattern Analysis and Machine Intelligence, IEEE Transactions on 15, 9 (1993), 850–863.

Kurt Koffka. 2013. Principles of Gestalt psychology. Vol. 44. Routledge.

Ming Li, Xin Chen, Xin Li, Bin Ma, and Paul Vit ´anyi. 2004. The similarity metric. Information Theory, IEEE Transactions on 50, 12 (2004), 3250–3264.

M. Ronnier Luo, Guihua Cui, and B. Rigg. 2001. The development of the CIE 2000 colour-difference formula: CIEDE2000. Color Research & Application 26, 5 (2001), 340–350.

Ali Mesbah and Mukul R. Prasad. 2011. Automated cross-browser compatibility testing. In Proceedings of the 33rd International Conference on Software Engineering. ACM, 561–570.

Eleni Michailidou, Simon Harper, and Sean Bechhofer. 2008. Visual complexity and aesthetic perception of web pages. In Proceedings of the 26th annual ACM international conference on Design of communication. ACM, 215–224.

Adriana Olmos and Frederick A. A. Kingdom. 2004. A biologically inspired algorithm for the recovery of shading and reflectance images. Perception 33, 12 (2004), 1463–1473.

Mateusz Pawlik and Nikolaus Augsten. 2015. Efficient computation of the tree edit distance. ACM Transactions on Database Systems (TODS) 40, 1 (2015), 3.

Routhu Srinivasa Rao and Syed Taqi Ali. 2015. A Computer Vision Technique to Detect Phishing Attacks. In Communication Systems and Network Technologies (CSNT), 2015 Fifth International Conference on. IEEE, 596–601.

Thiadmer Riemersma. 2008. Colour metric. (2008). Retrieved April 18, 2016 from http://www.compuphase.com/cmetric.htm

Jeanine Romano, Jeffrey D. Kromrey, Jesse Coraggio, and Jeff Skowronek. 2006. Appropriate statistics for ordinal level data: Should we really be using t-test and Cohen’s d for evaluating group differences on the NSSE and other surveys. In annual meeting of the Florida Association of Institutional Research. 1–33.

Tõnis Saar, Marlon Dumas, Marti Kaljuve, and Nataliia Semenenko. 2015. Browserbite: cross-browser testing via image processing. Software: Practice and Experience (2015).

Ali Shahbazi and James Miller. 2014. Extended subtree: a new similarity function for tree structured data. Knowledge and Data Engineering, IEEE Transactions on 26, 4 (2014), 864–877.

Peng Shi, Lianhong Ding, and Bingwu Liu. 2008. Similarity computation of Web pages. In Knowledge Acquisition and Modeling Workshop, 2008. KAM Workshop 2008. IEEE International Symposium on. IEEE, 777–780.

Herb Stevenson. 2012. Emergence: The Gestalt Approach to Change. (2012). Retrieved April 18, 2016 from http://www.clevelandconsultinggroup.com/articles/emergence-gestalt-approach-to-change.php

Yasufumi Takama and Noriaki Mitsuhashi. 2005. Visual similarity comparison for Web page retrieval. In Web Intelligence, 2005. Proceedings. The 2005 IEEE/WIC/ACM International Conference on. IEEE, 301–304.

Jeremy M. Wolfe, Keith R. Kluender, Dennis M. Levi, Linda M. Bartoshuk, Rachel S. Herz, Roberta L. Klatzky, Susan J. Lederman, and Daniel M. Merfeld. 2009. Sensation and Perception (2nd ed.). Sinauer Associates Inc., Massachusetts, MA.

Ou Wu, Haiqiang Zuo, Weiming Hu, and Bing Li. 2016. Multimodal Web Aesthetics Assessment Based on Structural SVM and Multitask Fusion Learning. IEEE Transactions on Multimedia 18, 6 (2016), 1062– 1076.

Zhen Xu and James Miller. 2015a. Identifying semantic blocks in Web pages using Gestalt laws of grouping. World Wide Web (2015), 1–22.

Zhen Xu and James Miller. 2015b. A New Webpage Classification Model Based on Visual In-formation Using Gestalt Laws of Grouping. In International Conference on Web Infor-mation Systems Engineering. Springer, 225–232.

CHAPTER 5 An Automated Testing Framework for Cross-Browser Visual Incompatibility Detection[7]

Abstract

Due to the rapid evolution of web applications and computer techniques, visual incompatibility of web pages has become a problem across different browsers and platforms influencing the functionality of the web applications. At the present, researchers have made progress to address such issues; in addition, many commercial tools have emerged as well. However, drawbacks still exist in the existing work, where fully automate testing at the system level is still not achieved. In this chapter, we attempt to propose a framework to detect the cross browser visual incompatibilities automatically. Highlights of the proposed framework include template based case organization, version based automation, and similarity embedded incompatibilities identification.

Keywords: Automated testing; Visual incompatibility; Visual similarity.

1 Introduction

Web applications have become more and more popular nowadays. Compared with traditional applications with a client-server architecture, they are cross-platform, fully-functional, and easier to deploy (ready-to-use and no installation or configuration required). Developers of web applications, work hard on the goal of providing a universally identical user experience. However, due to the incompatibilities among browsers (and platforms),

7 Xu, Zhen, and James Miller. "An Automated Testing Framework for Cross-Browser Visual Incompatibility Detection". Submitted to International Journal of Web Engineering and Technology.

this goal is difficult to achieve. Visual differences of a web page rendered across browsers, in some cases, are expected or acceptable (such as fonts of text). However, in many other cases, they are incorrect and therefore may cause reading problems (such as missing or incorrectly presented content). The latter inconsistencies are considered as the cross-browser visual incompatibility (VI) in this chapter.

The test of a web application to identify such VIs can be conducted manually, by reading and comparing each page through all the target browsers. This activity is highly manual and thus cost-intensive, time-consuming, and in many cases error-prone. On the one hand, a fully functional web application usually contains thousands of web pages, which makes it impossible to test all of them manually. On the other hand, many of the web pages are rendered from the same template, hence testing each of these pages is a repetitive and unnecessary task. In this chapter, we propose an automated testing framework to solve these problems. The highlights of the framework include:

- template based case organization – extract different web pages rendered by the same source template as a single test case;
- version based automation – rerun the test case when changes of the source code are detected; and
- incompatibility identification with similarity estimation – provide both the list of visual. Incompatibilities and the quantitative similarity score for each pair of browsers being compared.

The rest of the chapter is organized as follows. Section 2 discusses related work, including the advantages and limitations of currently existing cross-browser testing tools. Section 3 describes the automated testing framework. It covers VI detection algorithm and the automation schemes. Section 4 concludes the current progress and presents the future work.

2 Related Work

In this section, we will review existing research and tools regarding cross browser testing of web applications and web pages. There are many testing tools related to this area in the market. We will describe each in detail in this section by pointing out their pros and cons.

The research papers in the literature, regarding this area, are limited. Mesbah and Prasad (2011) propose an approach to automatically analyze web applications under various browsers and present the observed discrepancies on a pairwise basis. The analysis crawls the target web application first and then analyses the crawled results. Choudhary et al. (2010) investigate cross browser issues and propose an approach to automatically detect these issues based on differential testing. They implement their approach in the WebDiff tool with acceptable number of false positives. Later, they propose a more comprehensive tool, namely, CrossCheck, based on the WebDiff and the CrossT. The CrossCheck tool (Choudhary, et al., 2012) combines the benefits of WebDiff and CrossT, and can provide both visual difference detection and functional difference detection. Subsequently, they present another tool called X-Pert (2013). The above tools divided the detection of VIs into three aspects: structure XBI (cross-browser incompatibility) detection, text-content XBI detection, and visual-content XBI detection. The structure XBI detection employs the "alignment graph", which records the hierarchical and geometrical information of each DOM element (e.g., element 1 is above element 2 and they are left and right aligned). This is a novel idea of XBI detection as it narrows down the numeric coordinates of elements into a limited number of relations based on the relative position. The text-content XBI detection compares the text of elements. The potential problem of comparing textual strings is that in a multi-language web page scenario (e.g., the English and the French version of Google's home page), text is not the core content, and thus the pages are similar to users/developers while the comparison results suggests dissimilar, leading to false positive results. The visual-content XBI detection takes the screenshot images as the input – the images of the leaf DOM elements only, to be precise – and compares the color histogram using χ^2 distance. The limitation of it is that leaf elements represent only part, and in many cases only a small part of the whole page; and using color distribution to determine image similarity ignores the actual content, thus may also raise false positive results.

Figure 5.1 shows three tools that only support cross-IE incompatibility detections. The Expression Web SuperPreview (2011) supports only versions of IE 6 and 7 (IE 11 is in the list, but actually not supported). It provides functions such as side-by-side comparison, window size customization, and DOM inspection. The side-by-side comparison enables us to compare web pages with different browsers intuitively and conveniently on a single screen. The window size customization allows us to change the width and height of the view port to simulate different devices and screens. With the DOM inspection function, we can investigate the web pages in a responsive way. This tool returns error on many web pages (marked by the yellow circle in the figure); and when the page preview is acquired, it is limited in the current view port. Content outside of the view port will not be rendered (as shown in the blue circle). IETester (2017) can perform side-by-side comparison, but lacks in window size customization. With the extension of DebugBar, it can also perform DOM inspection. Although most versions of IE are claimed to be supported, many return errors. IE NetRenderer (2017) can only draw web pages with the target version of IE to generate screenshot image. Therefore, it provides no side-by-side comparison or DOM Inspection. By investigating the tool, we also observe that it does not support window customization.

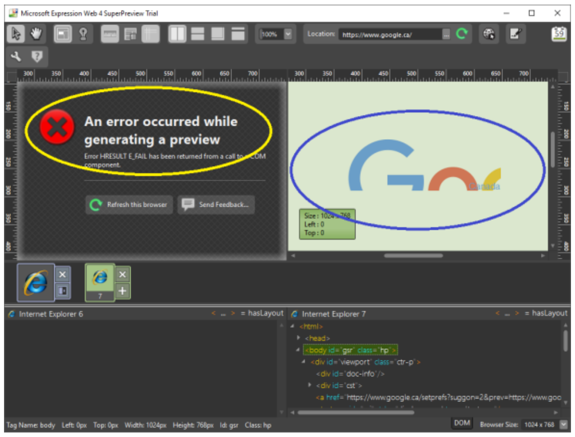
(a) Expression Web SuperPreview

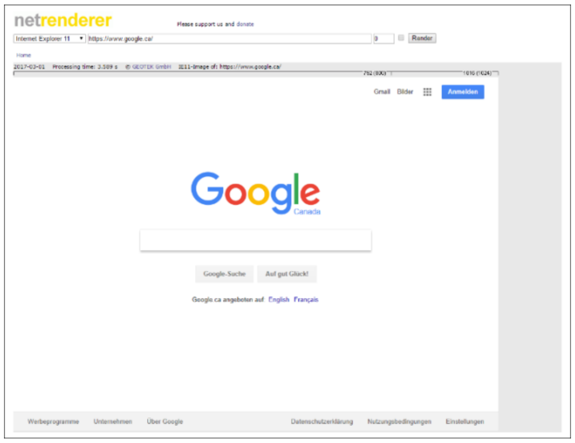
(b) IE NetRenderer

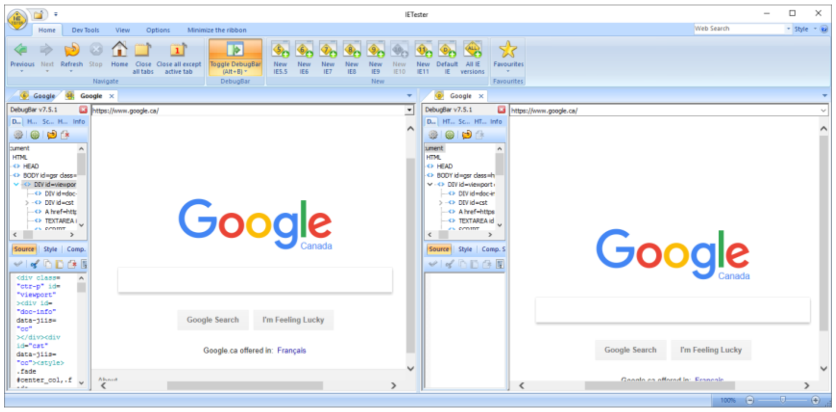
(c) IETester

Figure 5.1 The Three Tools for Cross-IE Incompatibility Detection

Browsershots (2005), Browsera (2017), BrowserBite (2017), BrowserStack (2017), and CrossBrowserTesting (2017) are five tools that support multi-browser and multi-platform detections. This meets the minimum request for VI detection. For the input, only Browsera can take multiple URLs as the input, while all the other tools allow only one

URL per test. Thus, for web application developers to conduct full-site tests, most tasks will have to be performed manually. Also, Browsershots, BrowserStack and CrossBrowserTesting provide configurations to customize window size. As for the detection, Browsershots, BrowserBite and BrowserStack load a web page with all selected browsers and then simply take all the screenshot images as the results, without doing any VI detection. On the other hand, Browsera and CrossBrowserTesting provides both screenshot images and detection reports, as shown in **Figure 5.2**.

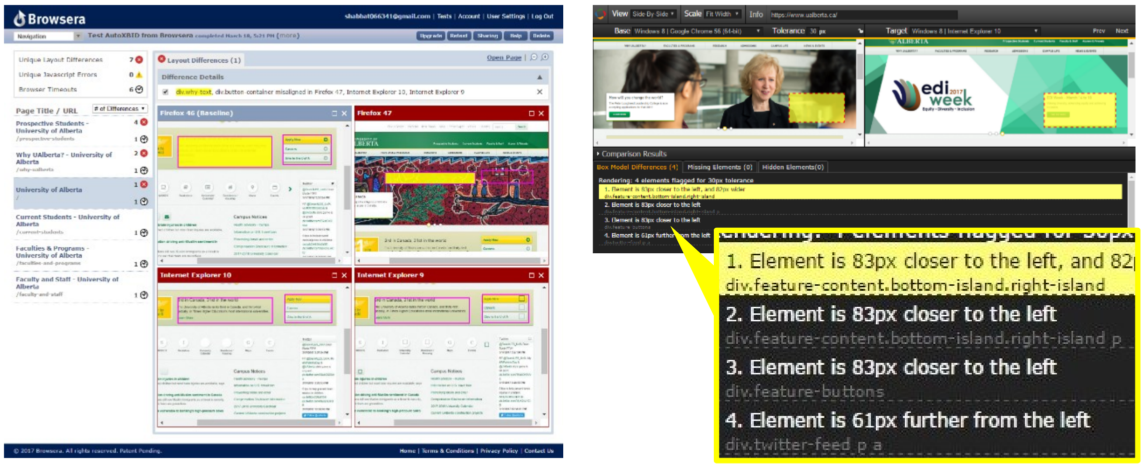

Test AutoXBID from Browsera completed March 18, 5:21 PM (more)

Unique Layout Differences 7
Unique Javascript Errors 0
Browser Timeouts 6

Page Title / URL	# of Differences
Prospective Students - University of Alberta /prospective-students	4 / 1
Why UAlberta? - University of Alberta /why-ualberta	2 / 1
University of Alberta /	1 / 1
Current Students - University of Alberta /current-students	1
Faculties & Programs - University of Alberta /faculties-and-programs	1
Faculty and Staff - University of Alberta /faculty-and-staff	1

Layout Differences (1)

Difference Details

div.why-text, div.button-container misaligned in Firefox 47, Internet Explorer 10, Internet Explorer 9

Firefox 46 (Baseline) | Firefox 47 | Internet Explorer 10 | Internet Explorer 9

© 2017 Browsera. All rights reserved. Patent Pending.

View: Side-By-Side; Scale: Fit Width; Info: https://www.ualberta.ca/

Base: Windows 8 | Google Chrome 56 (64-bit); Tolerance: 30 px; Target: Windows 8 | Internet Explorer 10

Comparison Results

Box Model Differences (4) | Missing Elements (0) | Hidden Elements(0)

Rendering: 4 elements flagged for 30px tolerance
1. Element is 83px closer to the left, and 82px wider
div.feature-content.bottom-island.right-island
2. Element is 83px closer to the left
div.feature-content.bottom-island.right-island p
3. Element is 83px closer to the left
div.feature-buttons
4. Element is 61px further from the left
div.twitter-feed p a

(a) Browsera (b) CrossBrowserTesting

Figure 5.2 Detection Reports of Browsera and CrossBrowserTesting

3 Automated Testing Framework

In our previous work (Xu and Miller, 2015), we developed a method to calculate the quantitative visual similarity of two web pages. The present chapter extends this method by adding an extra step to identify different elements between the two pages, and uses the extended method as the core function of the automated testing framework to detect VIs.

3.1 Automated Page-Level Detection of VIs

The page-level detection employs the above extended method as the core function of the proposed testing framework. This method extracts block trees from the web page rendered by two different browsers, and uses the two block trees to detect VIs.

3.1.1 Block Tree Extraction from Web Page

The DOM tree contains all the information from a web page, but only the visible elements contribute to the visualization of the web page. Therefore, the first step of the block tree extraction is to remove invisible DOM elements. The next step is to merge semantically related elements into blocks. This is done by translating and applying the Gestalt laws of grouping as follows.

- The Gestalt law of simplicity shows people's tendency to recognize the simplest representation of objects. To interpret this law, we take each DOM element as the simplest representation of objects.
- The Gestalt law of closure indicates that people are inclined to construct complete shapes from incomplete ones. A DOM element is often overlapped by its child DOM elements, leaving the shape incomplete, but people are still able to recognize it as a complete rectangle. As such, to interpret this law, we treat all DOM elements as complete rectangular objects.
- The Gestalt law of proximity states that people have the tendency to group close objects and separate distant ones. Therefore, to translate this law, we merge elements into blocks based on this distance. In the web page scenario, we compare the distances between each pair of adjacent sibling DOM elements, those with

smaller distances are "clustered" into a group, and those with larger distances are separated into different groups.

- The Gestalt law of similarity illustrates that people are prone to regard similar objects as a group. Here, similarity refers to the visual features related to background, foreground, and size. If any of a list of sibling DOM elements is different from others in the above three aspects, we put it into a different group.
- The Gestalt law of continuity describes people's tendency to group aligned objects. In other words, if any DOM element is not aligned with its siblings, it is put into a different group.
- The Gestalt law of common fate reveals that people are inclined to put objects with the same motion into the same group. To translate this law, we focus on the scrolling behaviors when it comes to motion trends. Most DOM elements move accordingly when the user scrolls a web page, but some other elements may stay still, or move slower or faster. Such elements that do not move in the same way with others are place into a different group.
- The Gestalt law of symmetry tells us that people tend to perceive symmetric objects as a single group. Since this law is not common in web pages, we do not consider it in the present chapter.
- The Gestalt law of past experience states that people are prone to rely on past experience when interpreting objects. Again, we do not consider this law in the present chapter, because it is beyond the scope of web page analysis.

Figure 5.3 shows an example of the block tree extracted from University of Alberta's home page. By applying the Gestalt laws of grouping, the semantically related

DOM elements are grouped into blocks. In **Figure 5.3**b, semantically related elements are marked with the same background colors. For example, as shown in the yellow circle at the lower left part, the news items are marked with the same background color. This is because they refer to the same topic. As a comparison, the three boxes in the middle area (marked in the black circle) contain image, text and buttons respectively, indicating that they are semantically non-related, so they are marked with different colors. **Figure 5.3**c shows partial of the block tree, where each line denotes a single block. From this figure, we can find that a) the DOM hierarchy is well maintained in the block tree; b) the root block consists of the "`BODY`" element from the DOM tree; and c) some blocks contain only one DOM element while others merge a group of elements into one block.

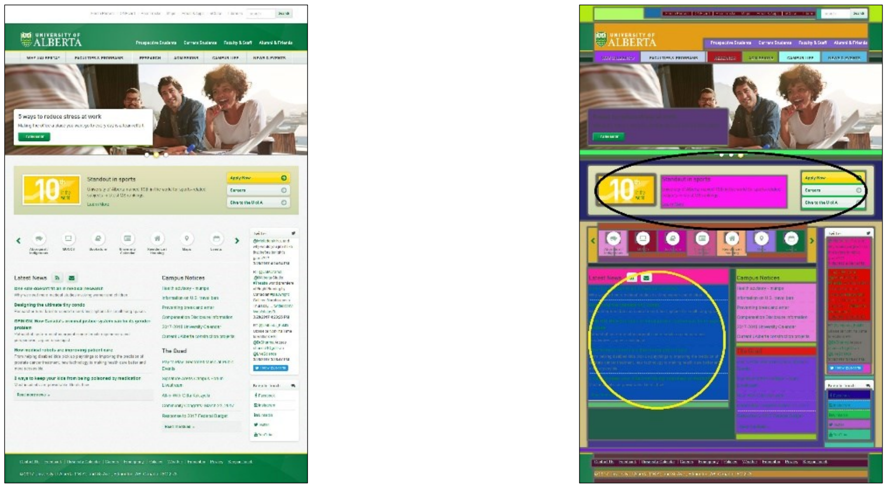
(a) Original Page (b) Analyzed Page

```
[BODY]: left=0,top=0,right=1007,bottom=1588; ...
|- [FORM,DIV]: left=-1988,top=-1999,right=1007,bottom=1588; ...
| |- [HEADER,DIV,FOOTER]: left=0,top=0,right=1007,bottom=1588; ...
| | |- [DIV,DIV,DIV]: left=0,top=0,right=1007,bottom=196; ...
| | | |- [DIV]: left=50,top=10,right=956,bottom=50; ...
| | | | |- [NAV,DIV]: left=218,top=10,right=956,bottom=48; ...
| | | | | |- [UL]: left=276,top=10,right=798,bottom=41; ...
| | | | | | |- [LI]: left=276,top=20,right=798,bottom=34; ...
| | | | | | | |- [UL]: left=276,top=22,right=798,bottom=34; ...
| | | | | | | | |- [A,A,A,A,A,A,A]: left=276,top=22,right=802,bottom=34; ...
| | | | | |- [INPUT,BUTTON]: left=802,top=13,right=956,bottom=45; ...
| | | |- [DIV]: left=50,top=61,right=956,bottom=151; ...
| | | | |- [A,NAV]: left=50,top=87,right=957,bottom=151; ...
| | | | | |- [UL]: left=416,top=115,right=957,bottom=144; ...
| | | | | | |- [A,A,A,A]: left=436,top=119,right=957,bottom=134; ...
| | | |- [NAV]: left=51,top=155,right=956,bottom=195; ...
| | | | |- [UL]: left=51,top=155,right=956,bottom=195; ...
| | | | | |- [LI]: left=52,top=155,right=956,bottom=195; ...
```

(c) Partial of the Block Tree

Figure 5.3 The Example of UAlberta's Home Page

3.1.2 VI Detection and Similarity Estimation

The two block trees retrieved from two browsers of a web page are compared to detect VIs. During the comparison, a *tree edit distance* (TED) based mapping scheme, the extended subtree model (Shahbazi and Miler, 2014), is employed. An overview of the model is given below:

- Subtree mapping. Regular TED mapping schemes only map tree nodes. However, in a web page scenario, content elements are stacked up so that lower elements are always covered by upper elements. Hence, when we see the content of a block in the web page, it is the content of a subtree that is rooted at the block. Consequently, the subtree mapping scheme is more accurate approach.

- One-time mapping. If two subtrees are mapped, then they will have common subtrees (if there are subtrees in them). However, to avoid duplications, we do not map these common subtrees again.
- Subtree weight determination. A subtree mapping has a weight that is equal to the mean value of the weights of the two subtrees. The weight of a subtree is equal to the number of nodes that take this subtree as their largest subtree.

The mapping of two block trees reflects the visual compatibilities, i.e., are the two corresponding blocks similar or not. Therefore, the detection of VIs is to locate blocks that are not in the mapping results. In another word, blocks that are added, deleted or changed from one tree to the other tree contain VIs. The quantitative similarity of the two block trees, the extended sub tree (EST) value, is calculated by (5-1):

$$S^*(X,Y) = \frac{\sqrt[\alpha]{\sum_{m_k \in M} \beta_k \times W(m_k)^\alpha}}{\max(|X|,|Y|)}, \tag{5-1}$$

where, X and Y are the two trees; $|X|$ and $|Y|$ are the sizes of the two trees, which equal to the numbers of nodes in X and Y, respectively; M is the mapping results; $W(m_k)$ is the weight of the mapping m_k; α is the coefficient to adjust the relation among mappings with different subtree sizes; and β_k is a geometrical parameter to reflect the importance of the mapping m_k with respect to the position of block k in X and Y. $\beta_k = 1$ when the node x_k of X and y_k of Y in m_k have the same depth, otherwise $\beta_k = \beta_0$, which is a constant in the range of $(0,1)$.

3.2 Automated System-Level Testing for VI Detections

System-level testing is designed to evaluate all the web pages in a web application. The automated testing framework should be able to discover objective functions, trigger actions, and report outcomes without human intervention. To achieve this goal, three modules are proposed to construct the testing framework, namely the source parser, the schedule builder and the result reporter.

3.2.1 Source Parser

The core task of this module is to discover the objective functions. In the web application scenario, to detect VIs, the objective functions cover all the web pages because all of these pages must (ideally) be bug-free. Development of modern web applications relies on page templates. That is, utilizing one template dynamically generates similar web pages. Consider Google's search result page, when a user types in "online shopping", the search result page displays dozens of online shopping related links; and when the user types in "health care", the page displays another dozens of links, which are similar in the layout with the previous page except the details. This is because the search result page utilizes a template that shows different content according to the inputs. To test a web application, it is useless and impractical to test all possible web pages. Instead, we only need to test one case for each page template. Consequently, to conduct automated testing, the practical objective functions should be narrowed down to include only unique page templates.

Consider a typical Django project as an example, each component app of a Django project contains a source file named "urls.py", where all the implemented URL entries are recorded and linked to the corresponding view methods. The view methods are further linked to the page templates that are used for displaying actual content. Therefore, in the Django project testing practice, the objective functions map to all these URL entries. To automatically test such projects, the source parser should be able to detect all possible URL entries. Meanwhile, some of these entries contain parameters, and thus, the source parser also needs to be able to detect these parameters and assign proper values to them. This may require accessing data models and querying databases.

3.2.2 Schedule Builder

As the name indicates, the schedule builder manages the schedule of testing automation. During the development of a web application, the source code keeps changing constantly, and it is necessary to repeat the tests through out the whole development period.

A straightforward solution to automatically repeat the tests is to set up a schedule based on the time. The second method we proposed to automatically run the tests is based on the source code changes. Not all the objective functions change all the time, so we should only re-test those that have changed and ignore those that have not changed. For instance, the developer may focus on one app of the web application today and another app tomorrow, so it is unnecessary to re-run tests on the second app. In this case, the schedule builder should monitor each template, and automatically triggers the actions to re-run the corresponding tests based on changes of the template's source codes (for example, re-test after a defined number of updates to the source code).

3.2.3 Result Reporter

The automatic testing framework runs without human intervention; therefore, once the results are produced, it is possible for users to ignore their implications if the framework does not notify the developer. This is acceptable if a test case passes, but when the result fails, the result reporter module must notify the developer. Content of the notifications include a true/false assertion (i.e., indicating whether the template page is rendered identically in the target browsers), a quantitative value of the visual similarity (where 1.0 indicates identical and 0.0 indicates completely different), and a list of differences between the rendered pages.

Priorities must be added to the notifications automatically, and the result reporter must display the outputs accordingly. This is because automatic repetitions of the scheduled tests will generate significant numbers of results, and only those failed results (i.e., VIs that have been detected) require the developer's attention. If the objective of a test is to confirm the template is rendered identically by all browsers, then all the results of "true", "1.0", or an empty list of differences are not important. In this case, the priority of these results should be set to lowest. As the opposite, the lower the similarity value (or the larger the difference list is), the higher the priority should be.

The difference list is easier to read if it is combined with the side-by-side display for locating VIs. Therefore, presentation of VIs must be done by rendering the web page in all the browsers simultaneously and highlighting the identified differences (for example, highlight them by changing the background colors or by outlining the borders of the related blocks).

Figure 5.4 shows the outline of the automated testing framework, where the green and yellow rectangles indicate the data and components of the framework, respectively; the green and yellow arrows denote the data and control flow, respectively; and the blue arrows refer to the notification flow.

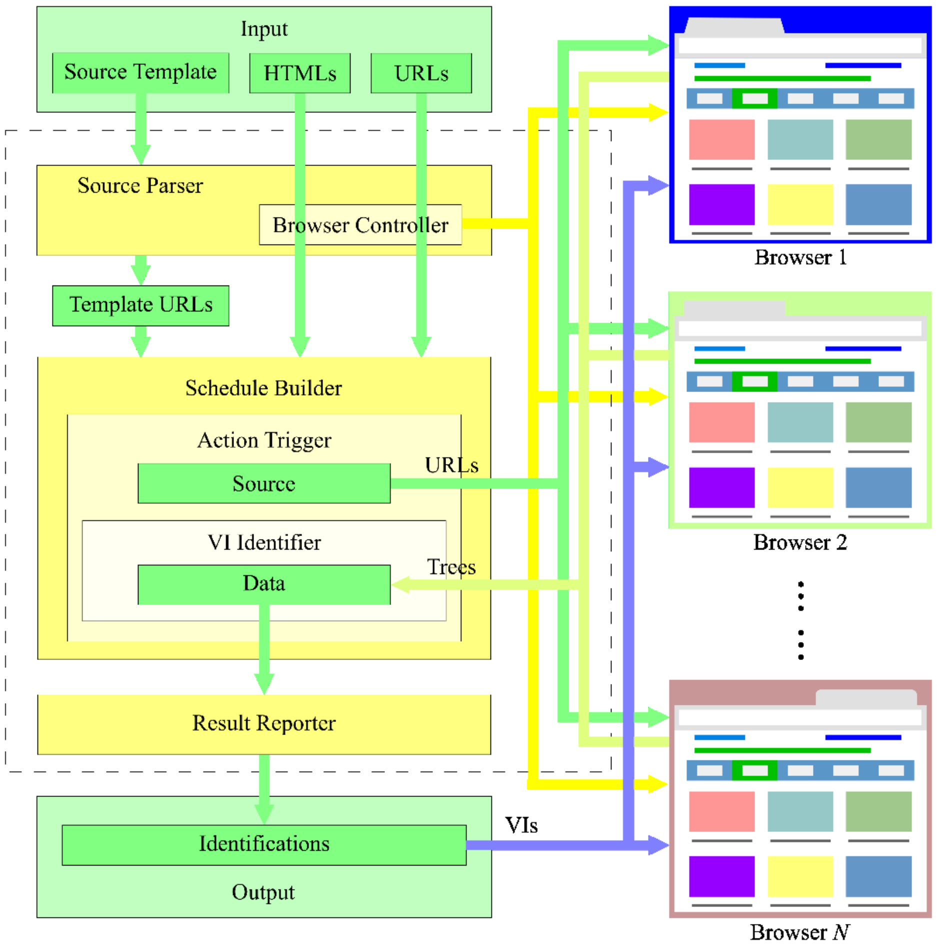

Figure 5.4 The Automated Testing Framework

- The framework accepts both templates of web applications and specific URLs/HTML code as the input. Although the templates require extra processing by the source parser, the specific URLs/HTML code can be directly input in the schedule builder.
- The browser controller registers and manages the supported browsers.
- The schedule builder manages the automation schedule, either by time, or by changes to the source code, or by both. According to the schedules, its subcomponent, the action trigger, conducts the testing process, where the sources are passed to the VI identifier for VI detection and similarity estimation.

- The result reporter collects all the test results, filters them by priorities, and notifies web application developers selectively. By updating the web pages in the browsers with the difference list, a side-by-side comparison provides fast location of VIs.

4 Automated Testing Tool

To conduction VI detection, the minimum request is that the automated testing tool must support multiple browsers and/or multiple platforms. The implementation, hence, is designed as a distributed system, where a central node communicates with and controls all leaf nodes. The leaf nodes run specific OSes and browsers and therefore consist of the testing farm, which renders the target web pages and collects the corresponding source data (i.e., the block trees). The central node deploys the automated testing tool as well as the target web application, and performs the testing automation. **Figure 5.5** shows a sequence diagram of the tool's testing process.

4.1 Browser and Platform Registration

During the initialization of the automated testing tool, the supported browsers and platforms are to be configured. The core thread of this distributed system that is located in the central node will send queries to all branches for browser detection. The active leaf nodes will respond to it with the configuration information, including the name and version of both its own operating system and installed browsers. Hardware configurations of the machine (either physical or virtual) could also be included if necessary, such as resolutions of mobile devices. **Figure 5.6** shows the two initialization dialogs of the tool, where the browser registration illustrates examples of local browsers.

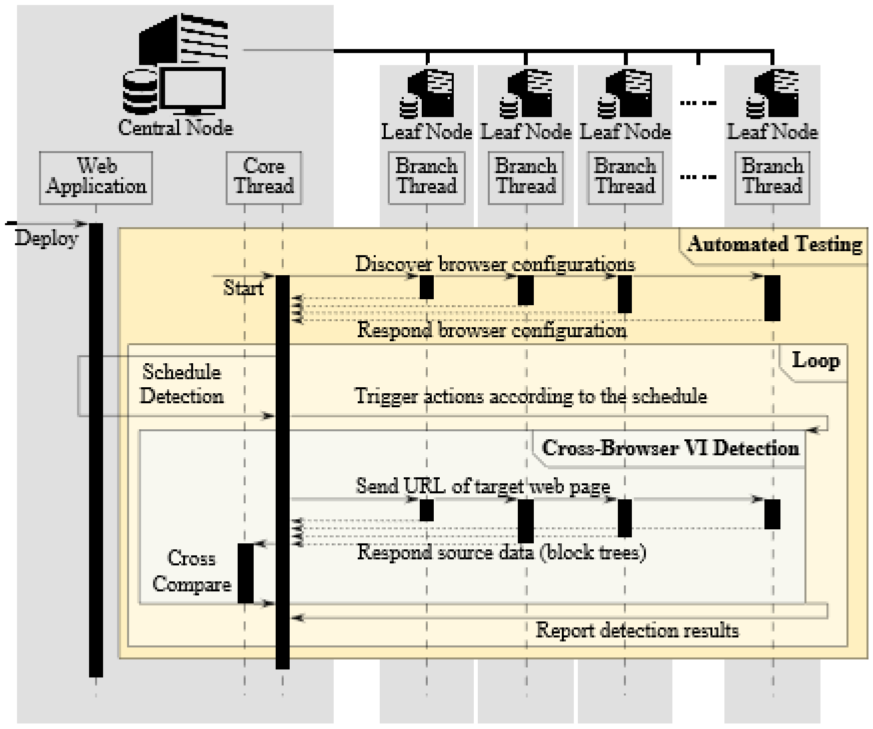

Figure 5.5 Sequence Diagram of the Automated Testing Tool

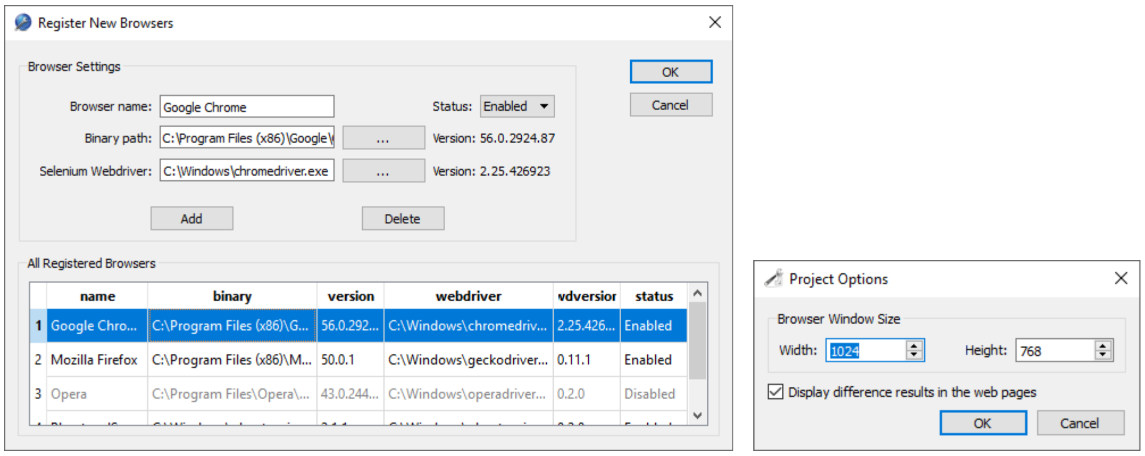

Browser Settings

Browser name: Google Chrome

Status: Enabled

Binary path: C:\Program Files (x86)\Google\

Version: 56.0.2924.87

Selenium Webdriver: C:\Windows\chromedriver.exe

Version: 2.25.426923

All Registered Browsers

	name	binary	version	webdriver	vdversior	status
1	Google Chro...	C:\Program Files (x86)\G...	56.0.292...	C:\Windows\chromedriv...	2.25.426...	Enabled
2	Mozilla Firefox	C:\Program Files (x86)\M...	50.0.1	C:\Windows\geckodriver...	0.11.1	Enabled
3	Opera	C:\Program Files\Opera\...	43.0.244...	C:\Windows\operadriver...	0.2.0	Disabled

Browser Window Size

Width: 1024

Height: 768

[✓] Display difference results in the web pages

(a) Browser Registration (b) Project Options

Figure 5.6 Initialization Dialogs of the Automated Testing Tool

4.2 Template Based Test Case Organization

The automated testing tool analyzes the source code that encode all the templates such as the full list of RESTful URLs, and generates test cases for each such template entry.

As mentioned in the previous section, this task is done by the source parser. If necessary, the source parser will dig further information (for example dynamic content in the URLs, such as the user ID “MarcoXZh” in “https://github.com/MarcoXZh/”) from sub apps and the web application’s database. Note this step is project dependant – different web applications require different strategies for code analysis.

Figure 5.7 shows example pseudocode of the source parser for Django project analysis. This algorithm takes a Django project’s project name and root directory as inputs. It searches the “manage.py” script for configurations of installed apps and databases (Line 6 to 8), and then parses the templates as follows:

```
1    ALGORITHM ParseSource_Django:
2        INPUT: project name: PN,
3               root directory PN: RD
4        OUTPUT: all template URLs: TS
5
6        config_script = get_config_script(RD.mangage.py)
7        apps = get_installed_apps(config_script)
8        database = get_database(config_script)
9        connect(database)
10       TS = [EMPTY_LIST]
11       FOR EACH app IN apps DO:
12           FOR EACH url, view IN urlpatterns(app.urls.py) DO:
13               IF contains_django_variables(url) THEN:
14                   variables = retrieve_variables(url)
15                   model = retrieve_model(view)
16                   sql_table = retrieve_sql_table(app.model)
17                   values = [EMPTY_LIST]
18                   FOR EACH var IN variables DO:
19                       value = query(sql_table, var)
20                       values.append(value)
21                   END FOR
22                   replace_all(url, variables, values)
23               END IF
24               TS.append(url)
25           END FOR
26       END FOR
27       close(database)
28       RETURN TS
29   END ALGORITHM
```

Figure 5.7 Extracting Templates from Django Projects

1) for each installed app, it checks its "urls.py" script to detect all supported URL patterns and the corresponding views;
2) for each URL pattern, if it contains variables, then the source parser needs to assign correct values by querying the view-model-table chain for all the variables (Line 13 to 23);
3) after assigning values to the variables, or if the pattern is a regular URL and contains no variables, the URL pattern is added to the template list; and
4) the full template list includes all the URL patterns of all the installed apps. Due to the templates list consisting of URL patterns only extracted from the "urls.py" script, it will not store duplicated URL entries, and at the same time cover all the supported URLs of the web application.

4.3 Version Based Automation

Once the templates are extracted from the web application's source code, the core thread sends signals to all the leaf nodes according to the predefined schedule for VI detection. This tool contains both time-driven schedules (i.e., triggers actions after a fixed time) and change-driven schedules (i.e., triggers actions after a fixed number of changes being made in the target source codes). Once the predefined time has expired or the predefined number of code changes has detected, a re-test is triggered. However, if the target source code remains unchanged (i.e., no changes of source code found by the diff process, or http response code of the target web page being 304), then the test will be skipped. **Figure 5.8** shows the scheduler builder of the tool, which combines the functions of template extraction and schedule configuration. Note the three source entries at the right-side list view are raw HTML code – a regular URL without variables and a variable-included URL. The “`|$1|`”, “`|$2|`”, etc. are the variable names, and the corresponding values are stored however not displayed. Testing frequency of the schedule builder can be configured as either change-based or time-based or both. Collection of the target test cases’ screenshots can be customized, too.

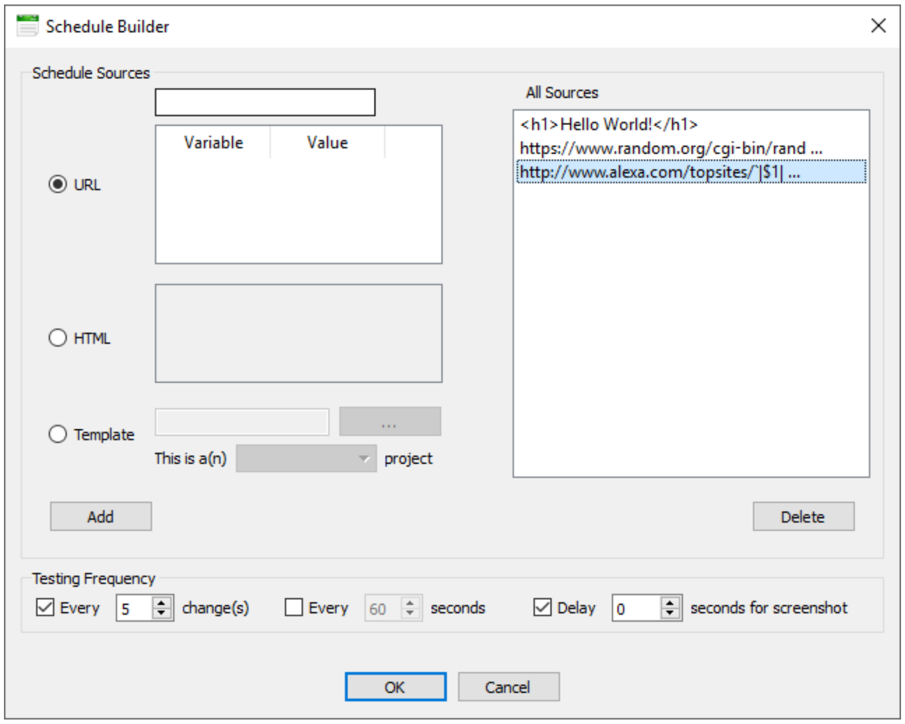

[✓ URL] HTML Template

All Sources
<h1>Hello World!</h1>
https://www.random.org/cgi-bin/rand ...
http://www.alexa.com/topsites/`|$1| ...

[✓] Every 5 change(s)
[ ] Every 60 seconds
[✓] Delay 0 seconds for screenshot

Figure 5.8 Schedule Builder of the Automated Testing Tool

4.4 Case Study

In this chapter, we evaluate the efficiency of the automated testing tool though the case of University of Alberta’s home page. Comprehensive experiments and result discussions can be found in (Xu and Miller, 2015). We run the tools to compare the page in two popular browsers: Google Chrome version 57 and Mozilla Firefox version 52, and on two platforms: Windows 10 and CentOS 7. By comparing the results of CrossBrowserTesting and our VI detection, the following conclusions can be derived:

1) Both CrossBrowserTesting and our automated testing tool can locate VIs of web pages among different browsers; and at the same time, both can make the correct conclusion without raising false positives if two versions of a web page are identical.
2) Results of CrossBrowserTesting contains only VIs, lacking in intuitive conclusions to determine how similar the two versions of a web page are. Thus, if a test result contains ten small VIs and another test result contains one big VIs, it is difficult to figure out the priority for developers to start debugging. As the comparison, our tool calculates the EST similarity, which enables the priority judgement. **Table 5.1** shows the EST values of the evaluation.

Table 5.1 EST Similarity Values of the Cross-Comparisons

Browser1 Browser 2	Windows-Chrome Windows-Firefox	CentOS-Chrome CentOS-Firefox	Windows-Chrome CentOS-Chrome	Windows-Firefox CentOS-Firefox
EST Value	1.0000	1.0000	0.9603	0.9603

3) During the tree comparison, our EST model maps sub trees instead of nodes, thus it can avoid potential duplications of VI detection. As previously shown in **Figure 5.2**b, CrossBrowserTesting identified four VIs caused by the X coordinates of the elements. However, the second and the third VIs are child elements of the element in the first VI. Due to the mismatch of the parent element's X coordinate from the two versions of the page, its child elements consequently mismatch, too, Therefore, the second and the third VIs are actually a duplication of the first VI. Our EST model, by absorbing comparisons of child elements and mapping subtrees, prevents such hierarchical false positives from being detected.

5 Conclusions

Diversity of present web browsers and platforms have brought cross browser issues to both web users and developers. To detect cross browser incompatibilities, many commercial tools have been developed and relevant topics have gained attention among researchers as well. In this chapter, we target the detection of VIs and attempt to propose a testing framework to detect these incompatibilities automatically. Three advantages exist in the automated testing framework. Firstly, the detection of VIs is based on source templates. By doing so, we narrow down the scale of testing. Second, automation is achieved by schedules based on both time and changes of the source code, which avoids human intervention and at the same time this further reduces the test ranges. Finally, the framework provides both a list of VIs (including a rendered presentation of these differences) and a quantitative similarity value as the result. This makes it possible to notify web application developers by priorities.

An automated testing tool is designed according to the framework. This tool allows the registration of browsers on both local and remote machines, and utilizes all these registered browsers to conduct VI detection. It extracts the templates depending on the type of the target web application. A Django example is employed showing that this tool can extract both plain URLs and URLs with variables, where the extraction of the latter is done by querying information from the web application's database. Version base automation of the tool is achieved by both time-driven and change-driven schedules. A case study is presented to illustrate the efficiency of the extended subtree model by comparing it with the CrossBrowserTesting. Conclusions reveal that the quantitative values indicate how similar the two browser versions of a web page are and serves as a reference to debug these

VIs; and the subtree mapping scheme has eliminated duplications of the VI detection results.

Acknowledgment

The authors would like to thank China Scholarship Council (CSC) for the financial support.

References

Expression Web SuperPreview, 2011. https://www.microsoft.com/en-ca/download/details.aspx?id=2020 (accessed 17.03.04).

IETester, 2017. http://www.my-debugbar.com/wiki/IETester/HomePage (accessed 17.03.04).

IE NetRenderer, 2017. https://netrenderer.com/ (accessed 17.03.04).

Browsershots, 2005. http://browsershots.org/ (accessed 17.03.04).

Browsera, 2017. http://www.browsera.com/ (accessed 17.03.04).

BrowserBite, 2017. http://browserbite.com/ (accessed 17.03.04).

BrowserStack, 2017. https://www.browserstack.com/ (accessed 17.03.04).

CrossBrowserTesting, 2017. https://crossbrowsertesting.com/ (accessed 17.03.04).

Ali Mesbah and Mukul R. Prasad. 2011. Automated cross-browser compatibility testing. In Proceedings of the 33rd International Conference on Software Engineering. ACM, 561–570.

Shauvik Roy Choudhary, Mukul R Prasad, and Alessandro Orso. 2012. Crosscheck: Combining crawling and differencing to better detect cross-browser incompatibilities in web applications. In 2012 IEEE Fifth International Conference on Software Testing, Verification and Validation. IEEE, 171–180.

Shauvik Roy Choudhary, Mukul R Prasad, and Alessandro Orso. 2013. X-PERT: accurate identification of cross-browser issues in web applications. In Proceedings of the 2013 International Conference on Software Engineering. IEEE Press, 702–711.

Shauvik Roy Choudhary, Husayn Versee, and Alessandro Orso. 2010. WEBDIFF: Automated identification of cross-browser issues in web applications. In Software Maintenance (ICSM), 2010 IEEE International Conference on. IEEE, 1–10.

Zhen Xu and James Miller. 2017. Estimating Similarity of Rich Internet Pages Using Visual Information, International Journal of Web Engineering and Technology.

Ali Shahbazi and James Miller. 2014. Extended subtree: a new similarity function for tree structured data. Knowledge and Data Engineering, IEEE Transactions on 26, 4 (2014), 864–877.

CHAPTER 6 Conclusions

1 Summary of Thesis

The purpose of this thesis is to investigate issues existing in the field of web pages, including the detection of semantic content, visual similarity, and cross-browser incompatibilities. To address these issues, we propose four research topics and present them in separate chapters that follow the introduction chapter. In this section, we will describe the accomplishments within each topic in both terms of their strengths and limitations.

In Chapter 2, we present our first journal paper, which develops an approach to identify semantic blocks in web pages. Since traditional methods cannot work well for modern web pages, we seek to introduce human perception into this topic. To remove the hierarchical inconsistencies between the visual layout and the DOM tree of web pages, we propose the layer tree. Based on it, we interpret the Gestalt Laws of grouping by novel measurements such as the normalized Hausdorff distance, the CIE-Lab color difference, and the normalized compression distance. A classifier is trained finally to operationalize the interpreted laws. Semantic blocks are extracted by applying the translated Gestalt laws to the layer tree. For this topic, we have achieved what we proposed in the introduction chapter. A limitation of the proposed technique is that it cannot work well with large web pages.

In Chapter 3, we present our second journal paper, which provides a method to detect web page similarity for modern rich-format web pages. Unlike existing approaches that adopt DOM trees or images, the new method considers both structural and visual information of the web pages. Based on the idea of the block tree, we propose a visual similarity measurement that use tree edit distance to calculate visual similarity between web pages. As stated in the introduction section, we have succeeded in presenting a way to detect web page similarity. One limitation of the proposed method is that tree edit distance is not the perfect data structure to describe web pages, because its mapping detection is based on nodes while web pages visualization is based on sub trees.

In Chapter 4, we present our third journal paper, which improves the visual similarity measurement by conducting empirical experiments to determine the measurements for Gestalt laws translation and replacing the tree edit distance with extended subtree model. By using this visual similarity measurement, we conduct experiment to evaluate visual similarity of different web pages. In this topic, we solved the limitation of the second topic described in the previous paragraph. Specifically, we introduced extended sub tree concept to represent web pages in order to obtain a more accurate comparison.

In Chapter 5, we present our fourth journal paper, which focuses on the development of an automated testing framework to detect cross-browser visual incompatibilities between web pages. An automated testing tool is designed according to the framework, by using the improved visual similarity.

2 Publications

1) Papers:

- Campbell, Joshua Charles, Chenlei Zhang, Zhen Xu, Abram Hindle, James Miller, Deficient documentation detection: a methodology to locate deficient project documentation using topic analysis," 10th Working Conference on Mining Software Repositories, pp. 57-60, 2013.
- Xu, Zhen, and James Miller. A New Webpage Classification Model Based on Visual Information Using Gestalt Laws of Grouping. International Conference on Web Information Systems Engineering. Springer International Publishing, 2015.

2) Posters and Presentations:

- Zhen Xu, Fadwa Estuka, James Miller. Identifying Semantic Blocks in Web Pages Using Gestalt Laws of Grouping. 25th Annual International Conference on Computer Science and Software Engineering.
- Zhen Xu, James Miller, Syed Tauhid Zuhori. A New Web Page Classification Model based on Visual Information using Gestalt Laws of Grouping. 25th Annual International Conference on Computer Science and Software Engineering.
- Zhen Xu, James Miller. An Empirical Metric for Web Page Visual Similarity based on the Gestalt Laws of Grouping. Consortium fro Software Engineering Research, 2016.
- Zhen Xu, James Miller. Cross-Browser Differences Detection based on an Empirical Metric for Web Page Visual Similarity. 26th Annual International Conference on Computer Science and Software Engineering.

Bibliography

Albrecht, P., M¨uller, A.-K., Ringelstein, M., Finis, D., Geerling, G., Cohn, E., Aktas, O., Hartung, H.-P., Hefter, H., Methner, A., 2013. Retinal neurodegeneration in wilsons disease revealed by spectral domain optical coherence tomography. In: Neurology. Vol. 80. Lippincott Williams & Wilkins 530 WALNUT ST, PHILADELPHIA, PA 19106-3621 USA.

Adriana Olmos and Frederick A. A. Kingdom. 2004. A biologically inspired algorithm for the recovery of shading and reflectance images. Perception 33, 12 (2004), 1463–1473.

Alain Hore and Djemel Ziou. 2010. Image quality metrics: PSNR vs. SSIM. In Pattern Recognition (ICPR), 2010 20th International Conference on. IEEE, 2366–2369.

Ali Mesbah and Mukul R. Prasad. 2011. Automated cross-browser compatibility testing. In Proceedings of the 33rd International Conference on Software Engineering. ACM, 561–570.

Ali Shahbazi and James Miller. 2014. Extended subtree: a new similarity function for tree structured data. Knowledge and Data Engineering, IEEE Transactions on 26, 4 (2014), 864–877.

Anthony Y Fu, Wenyin Liu, and Xiaotie Deng. 2006. Detecting phishing web pages with visual similarity assessment based on earth mover's distance (EMD). IEEE transactions on dependable and secure computing 3, 4 (2006), 301–311.

Baluja, S., 2006. Browsing on small screens: recasting web-page segmentation into an efficient machine learning framework. In: Proceedings of the 15th international conference on World Wide Web. ACM, pp. 33–42.

Bennett, C. H., G´acs, P., Li, M., Vit´anyi, P. M., Zurek, W. H., 1998. Information distance. IEEE Transactions on information theory 44 (4), 1407–1423.

Browsera, 2017. http://www.browsera.com/ (accessed 17.03.04).

Buttler, D., 2004. A short survey of document structure similarity algorithms. Tech. rep., Lawrence Livermore National Laboratory (LLNL), Livermore, CA.

Cai, D., Yu, S., Wen, J.-R., Ma, W.-Y., 2003a. Extracting content structure for web pages based on visual representation. In: Asia-Pacific Web Conference. Springer, pp. 406–417.

Cai, D., Yu, S., Wen, J.-R., Ma, W.-Y., 2003b. Vips: a vision-based page segmentation algorithm.

Canny, J., 1986. A computational approach to edge detection. IEEE Transactions on pattern analysis and machine intelligence (6), 679–698.

Cao, J., Mao, B., Luo, J., 2010. A segmentation method for web page analysis using shrinking and dividing. International Journal of Parallel, Emergent and Distributed Systems 25 (2), 93–104.

Chakrabarti, D., Kumar, R., Punera, K., 2008. A graph-theoretic approach to webpage segmentation. In: Proceedings of the 17th international conference on World Wide Web. ACM, pp. 377–386.

Chaudhuri, B. B., Rosenfeld, A., 1999. A modified hausdorff distance between fuzzy sets. Information Sciences 118 (1), 159–171.

Chechik, G., Sharma, V., Shalit, U., Bengio, S., 2010. Large scale online learning of image similarity through ranking. Journal of Machine Learning Research 11 (Mar), 1109–1135.

Cilibrasi, R. L., et al., 2007. Statistical inference through data compression.

Cohen, J., 1960. A coefficient of agreement for nominal scales. Educational and psychological measurement 20 (1), 37–46.

Connolly, C., Fleiss, T., 1997. A study of efficiency and accuracy in the transformation from rgb to cielab color space. IEEE Transactions on Image Processing 6 (7), 1046–1048.

Connor, R., Simeoni, F., Iakovos, M., Moss, R., 2011. A bounded distance metric for comparing tree structure. Information Systems 36 (4), 748–764.

Cording, P. H., Lyngby, K., 2011. Algorithms for web scraping. PDF] Available: http://www2. imm. dtu. dk/pubdb/views/publicationdetails. php.

CrossBrowserTesting, 2017. https://crossbrowsertesting.com/ (accessed 17.03.04).

Daniel P. Huttenlocher, Gregory A. Klanderman, and William J. Rucklidge. 1993. Comparing images using the Hausdorff distance. Pattern Analysis and Machine Intelligence, IEEE Transactions on 15, 9 (1993), 850–863.

Dorner, D., 1996. The logic of failure: Recognizing and avoiding error in complex situations. Basic Books.

Dubuisson, M.-P., Jain, A. K., 1994. A modified hausdorff distance for object matching. In: Pattern Recognition, 1994. Vol. 1-Conference A: Computer Vision & Image Processing., Proceedings of the 12th IAPR International Conference on. Vol. 1. IEEE, pp. 566 – 568.

Eleni Michailidou, Simon Harper, and Sean Bechhofer. 2008. Visual complexity and aesthetic perception of web pages. In Proceedings of the 26th annual ACM international conference on Design of communication. ACM, 215–224.

Expression Web SuperPreview, 2011. https://www.microsoft.com/en-ca/download/details.aspx?id=2020 (accessed 17.03.04).

Francisco Claude, Antonio Farina, Miguel A. Mart´ınez-Prieto, and Gonzalo Navarro. 2010. Compressed qgram indexing for highly repetitive biological sequences. In BioInformatics and BioEngineering (BIBE), 2010 IEEE International Conference on. IEEE, 86–91.

Gupta, S., Kaiser, G., Neistadt, D., Grimm, P., 2003. Dom-based content extraction of html documents. In: Proceedings of the 12th international conference on World Wide Web. ACM, pp. 207–214.

Gwet, K. L., 2014. Handbook of inter-rater reliability: The definitive guide to measuring the extent of agreement among raters. Advanced Analytics, LLC.

Hattori, G., Hoashi, K., Matsumoto, K., Sugaya, F., 2007. Robust web page segmentation for mobile terminal using content-distances and page layout information. In: Proceedings of the 16th international conference on World Wide Web. ACM, pp. 361–370.

Hauzeur, J., Mathy, L., De Maertelaer, V., 1999. Comparison between clinical evaluation and ultrasonography in detecting hydrarthrosis of the knee. The Journal of rheumatology 26 (12), 2681–2683.

Herb Stevenson. 2012. Emergence: The Gestalt Approach to Change. (2012). Retrieved April 18, 2016 from http://www.clevelandconsultinggroup.com/articles/emergence-gestalt-approach-to-change.php

Hern´andez, I., Rivero, C. R., Ruiz, D., Corchuelo, R., 2014. Cala: An unsupervised url-based web page classification system. Knowledge-Based Systems 57, 168–180.

Huttenlocher, D. P., Klanderman, G. A., Rucklidge, W. J., 1993. Comparing images using the hausdorff distance. IEEE Transactions on pattern analysis and machine intelligence 15 (9), 850–863.

IE NetRenderer, 2017. https://netrenderer.com/ (accessed 17.03.04).

IETester, 2017. http://www.my-debugbar.com/wiki/IETester/HomePage (accessed 17.03.04).

Jeanine Romano, Jeffrey D. Kromrey, Jesse Coraggio, and Jeff Skowronek. 2006. Appropriate statistics for ordinal level data: Should we really be using t-test and Cohen's d for evaluating group differences on the NSSE and other surveys. In annual meeting of the Florida Association of Institutional Research. 1–33.

Jeremy M. Wolfe, Keith R. Kluender, Dennis M. Levi, Linda M. Bartoshuk, Rachel S. Herz, Roberta L. Klatzky, Susan J. Lederman, and Daniel M. Merfeld. 2009. Sensation and Perception (2nd ed.). Sinauer Associates Inc., Massachusetts, MA.

Johnson, G. M., Fairchild, M. D., 2003. A top down description of s-cielab and ciede2000. Color Research & Application 28 (6), 425–435.

Jyotish Chandra Banerjee. 1994. Encyclopaedic Dictionary of psychological terms. MD Publications Pvt. Ltd., New Delhi.

Kang, J., Yang, J., Choi, J., 2010. Repetition-based web page segmentation by detecting tag patterns for small-screen devices. IEEE Transactions on Consumer Electronics 56 (2).

Koffka, K., 2013. Principles of Gestalt psychology. Vol. 44. Routledge.

Kohlsch¨utter, C., Nejdl, W., 2008. A densitometric approach to web page segmentation. In: Proceedings of the 17th ACM conference on Information and knowledge management. ACM, pp. 1173–1182.

Kurt Koffka. 2013. Principles of Gestalt psychology. Vol. 44. Routledge.

Kwitt, R., Uhl, A., 2008. Image similarity measurement by kullback-leibler divergences between complex wavelet subband statistics for texture retrieval. In: Image Processing, 2008. ICIP 2008. 15th IEEE International Conference on. IEEE, pp. 933–936.

Landis, J. R., Koch, G. G., 1977. The measurement of observer agreement for categorical data. biometrics, 159–174.

Lee, J.-H., Yeh,W.-C., Chuang, M.-C., 2015.Web page classification based on a simplified swarm optimization. Applied Mathematics and Computation 270, 13–24.

Li, M., Chen, X., Li, X., Ma, B., Vit´anyi, P. M., 2004. The similarity metric. IEEE transactions on Information Theory 50 (12), 3250–3264.

Lin, S.-H., Ho, J.-M., 2002. Discovering informative content blocks from web documents. In: Proceedings of the eighth ACM SIGKDD international conference on Knowledge discovery and data mining. ACM, pp. 588–593.

Liu, H. X.,Wu, B., Liu, Y., Huang, M., Xu, Y. F., 2013. A discussion on printing color difference tolerance by ciede2000 color difference formula. In: Applied Mechanics and Materials. Vol. 262. Trans Tech Publ, pp. 96–99.

Liu, Z., Lagani`ere, R., 2007. Phase congruence measurement for image similarity assessment. Pattern Recognition Letters 28 (1), 166–172.

Luo, M. R., Cui, G., Rigg, B., 2001. The development of the cie 2000 colour-diffierence formula: Ciede2000. Color Research & Application 26 (5), 340–350.

M. Ronnier Luo, Guihua Cui, and B. Rigg. 2001. The development of the CIE 2000 colour-difference formula: CIEDE2000. Color Research & Application 26, 5 (2001), 340–350.

M¨uller-Molina, A. J., Hirata, K., Shinohara, T., 2008. A tree distance function based on multi-sets. In: Pacific-Asia Conference on Knowledge Discovery and Data Mining. Springer, pp. 87–98.

María Alpuente and Daniel Romero. 2009. A visual technique for web pages comparison. Electronic Notes in Theoretical Computer Science 235 (2009), 3–18.

Mateusz Pawlik and Nikolaus Augsten. 2015. Efficient computation of the tree edit distance. ACM Transactions on Database Systems (TODS) 40, 1 (2015), 3.

McCallum, A., Nigam, K., et al., 1998. A comparison of event models for naive bayes text classification. In: AAAI-98 workshop on learning for text categorization. Vol. 752. Madison, WI, pp. 41–48.

Ming Li, Xin Chen, Xin Li, Bin Ma, and Paul Vit ´anyi. 2004. The similarity metric. Information Theory, IEEE Transactions on 50, 12 (2004), 3250–3264.

Onan, A., 2016. Classifier and feature set ensembles for web page classification. Journal of Information Science 42 (2), 150–165.

Ou Wu, Haiqiang Zuo, Weiming Hu, and Bing Li. 2016. Multimodal Web Aesthetics Assessment Based on Structural SVM and Multitask Fusion Learning. IEEE Transactions on Multimedia 18, 6 (2016), 1062– 1076.

Palmer, S. E., 1990. Modern theories of gestalt perception. Mind & Language 5 (4), 289–323.

Peng Shi, Lianhong Ding, and Bingwu Liu. 2008. Similarity computation of Web pages. In Knowledge Acquisition and Modeling Workshop, 2008. KAM Workshop 2008. IEEE International Symposium on. IEEE, 777–780.

Pereira, A. C., Eggertsson, H., Martinez-Mier, E. A., Mialhe, F. L., Eckert, G. J., Zero, D. T., 2009. Validity of caries detection on occlusal surfaces and treatment decisions based on results from multiple caries-detection methods. European journal of oral sciences 117 (1), 51–57.

Refaeilzadeh, P., Tang, L., Liu, H., 2009. Cross-validation. In: Encyclopedia of database systems. Springer, pp. 532–538.

Reis, D. d. C., Golgher, P. B., Silva, A. S., Laender, A., 2004. Automatic web news extraction using tree edit distance. In: Proceedings of the 13th international conference on World Wide Web. ACM, pp. 502–511.

Rohlfing, T., 2012. Image similarity and tissue overlaps as surrogates for image registration accuracy: widely used but unreliable. IEEE transactions on medical imaging 31 (2), 153–163.

Roshanbin, N., Miller, J., 2011. Finding homoglyphs-a step towards detecting unicode-based visual spoofing attacks. Web Information System Engineering–WISE 2011, 1–14.

Routhu Srinivasa Rao and Syed Taqi Ali. 2015. A Computer Vision Technique to Detect Phishing Attacks. In Communication Systems and Network Technologies (CSNT), 2015 Fifth International Conference on. IEEE, 596–601.

Saar, T., Dumas, M., Kaljuve, M., Semenenko, N., 2016. Browserbite: cross-browser testing via image processing.

Sampat, M. P., Wang, Z., Gupta, S., Bovik, A. C., Markey, M. K., 2009. Complex wavelet structural similarity: A new image similarity index. IEEE transactions on image processing 18 (11), 2385–2401.

Shahbazi, A., Miller, J., 2014. Extended subtree: a new similarity function for tree structured data. IEEE Transactions on knowledge and Data Engineering 26 (4), 864–877.

Sharma, G., Wu, W., Dalal, E. N., 2005. The ciede2000 color-diffierence formula: Implementation notes, supplementary test data, and mathematical observations. Color Research & Application 30 (1), 21–30.

Shauvik Roy Choudhary, Husayn Versee, and Alessandro Orso. 2010. WEBDIFF: Automated identification of cross-browser issues in web applications. In Software Maintenance (ICSM), 2010 IEEE International Conference on. IEEE, 1–10.

Shauvik Roy Choudhary, Mukul R Prasad, and Alessandro Orso. 2012. Crosscheck: Combining crawling and differencing to better detect cross-browser incompatibilities in web applications. In 2012 IEEE Fifth International Conference on Software Testing, Verification and Validation. IEEE, 171–180.

Shauvik Roy Choudhary, Mukul R Prasad, and Alessandro Orso. 2013. X-PERT: accurate identification of cross-browser issues in web applications. In Proceedings of the 2013 International Conference on Software Engineering. IEEE Press, 702–711.

Sim, D.-G., Kwon, O.-K., Park, R.-H., 1999. Object matching algorithms using robust hausdorff distance measures. IEEE Transactions on image processing 8 (3), 425–429.

Simon Harper, Eleni Michailidou, and Robert Stevens. 2009. Toward a definition of visual complexity as an implicit measure of cognitive load. ACM Transactions on Applied Perception (TAP) 6, 2 (2009), 10.

Software: Practice and Experience 46 (11), 1459–1477.

Song, R., Liu, H.,Wen, J.-R., Ma,W.-Y., 2004. Learning block importance models for web pages. In: Proceedings of the 13th international conference on World Wide Web. ACM, pp. 203–211.

Sternberg, R. J., Sternberg, K., 2016. Cognitive psychology. Nelson Education.

Stevenson, H., 2012. Emergence: The gestalt approach to change. Unleashing Executive and Orzanizational Potential. Retrieved 7.

Sukru Eraslan, Yeliz Yesilada, and Simon Harper. 2016. Scanpath Trend Analysis on Web Pag-es: Clustering Eye Tracking Scanpaths. ACM Transactions on the Web (TWEB) 10, 4 (2016), 20.

Tai, K.-C., 1979. The tree-to-tree correction problem. Journal of the ACM (JACM) 26 (3), 422–433.

Teh-Chung Chen, Scott Dick, and James Miller. 2010. Detecting visually similar web pages: Application to phishing detection. ACM Transactions on Internet Technology (TOIT) 10, 2 (2010), 5.

Terwijn, S. A., Torenvliet, L., Vit´anyi, P. M., 2011. Nonapproximability of the normalized information distance. Journal of Computer and System Sciences 77 (4), 738–742.

Tewarie, P., Balk, L., Costello, F., Green, A., Martin, R., Schippling, S., Petzold, A., 2012. The oscar-ib consensus criteria for retinal oct quality assessment. PloS one 7 (4), e34823.

Thiadmer Riemersma. 2008. Colour metric. (2008). Retrieved April 18, 2016 from http://www.compuphase.com/cmetric.htm

Tõnis Saar, Marlon Dumas, Marti Kaljuve, and Nataliia Semenenko. 2015. Browserbite: cross-browser testing via image processing. Software: Practice and Experience (2015).

Unwin, N., Alberti, K., Bhopal, R., Harland, J., Watson, W., White, M., 1998. Comparison of the current who and new ada criteria for the diagnosis of diabetes mellitus in three ethnic groups in the uk. Diabetic medicine 15 (7), 554–557.

Wei, Y., Wang, B., Liu, Y., Lv, F., 2014. Research on webpage similarity computing technology based on visual blocks. In: Chinese National Conference on Social Media Processing. Springer, pp. 187–197.

Xu, Z., Miller, J., 2016. Identifying semantic blocks in web pages using gestalt laws of grouping. World Wide Web. 19 (5), 957–978.

Yasufumi Takama and Noriaki Mitsuhashi. 2005. Visual similarity comparison for Web page retrieval. In Web Intelligence, 2005. Proceedings. The 2005 IEEE/WIC/ACM International Conference on. IEEE, 301–304.

Yu, S., Cai, D., Wen, J.-R., Ma, W.-Y., 2003. Improving pseudo-relevance feedback in web information retrieval using web page segmentation. In: Proceedings of the 12th international conference on World Wide Web. ACM, pp. 11–18.

Zhai, Y., Liu, B., 2006. Structured data extraction from the web based on partial tree alignment. IEEE Transactions on Knowledge and Data Engineering 18 (12), 1614–1628. 12

Zhao, C., Shi, W., Deng, Y., 2005. A new hausdorff distance for image matching. Pattern Recognition Letters 26 (5), 581–586.

Zhen Xu and James Miller. 2015a. Identifying semantic blocks in Web pages using Gestalt laws of grouping. World Wide Web (2015), 1–22.

Zhen Xu and James Miller. 2015b. A New Webpage Classification Model Based on Visual In-formation Using Gestalt Laws of Grouping. In International Conference on Web Infor-mation Systems Engineering. Springer, 225–232.

Zhen Xu and James Miller. 2017. Estimating Similarity of Rich Internet Pages Using Visual Information, International Journal of Web Engineering and Technology.